Supporting Information

Squaramide calix[4]pyrroles for anion transport

Patrick Wang,[a] Mohamed Fares[b], David Hibbs[b], Jonathan Du[b], Philip A. Gale*[c]

[a] School of Chemistry, The University of Sydney, NSW, Australia.

[b] School of Pharmacy, The University of Sydney, NSW, Australia

[c] School of Mathematical and Physical Sciences, Faculty of Science, University of Technology Sydney, NSW, Australia.

Contents

Synthesis

Synthetic Procedures

Chemicals were purchased from commercial sources and used without purification unless otherwise stated. Anhydrous solvents were collected from an Inert Corp PureSolv MD7 solvent purification system.

NMR spectra were recorded on Bruker Avance NEO 300, Bruker AVIII 400, Bruker AVIII 500, Bruker NEO 500 NMR, or Bruker AVIII 600 spectrometers in the indicated solvent at 298 K. Chemical shifts are reported relative to the deuterated solvent used. Spectra resolution are indicated before the chemical shifts.

Low-resolution mass spectrometry (LR-MS) was collected using positive and negative electrospray ionisation on a Bruker amaZon SL mass spectrometer. High-resolution mass spectrometry (HR-MS) was collected on a Bruker Solarix 2XR mass spectrometer by Sydney Analytical. All mass spectrometry data are reported as *m/z*.

3-Ethoxy-4-(phenylamino)cyclobut-3-ene-1,2-dione (ES1)

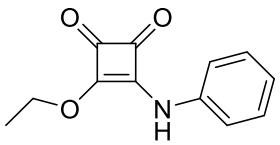

Diethyl squarate (0.5319 g, 3.13 mmol) was suspended with zinc triflate (0.0671 g, 0.18 mmol) and aniline (0.3531 g, 3.79 mmol) in absolute ethanol (30 mL). The mixture was stirred at RT for 23 h before removing the solvent under vacuum. The residue was washed with 1 M NH_4Cl (3 × 30 mL) and water (3 × 30 mL). The solid was washed with hot diethyl ether (200 mL) and the filtrate concentrated under vacuum to give the product as a pale-yellow powder. Yield 0.5189 g (76 %).

^{1}H NMR (300 MHz, DMSO-d_6) δ: 10.74 (s, 1H), 7.40 – 7.29 (m, 4H), 7.16 – 7.08 (m, 1H), 4.77 (q, *J* = 7.1 Hz, 2H), 1.42 (t, *J* = 7.1 Hz, 3H). **LR-MS** (ESI+) $[M+Na]^+$: 240.11 *m/z*.

3-Ethoxy-4-((4-nitrophenyl)amino)cyclobut-3-ene-1,2-dione (ES2)

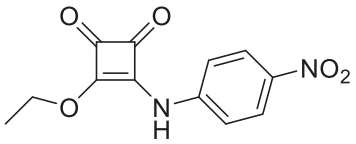

Diethyl squarate (0.4981 g, 2.93 mmol) was suspended with zinc triflate (0.0831 g, 0.23 mmol) and 4-nitroaniline (0.4359 g, 3.16 mmol). The mixture was stirred at RT for 22 h before removing the solvent under vacuum. The residue was washed with 1 M NH_4Cl (3 × 30 mL) and water (3 × 30 mL). The final product was recrystallised from MeCN (20 mL) as an orange crystalline powder. Yield 0.4531 g (59 %).

^{1}H NMR (300 MHz, DMSO-d_6) δ: 11.22 (s, 1H), 8.24 (d, *J* = 9.2 Hz, 2H), 7.60 (d, *J* = 9.2 Hz, 1H), 4.81 (q, *J* = 7.1 Hz, 2H), 1.45 (t, *J* = 7.1 Hz, 3H): **LR-MS** (ESI−) $[M-H]^-$: 261.06 *m/z*.

3-Ethoxy-4-((4-(trifluoromethyl)phenyl)amino)cyclobut-3-ene-1,2-dione (ES3)

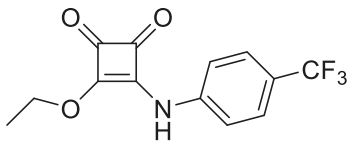

Diethyl squarate (1.0845 g, 6.37 mmol) was dissolved in absolute ethanol (10 mL) before adding 4-(trifluoromethyl)aniline (1.3394 g, 5.85 mmol) and zinc triflate (0.1665 g, 0.458 mmol). The solution was stirred at RT for 21 h, then filtered and the solid washed with excess hexane until the filtrate was colourless. The product was dried as a pale yellow powder. Yield 1.7509 g (98 %).

^{1}H NMR (300 MHz, DMSO-d_6) δ: 11.01 (s, 1H), 7.72 (d, J = 8.6 Hz, 2H), 7.57 (d, J = 8.4 Hz, 2H), 4.79 (q, J = 7.1 Hz, 2H), 1.43 (t, J = 7.1 Hz, 3H): **LR-MS** (ESI+) $[M+Na]^+$: 308.10 *m/z*.

3-((3,5-Bis(trifluoromethyl)phenyl)amino)-4-ethoxycyclobut-3-ene-1,2-dione (ES4)

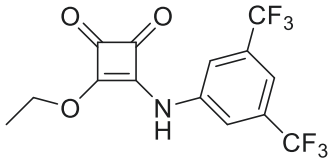

Diethyl squarate (1.3007 g, 7.64 mmol) was dissolved in absolute ethanol (15 mL) before adding 3,5-bis(trifluoromethyl)aniline (1.7464 g, 7.62 mmol) and zinc triflate (0.1649 g, 0.454 mmol). The solution was stirred at RT for 21 h. The mixture was filtered and washed with water (2 × 10 mL), cold absolute ethanol (2 × 10 mL), and finally hexane (3 × 60 mL). The product was dried into a pale-yellow powder. Yield 1.7466 g (65 %).

^{1}H NMR (300 MHz, DMSO-d_6) δ: 11.19 (s, 1H), 8.03 (s, 2H), 7.76 (s, 1H), 4.80 (q, *J* = 7.1 Hz, 2H), 1.42 (t, *J* = 7.1 Hz, 3H): **LR-MS** (ESI+) $[M+Na]^+$: 376.02 *m/z*.

3-Ethoxy-4-((4-methoxyphenyl)amino)cyclobut-3-ene-1,2-dione (ES5)

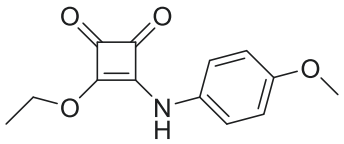

Diethyl squarate (0.5117 g, 3 .01 mmol) and zinc triflate (0.2884 g, 0.790 mmol) were suspended in absolute ethanol (10 mL) before adding a solution of *p*-anisidine (0.3482 g, 2.83 mmol) in absolute ethanol (15 mL). The mixture was stirred at RT for 19 h before concentrating under reduced pressure. The residue was washed with 1 M NH_4Cl (3 × 30 mL) and water (3 × 30 mL). The solid was then refluxed in hot hexane for 1 h before hot filtering to give the product as a grey powder. Yield 0.5301 g (76 %).

^{1}H NMR (300 MHz, DMSO-d_6) δ: 10.61 (s, 1H), 7.27 (d, *J* = 8.4 Hz, 2H), 6.92 (d, *J* = 9.0 Hz, 2H), 4.74 (q, *J* = 7.1 Hz, 2H), 3.73 (s, 3H), 1.40 (t, *J* = 7.1 Hz, 3H): **LR-MS** (ESI+) $[M+H]^+$: 248.11 *m/z*.

3-Ethoxy-4-((perfluorophenyl)amino)cyclobut-3-ene-1,2-dione (ES6)

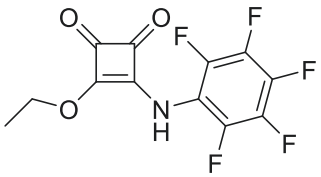

Diethyl squarate (0.5342 g, 3.14 mmol) was suspended with pentafluoroaniline (0.5387 g, 2.94 mmol) and zinc triflate (0.2572 g, 0.708 mmol) in absolute ethanol (10 mL). The mixture was stirred at RT for 17 h and the solvent removed under reduced pressure. The crude product was purified via flash chromatography, eluting with hexane/ethyl acetate (9:1) to give a clear oil which dried into a white solid after concentrating under reduced pressure in the presence of *n*-hexane. The solid was washed with excess *n*-hexane to remove excess diethyl squarate and dried to give the product as a white powder. Yield 0.4959 g (55 %).

^{1}H NMR (500 MHz, DMSO-d_6) δ: 11.12 (s, 1H), 4.69 (q, *J* = 7.1 Hz, 2H), 1.35 (t, *J* = 7.1 Hz, 3H): **LR-MS** (ESI−) $[M-H]^-$: 305.97 *m/z*.

3-(Butylamino)-4-ethoxycyclobut-3-ene-1,2-dione (ES7)

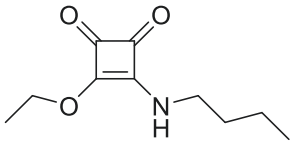

N-butylamine (0.4241 g, 5.80 mmol) was added to a solution of diethyl squarate (1.0760 g, 6.32 mmol) in MeCN (6 mL). The reaction was stirred at RT for 17 h before filtering and concentrating the filtrate under reduced pressure to a yellow oil. The crude product was purified via flash chromatography, eluting with hexane/ethyl acetate (7:3) to give a clear oil which dried into a white solid after concentrating under reduced pressure in the presence of *n*-hexane. Yield 0.9766 g (85 %).

^{1}H NMR (300 MHz, DMSO-d_6) δ: 8.70 (s, 1H), 4.72 – 4.58 (m, 2H), 3.47 (t, *J* = 6.9 Hz, 1H), 3.28 (t, *J* = 6.9 Hz, 1H), 1.57 – 1.41 (m, 2H), 1.41 – 1.20 (m, 4H), 0.87 (t, *J* = 7.3 Hz, 3H). **LR-MS** (ESI+) $[M+H]^+$: 198.19 *m/z*.

2-(2-Oxopropyl)isoindoline-1,3-dione (I1)

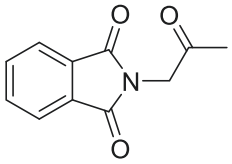

Potassium phthalimide (25.7095 g, 138.8 mmol) was suspended in acetone (75 mL) with chloroacetone (12.2412 g, 132.3 mmol). The mixture was refluxed at 80 °C for 10 h and the solvent removed under reduced pressure. The solid was dissolved in DCM (100 mL) and washed with water (2 × 100 mL) followed by 10% Na_2CO_3 (2 × 100 mL). The organic layer was dried over $MgSO_4$ and concentrated under reduced pressure to give a yellow oil, which crystallised into a white solid after cooling. The solid was washed with excess water and dried to give the product as a white crystalline powder. Yield 22.6823 g (84 %).

^{1}H NMR (300 MHz, DMSO-d_6) δ: 7.98 – 7.82 (m, 4H), 4.58 (s, 2H), 2.24 (s, 3H): **LR-MS** (ESI+) $[M+Na]^+$: 226.09 *m/z*.

2-(2,2-Di(1H-pyrrol-2-yl)propyl)isoindoline-1,3-dione (I2)

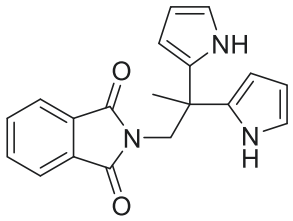

I1 (2.2441 g, 11.04 mmol) was mixed with distilled pyrrole (10 mL, 144.1 mmol) at 0 °C under an inert atmosphere. TFA (0.8 mL, 10.45 mmol) was added to the mixture dropwise and the solution stirred for 18 h, allowing to warm up to RT. The solution was diluted with water (100 mL) and extracted with DCM (3 × 40 mL). The organic layer was dried over $MgSO_4$ and concentrated under reduced pressure to give a dark oil. The crude product was purified via flash chromatography, eluting with hexane/ethyl acetate (19:1). Fractions were combined and concentrated under reduced pressure to give a yellow oil which solidified into a solid on cooling. The solid was refluxed in *n*-hexane (200 mL), hot filtered, then washed with hot *n*-hexane until the filtrate was colourless. The solid was dried to give the product as a pale-yellow powder. Yield 1.3330 g (38 %).

^{1}H NMR (300 MHz, DMSO-d_6) δ: 10.39 (s, 2H), 7.80 (s, 4H), 6.58 (d, J = 2.1 Hz, 2H), 5.89 – 5.82 (m, 2H), 5.80 – 5.76 (m, 2H), 4.07 (s, 2H), 1.57 (s, 3H): **LR-MS** (ESI+) $[M+Na]^+$: 342.14 *m/z*.

2-((5,10,10,15,15,20,20-Heptamethyl-5H,10H,15H,20H,22H,24H-porphyrin-5-yl)methyl)isoindoline-1,3-dione (I3)

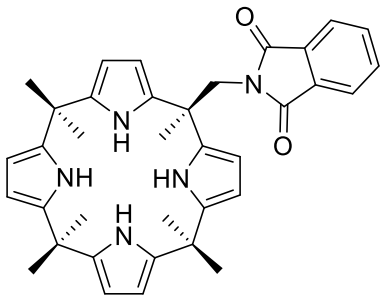

I2 (1.1447 g, 3.58 mmol) was dissolved in dry DCM (55 mL) at 0 °C under an inert atmosphere. Distilled pyrrole (1.3 mL, 18.74 mmol) and acetone (2.75 mL, 37.12 mmol) were added to the solution. TFA (0.6 mL, 7.84 mmol) was added dropwise, and the solution stirred for 18 h, allowing to warm up to RT. The solution was quenched with 1 M NaOH (50 mL) and the organic layer washed with water (3 × 100 mL) and brine (50 mL). The organic layer was dried over $MgSO_4$ and concentrated under reduced pressure to give a brown solid. The crude product was purified via flash chromatography, eluting with hexane/ethyl acetate (9:1) to give the final product as a pale-yellow powder. Yield 0.7745 g (38 %).

^{1}H NMR (300 MHz, DMSO-d_6) δ: 9.55 (s, 2H), 9.29 (s, 2H), 7.79 (s, 4H), 5.88 – 5.41 (m, 8H), 4.12 (s, 2H), 1.65 – 1.41 (m, 21H): **LR-MS** (ESI+) $[M+Na]^+$: 596.27 *m/z*.

(5,10,10,15,15,20,20-Heptamethyl-5H,10H,15H,20H,22H,24H-porphyrin-5-yl)methanamine (I4)

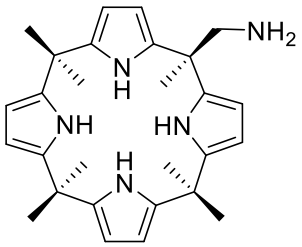

I3 (0.1963 g, 0.342 mmol) was suspended in absolute ethanol (10 mL). Hydrazine monohydrate (0.13 mL) was added dropwise to the mixture and refluxed for 24 h. The solution was cooled then diluted with 2.5 M NaOH (100 mL) and extracted with DCM (3 × 50 mL). The combined organic layers were washed with water (2 × 100 mL) then dried over $MgSO_4$ and concentrated to give the final product as a pale-yellow powder. Yield 0.1492 g (98 %).

^{1}H NMR (300 MHz, DMSO-d_6) δ: 9.21 (s, 4H), 5.78 – 5.65 (m, 8H), 2.94 (s, 2H), 1.65 – 1.35 (m, 21H), 1.29 (s, 2H): **LR-MS** (ESI+) $[M+H]^+$: 444.27 *m/z*.

3-(((5,10,10,15,15,20,20-Heptamethyl-5H,10H,15H,20H,22H,24H-porphyrin-5-yl)methyl)amino)-4-(phenylamino)cyclobut-3-ene-1,2-dione (1)

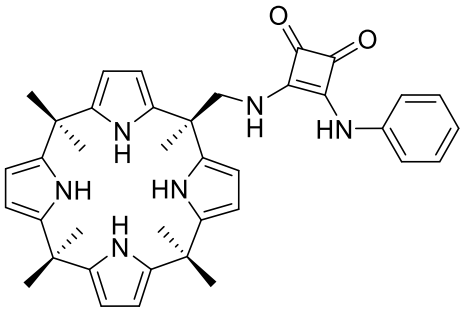

I4 (0.1486 g, 0.335 mmol) was suspended with **ES1** (0.0769 g, 0.354 mmol) in methanol (25 mL). The mixture was refluxed for 12 h and cooled to RT. The mixture was filtered and dried to give the product as fine white needles. Yield 0.1755 g (85 %). Melting point: 170.2 – 180.6 °C (decomposed).

^{1}H NMR (600 MHz, DMSO-d_6) δ: 9.76 (s, 1H), 9.25 (d, *J* = 16.0 Hz, 4H), 7.46–7.38 (m, 3H), 7.35–7.29 (m, 2H), 7.01 (tt, *J* = 7.4, 1.1 Hz, 1H), 5.85 (t, *J* = 3.0 Hz, 2H), 5.80 (t, *J* = 3.0 Hz, 2H), 5.65 (p, *J* = 3.2 Hz, 4H), 4.14 (d, *J* = 6.4 Hz, 2H), 1.73–0.97 (m, 21H): **^{13}C NMR** (151 MHz, DMSO-d_6) δ: 183.9, 180.5, 169.7, 163.4, 139.2, 139.0, 138.6, 138.5, 134.4, 129.4, 122.6, 118.1, 103.5, 102.6, 101.7, 101.6, 52.4, 40.1, 34.6, 34.3, 29.3, 28.8, 28.7, 28.3, 23.9: **LR-MS** (ESI−) $[M-H]^-$: 613.36 *m/z*: **HR-MS** (ESI+) calculated for $[M-H]^-$: 613.32965 *m/z*, found $[M-H]^-$: 613.32937 *m/z*.

3-(((5,10,10,15,15,20,20-Heptamethyl-5H,10H,15H,20H,22H,24H-porphyrin-5-yl)methyl)amino)-4-((4-nitrophenyl)amino)cyclobut-3-ene-1,2-dione (2)

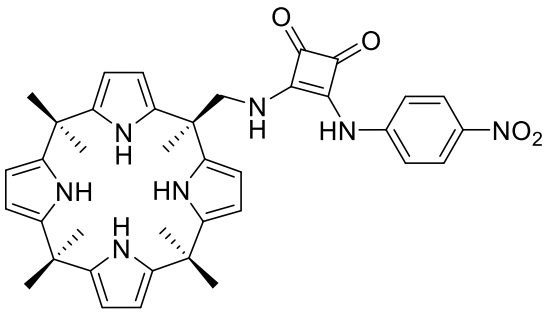

I4 (0.1318 g, 0.297 mmol) was suspended with **ES2** (0.0797 g, 0.304 mmol) in methanol (20 mL). The mixture was refluxed for 13 h then cooled to RT. The mixture was filtered and dried to give the final product as an orange solid. Yield 0.1656 g (85 %). Melting point: 227.0 – 231.9°C (decomposed).

^{1}H NMR (600 MHz, DMSO-d_6) δ: 10.28 (s, 1H), 9.27 (d, *J* = 36.6 Hz, 4H), 8.21 (d, *J* = 9.2 Hz, 2H), 7.64 (s, 1H), 7.58 (d, *J* = 9.2 Hz, 2H), 5.83 (dt, *J* = 28.4, 3.0 Hz, 4H), 5.63 (p, *J* = 3.1 Hz, 4H), 4.14 (s, 2H), 1.58–1.47 (m, 21H): **^{13}C NMR** (151 MHz, DMSO-d_6) δ: 185.1, 180.3, 170.7, 162.0, 145.3, 141.4, 139.3, 138.6, 138.5, 134.3, 125.7, 117.7, 103.5, 102.7, 101.6, 101.6, 52.6, 40.1, 40.1, 34.6, 34.3, 29.4, 28.8, 28.6, 28.1, 23.9: **LR-MS** (ESI−) $[M-H]^-$: 658.36 *m/z*: **HR-MS** (ESI−) calculated for $[M-H]^-$: 658.31473 *m/z*, found $[M-H]^-$: 658.31459 *m/z*.

3-(((5,10,10,15,15,20,20-Heptamethyl-5H,10H,15H,20H,22H,24H-porphyrin-5-yl)methyl)amino)-4-((4-(trifluoromethyl)phenyl)amino)cyclobut-3-ene-1,2-dione (3)

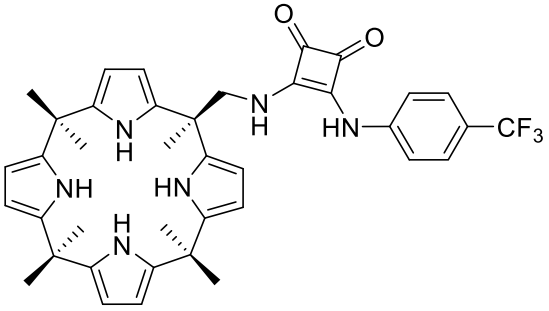

I4 (0.1340 g, 0.302 mmol) was suspended with **ES3** (0.0866 g, 0.304 mmol) in methanol (20 mL). The mixture was refluxed for 12 h then cooled to RT. The mixture was filtered and dried to give the final product as a white solid. Yield 0.1565 g (76 %). Melting point: 179.0 – 229.0 °C (decomposed)

^{1}H NMR (500 MHz, DMSO-d_6) δ: 10.03 (s, 1H), 9.25 (d, *J* = 22.1 Hz, 4H), 7.62 (dd, *J* = 51.7, 8.4 Hz, 4H), 7.53 (s, 1H), 5.82 (d, *J* = 23.6 Hz, 4H), 5.64 (s, 4H), 4.14 (d, *J* = 6.2 Hz, 2H), 1.56–1.46 (m, 21H): **^{13}C NMR** (126 MHz, DMSO-d_6) δ: 185.0, 180.9, 170.6, 163.2, 143.0, 139.7, 138.98, 138.96, 134.8, 127.1, 125.0, 122.8, 118.4, 103.9, 103.1, 102.1, 102.0, 53.0, 40.5, 40.4, 40.2, 40.0, 35.0, 34.7, 29.8, 29.2, 29.0, 28.6, 24.4: **^{19}F NMR** (471 MHz, DMSO-d_6) δ: −60.14: **LR-MS** (ESI−) $[M-H]^-$: 681.35 *m/z*: **HR-MS** (ESI−) calculated for $[M-H]^-$: 681.31703 *m/z*, found $[M-H]^-$: 681.31672 *m/z*.

3-((3,5-Bis(trifluoromethyl)phenyl)amino)-4-(((5,10,10,15,15,20,20-heptamethyl-5H,10H,15H,20H,22H,24H-porphyrin-5-yl)methyl)amino)cyclobut-3-ene-1,2-dione (4)

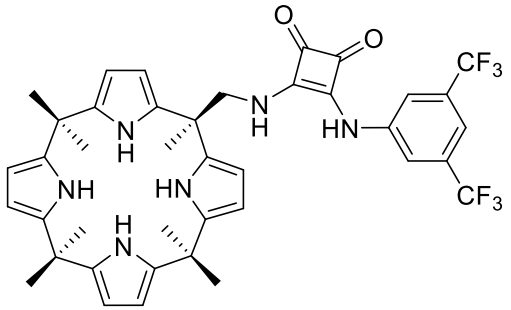

I4 (0.1331 g, 0.300 mmol) was suspended with **ES4** (0.1066 g, 0.302 mmol) in methanol (20 mL). The mixture was refluxed for 12 h then cooled to RT. The mixture was filtered and dried to give the final product as a white powder. Yield 0.1677 g (74 %). Melting point: 173.4 – 178.4 °C (decomposed)

^{1}H NMR (500 MHz, DMSO-d_6) δ: 10.22 (d, *J* = 9.0 Hz, 1H), 9.25 (d, *J* = 19.5 Hz, 4H), 8.02 (s, 2H), 7.65 (s, 1H), 7.53 (s, 1H), 5.83 (dt, *J* = 26.4, 3.0 Hz, 4H), 5.63 (d, *J* = 2.5 Hz, 4H), 4.13 (d, *J* = 5.4 Hz, 2H), 1.56–1.45 (m, 21H): **^{13}C NMR** (126 MHz, DMSO-d_6) δ: 184.5, 180.6, 170.4, 162.3, 141.1, 139.3, 138.5, 134.3, 131.4, 123.2, 118.1, 114.7, 103.6, 102.7, 101.8, 101.6, 101.6, 52.6, 40.2, 40.1, 39.9, 39.8, 34.6, 34.3, 29.3, 28.7, 28.6, 28.2, 24.0: **^{19}F NMR** (471 MHz, DMSO-d_6) δ −61.75: **LR-MS** (ESI−) $[M-H]^-$: 749.33 *m/z*: **HR-MS** (ESI−) calculated for $[M-H]^-$: 749.30442 *m/z*, found $[M-H]^-$: 749.30431 *m/z*.

3-(((5,10,10,15,15,20,20-Heptamethyl-5H,10H,15H,20H,22H,24H-porphyrin-5-yl)methyl)amino)-4-((4-methoxyphenyl)amino)cyclobut-3-ene-1,2-dione (5)

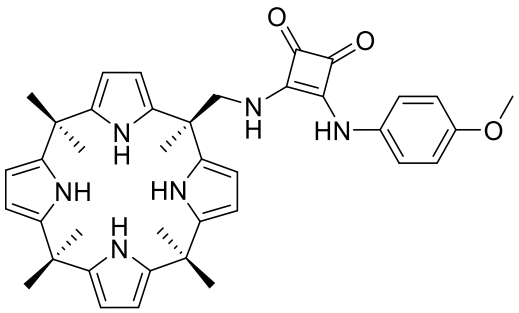

I4 (0.1254 g, 0.283 mmol) was suspended with **ES5** (0.0698 g, 0.282 mmol) in methanol (20 mL). The mixture was refluxed for 18 h then cooled to RT. The mixture was filtered and dried to give the final product as a light grey powder. Yield 0.0715 g (39 %). Melting point: 271.8 – 298.5 °C (decomposed).

^{1}H NMR (600 MHz, DMSO-d_6) δ: 9.65 (s, 1H), 9.25 (d, *J* = 10.7 Hz, 4H), 7.31 (d, *J* = 8.8 Hz, 3H), 6.90 (d, *J* = 9.0 Hz, 2H), 5.82 (dt, *J* = 24.1, 3.0 Hz, 4H), 5.65 (t, *J* = 2.9 Hz, 4H), 4.13 (d, *J* = 6.4 Hz, 2H), 3.72 (s, 3H), 1.55–1.47 (m, 21H): **^{13}C NMR** (151 MHz, DMSO-d_6) δ: 183.8, 181.1, 169.7, 163.9, 155.7, 139.6, 138.98, 138.96, 134.9, 132.6, 120.1, 115.0, 103.9, 103.1, 102.1, 102.0, 55.7, 52.7, 40.5, 35.0, 34.8, 29.7, 29.2, 29.1, 28.7, 24.3: **LR-MS** (ESI−) $[M-H]^-$: 643.39 *m/z*: **HR-MS** (ESI−) calculated for $[M-H]^-$: 643.34021 *m/z*, found $[M-H]^-$: 643.34098 *m/z*.

3-(((5,10,10,15,15,20,20-Heptamethyl-5H,10H,15H,20H,22H,24H-porphyrin-5-yl)methyl)amino)-4-((perfluorophenyl)amino)cyclobut-3-ene-1,2-dione (6)

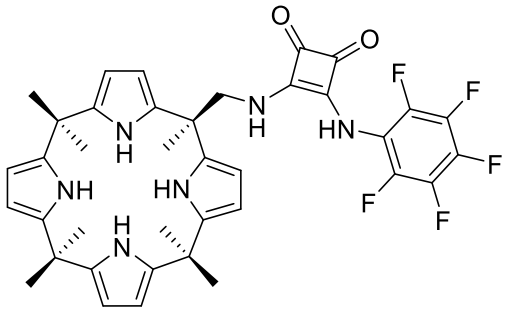

I4 (0.1257 g, 0.283 mmol) was suspended with **ES6** (0.0873 g, 0.284 mmol) in methanol (20 mL). The mixture was refluxed for 18 h then cooled to RT. The solvent was removed under reduced pressure and the crude product purified via flash chromatography, eluting with hexane/ethyl acetate (6:4). The relevant fractions were combined, concentrated to give a white powder, then washed with diethyl ether (30 mL) and dried to give the product as a white powder. Yield 0.0663 g (33 %). Melting point: 259.5 – 275.5 °C (decomposed).

^{1}H NMR (500 MHz, acetone-d_6) δ: 8.71 (s, 1H), 8.14 (d, *J* = 21.8 Hz, 4H), 6.67 (s, 1H), 5.90 (t, *J* = 3.1 Hz, 2H), 5.84 (t, *J* = 3.0 Hz, 2H), 5.77 (d, *J* = 2.7 Hz, 4H), 4.19 (d, *J* = 6.2 Hz, 2H), 1.58 (s, 3H), 1.52–1.49 (m, 18H): **^{13}C NMR** (126 MHz, acetone-d_6) δ: 186.2, 181.7, 169.9, 164.1, 142.4, 139.5, 138.6, 138.2, 137.7, 133.8, 114.4, 104.0, 102.9, 102.5, 102.2, 52.2, 40.5, 35.0, 34.9, 27.9, 27.6, 23.2: **^{19}F NMR** (471 MHz, acetone-d_6) δ: −151.03 (d, *J* = 22.3 Hz), −161.66, −165.16 (t, *J* = 21.8 Hz): **LR-MS** (ESI−) $[M-H]^-$: 703.34 *m/z*: **HR-MS** (ESI−) calculated for $[M-H]^-$: 703.28254 *m/z*, found $[M-H]^-$: 703.28327 *m/z*.

3-(Butylamino)-4-(((5,10,10,15,15,20,20-heptamethyl-5H,10H,15H,20H,22H,24H-porphyrin-5-yl)methyl)amino)cyclobut-3-ene-1,2-dione (7)

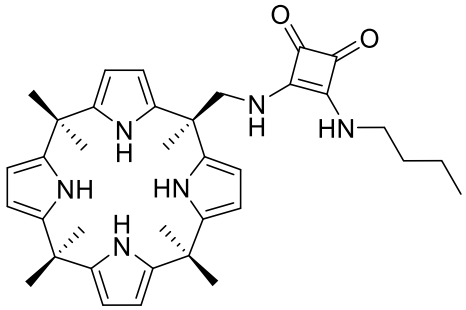

I4 (0.1492 g, 0.336 mmol) was suspended with **ES7** (0.0660 g, 0.335 mmol) in methanol (20 mL). The mixture was refluxed for 10 h and cooled to RT. The solvent was removed under reduced pressure and the residue purified via flash chromatography, eluting with DCM/MeOH (2.5%). The product was dried as a pale yellow powder. Yield 0.0834 g (42 %).

^{1}H NMR (400 MHz, DMSO-d_6) δ: 9.22 (s, 4H), 7.45 (s, 2H), 7.01 (s, 2H), 5.82 – 5.75 (m, 4H), 5.69 – 5.61 (m, 4H), 4.05 (d, *J* = 6.2 Hz, 2H), 3.47 (d, *J* = 5.9 Hz, 2H), 1.55 – 1.39 (m, 21H), 1.35 – 1.21 (m, 2H), 0.89 (t, *J* = 7.3 Hz, 3H): **LR-MS** (ESI+) $[M+Na]^+$: 617.32 m/z.

***meso*-octamethylcalix[4]pyrrole (8)**

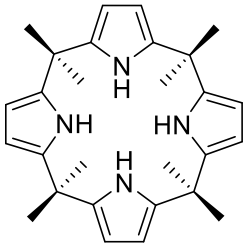

Distilled pyrrole (0.15 mL, 2.16 mmol) and acetone (0.17 mL, 2.30 mmol) were added to DCM (10 mL) under an inert atmosphere. TFA (0.1332 g, 1.17 mmol) was added dropwise to the solution and stirred at RT for 46 h. The reaction was diluted with DCM (100 mL) and then washed with saturated $NaHCO_3$ (60 mL), followed by brine (60 mL). The organic layer was dried over $MgSO_4$ before filtering and concentrating under reduced pressure to give a brown solid. The crude product was purified via flash chromatography, eluting with hexane/ethyl acetate (19:1) to give a white powder. Yield 0.1933 g (42 %).

^{1}H NMR (300 MHz, DMSO-d_6) δ: 9.25 (s, 4H), 5.68 (d, J = 2.4 Hz, 8H), 1.50 (s, 24H): **LR-MS** (ESI−) $[M-H]^-$: 427.34 m/z.

Characterisation spectra

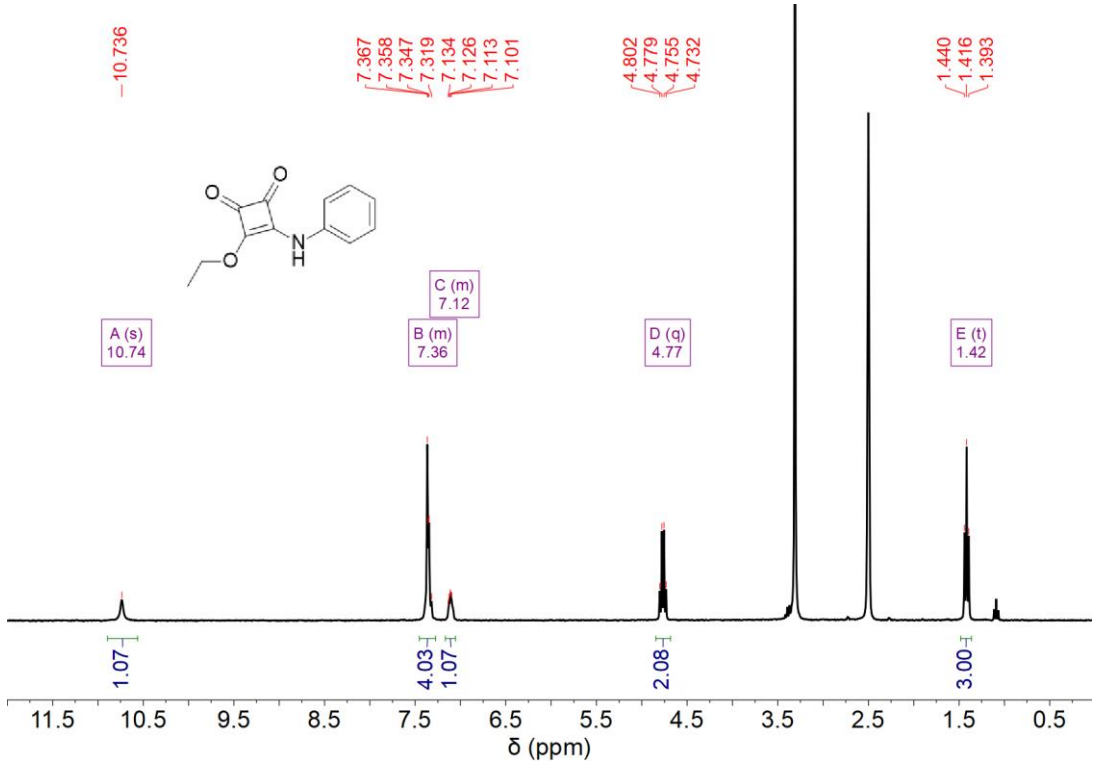

Figure S1. ^{1}H NMR (300 MHz, DMSO-d_6) spectrum of **ES1**.

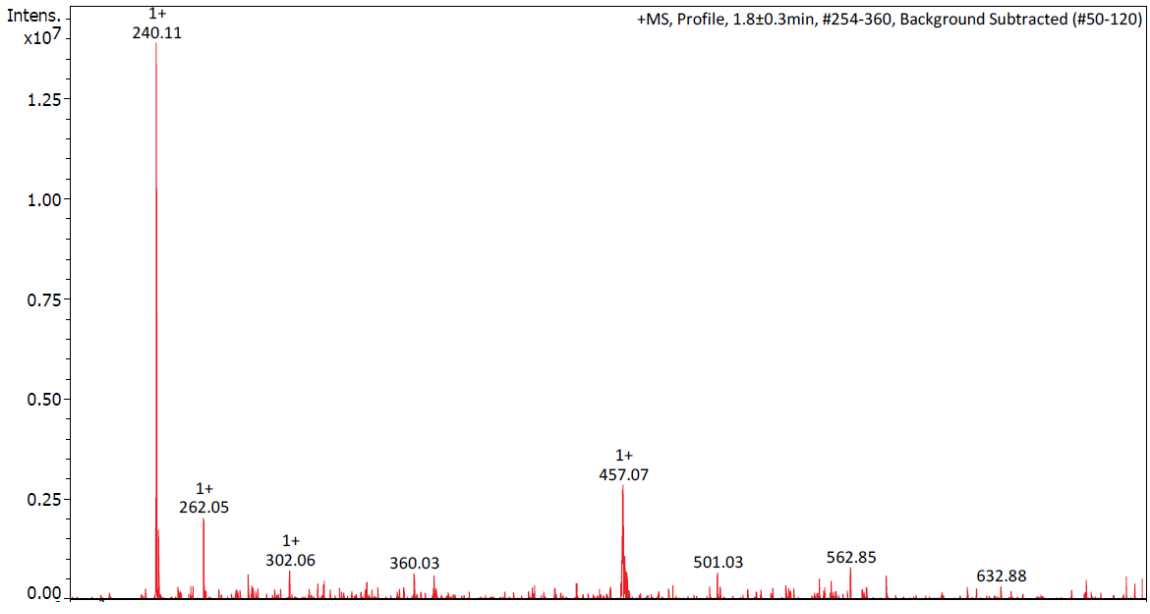

Figure S2. LR-MS (ESI+) of **ES1**.

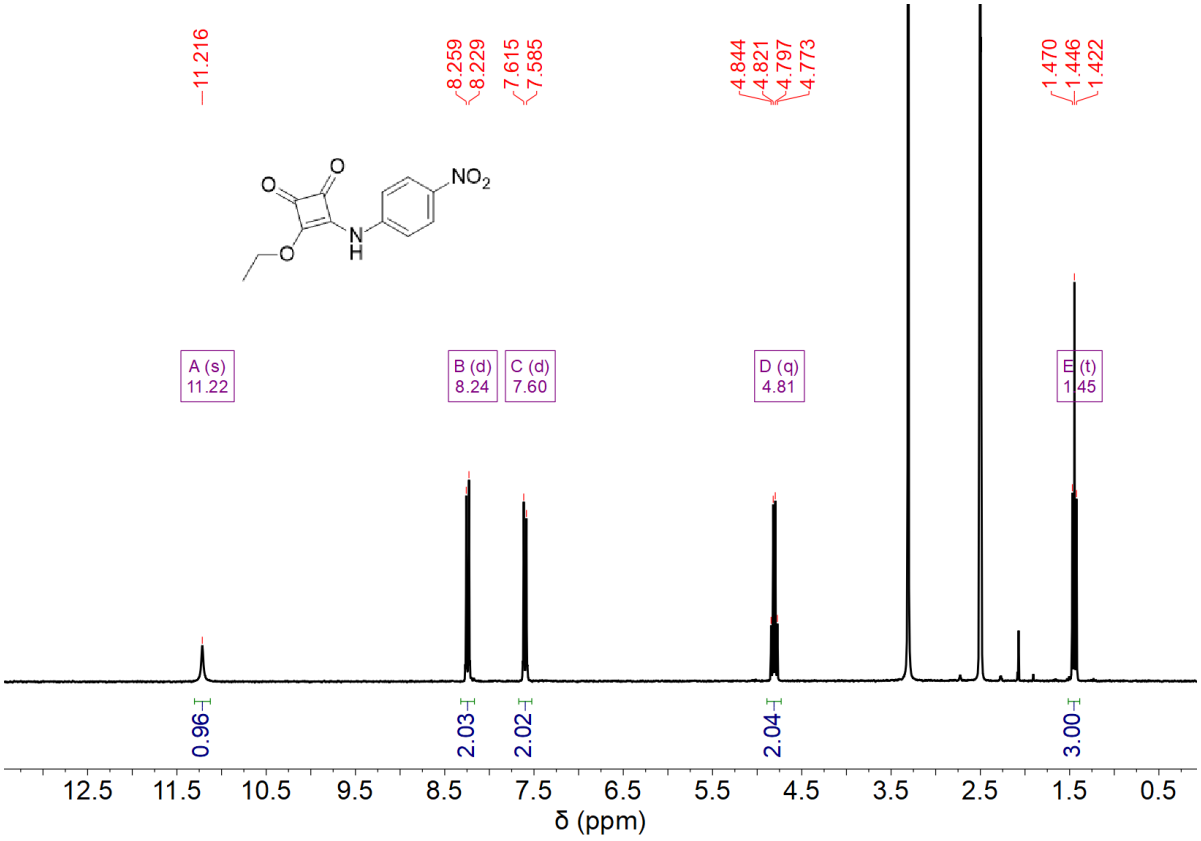

Figure S3. ^{1}H NMR (300 MHz, DMSO-d_6) spectrum of **ES2**.

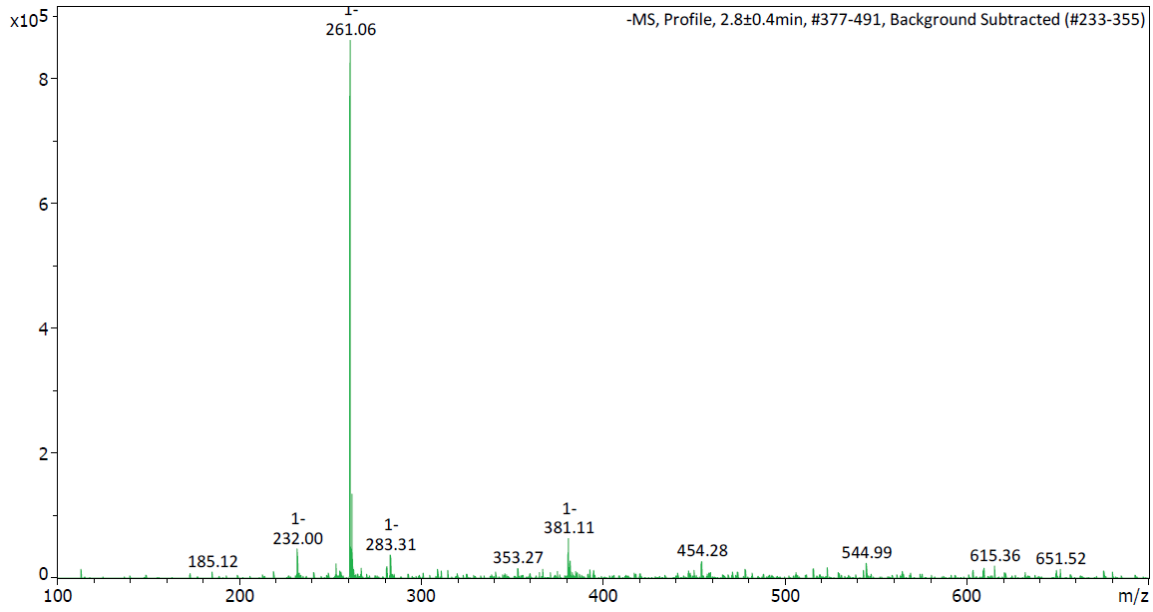

Figure S4. LR-MS (ESI−) of **ES2**.

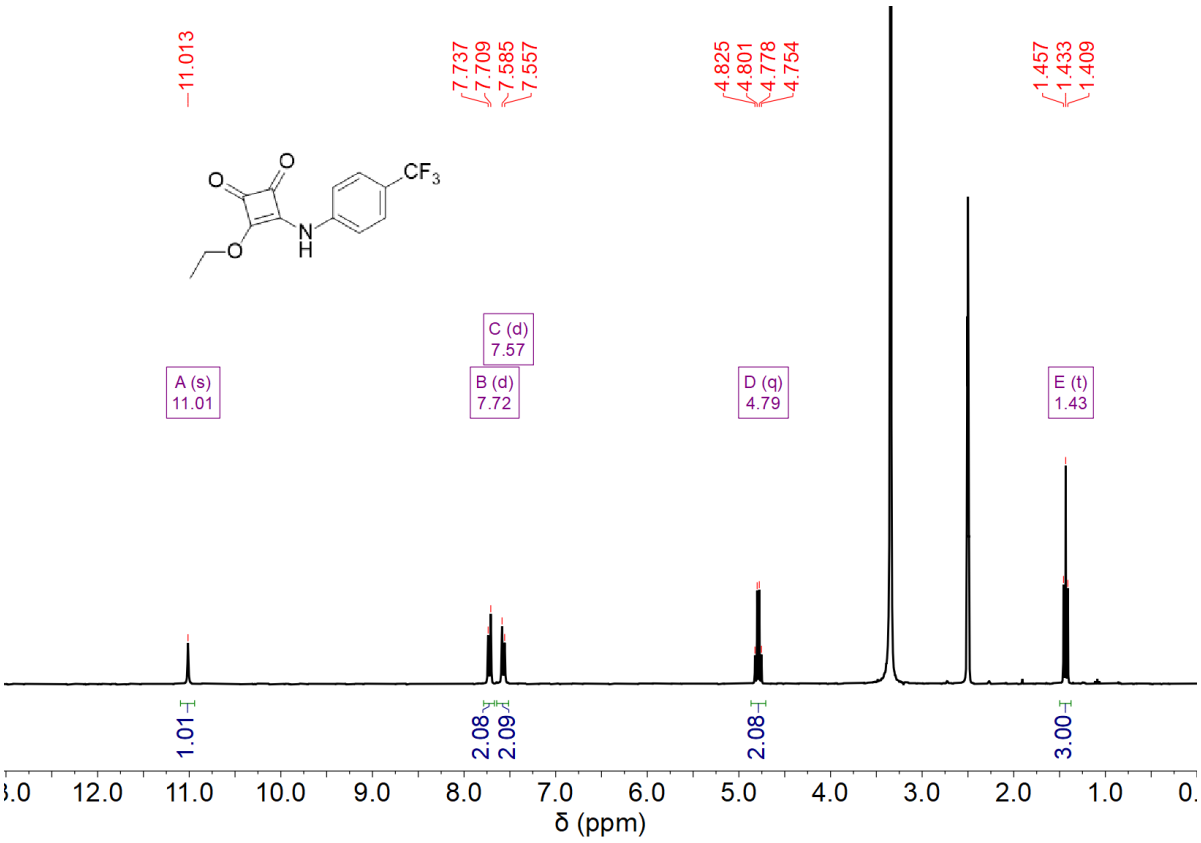

Figure S5. ^{1}H NMR (300 MHz, DMSO-d_6) spectrum of **ES3**.

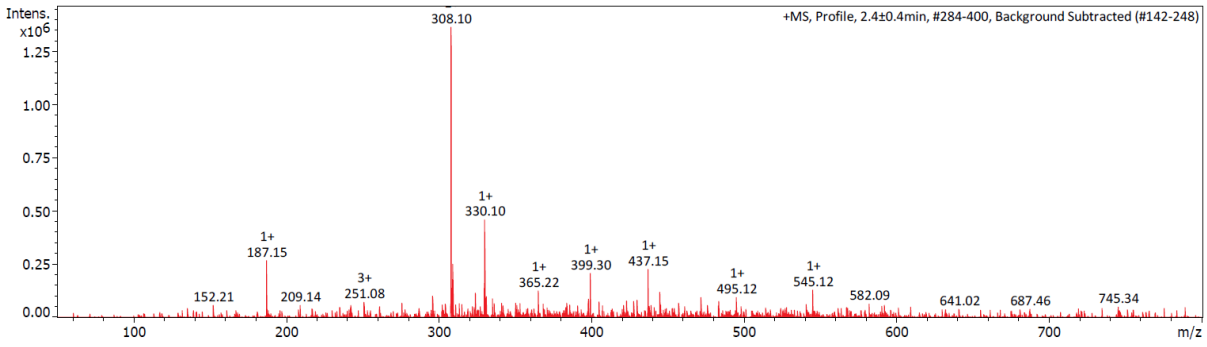

Figure S6. LR-MS (ESI+) of **ES3**.

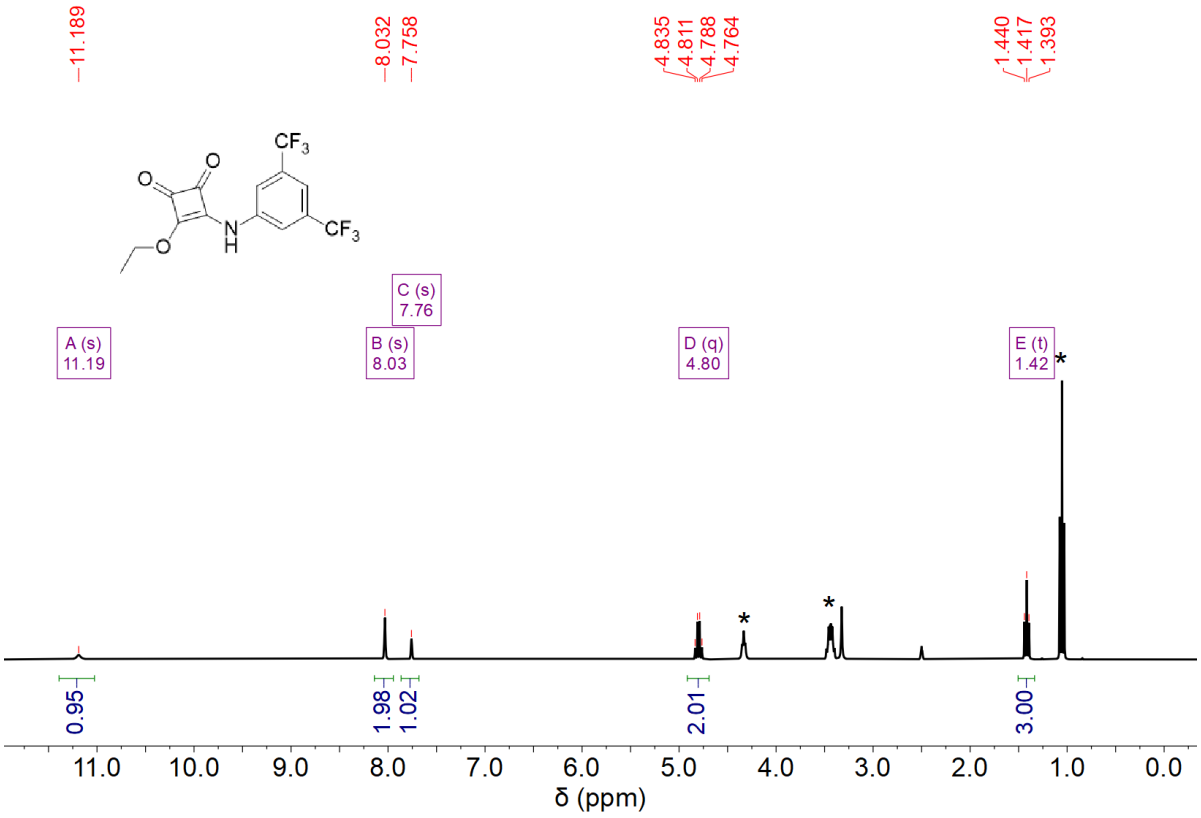

Figure S7. ^{1}H NMR (300 MHz, DMSO-d_6) spectrum of **ES4**. * are residual ethanol peaks.

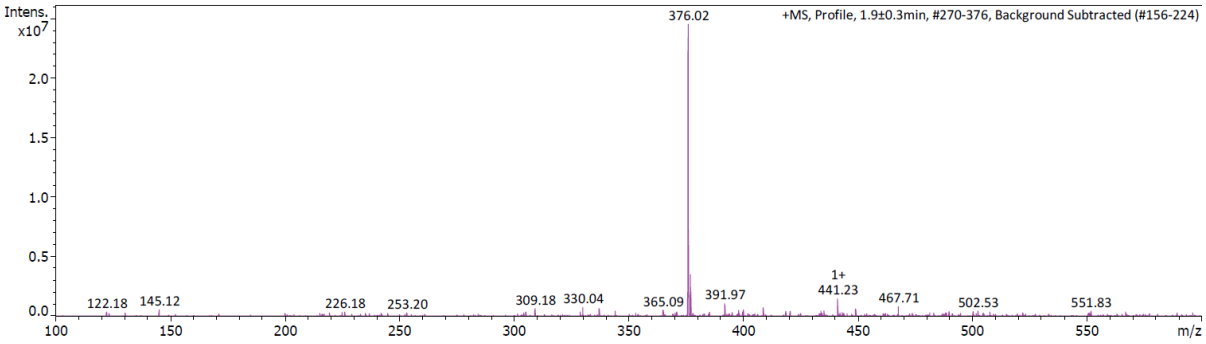

Figure S8. LR-MS (ESI+) of **ES4**.

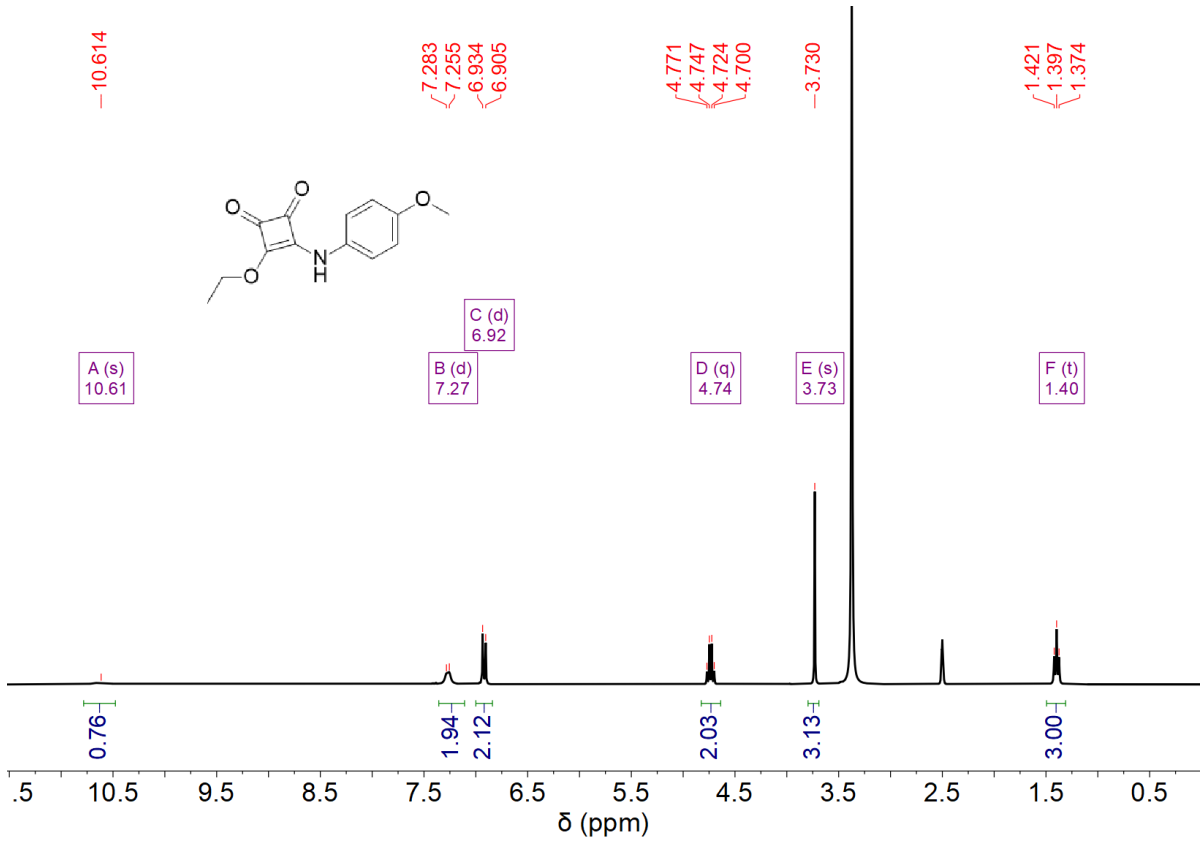

Figure S9. ^{1}H NMR (300 MHz, DMSO-d_6) spectrum of **ES5**.

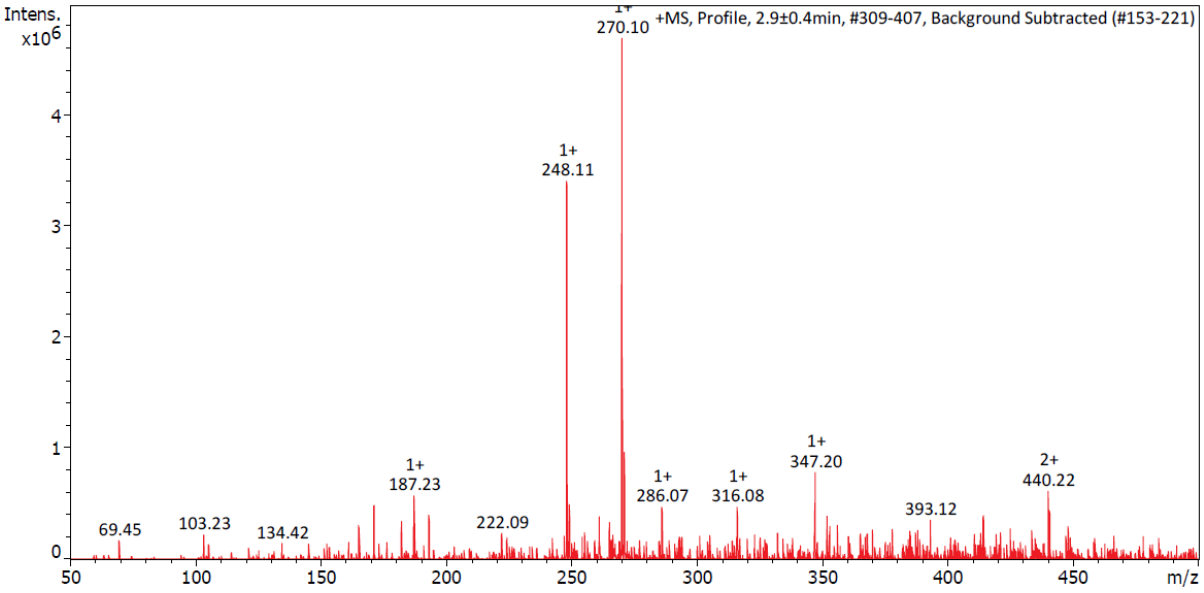

Figure S10. LR-MS (ESI+) of **ES5**.

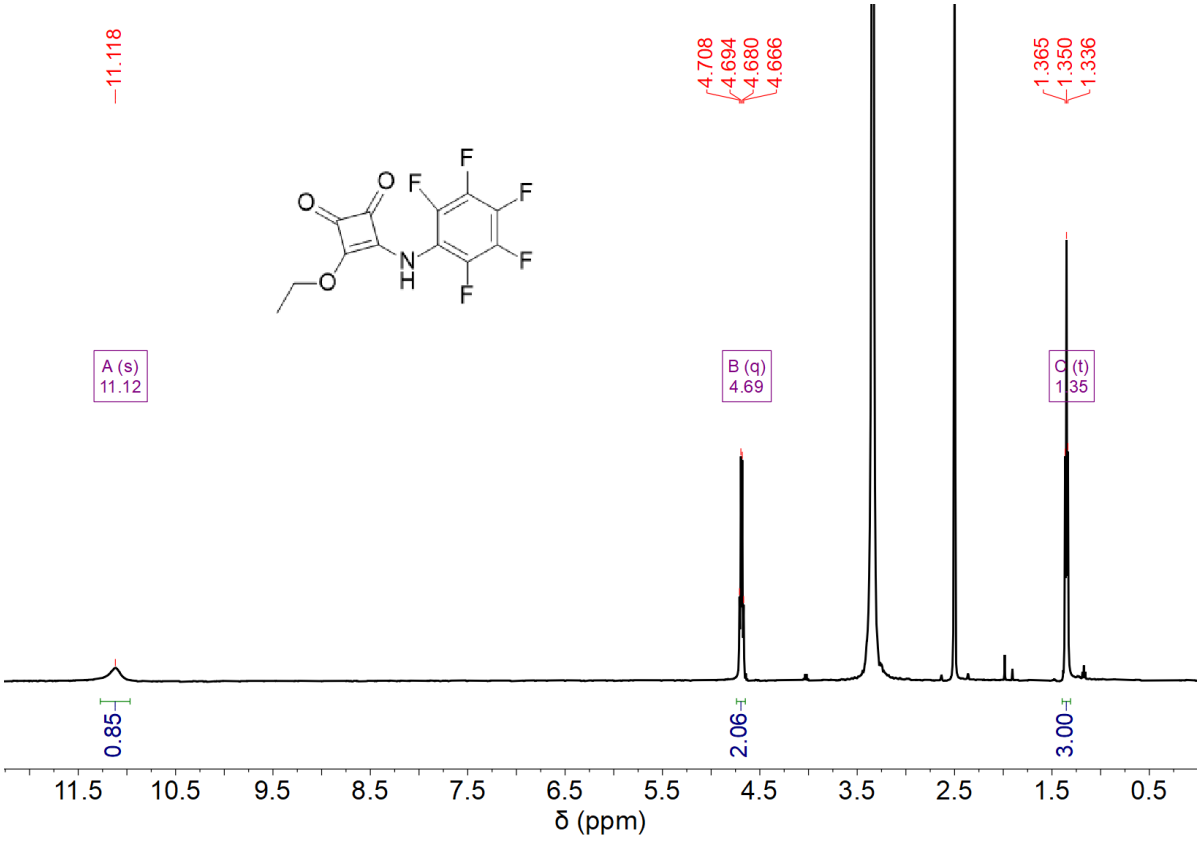

Figure S11. ^{1}H NMR (300 MHz, DMSO-d_6) spectrum of **ES6**.

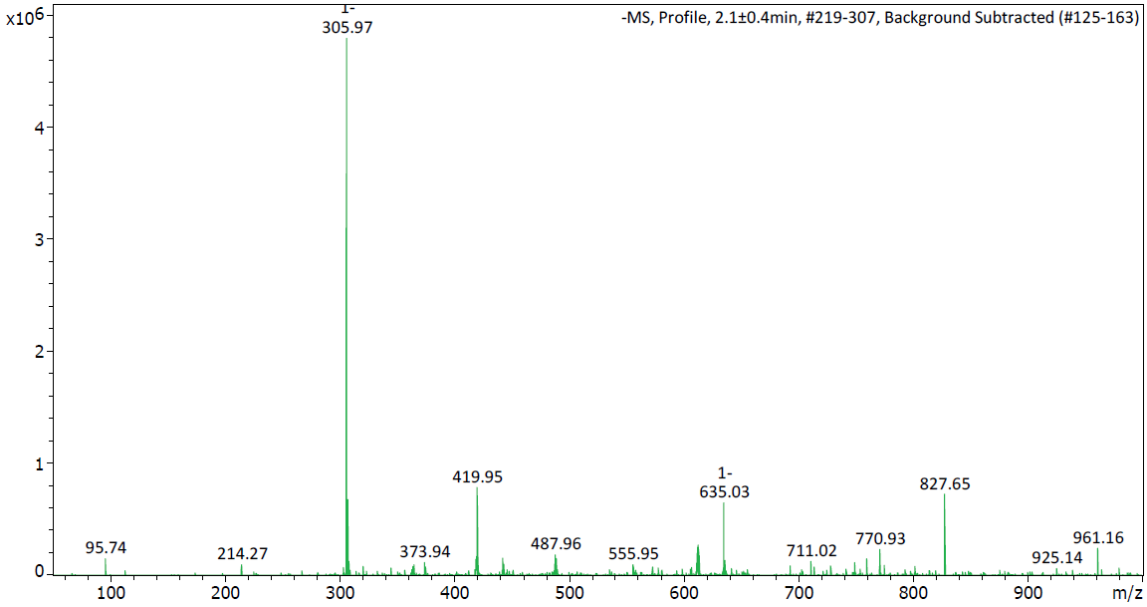

Figure S17. LR-MS (ESI−) of **ES6**.

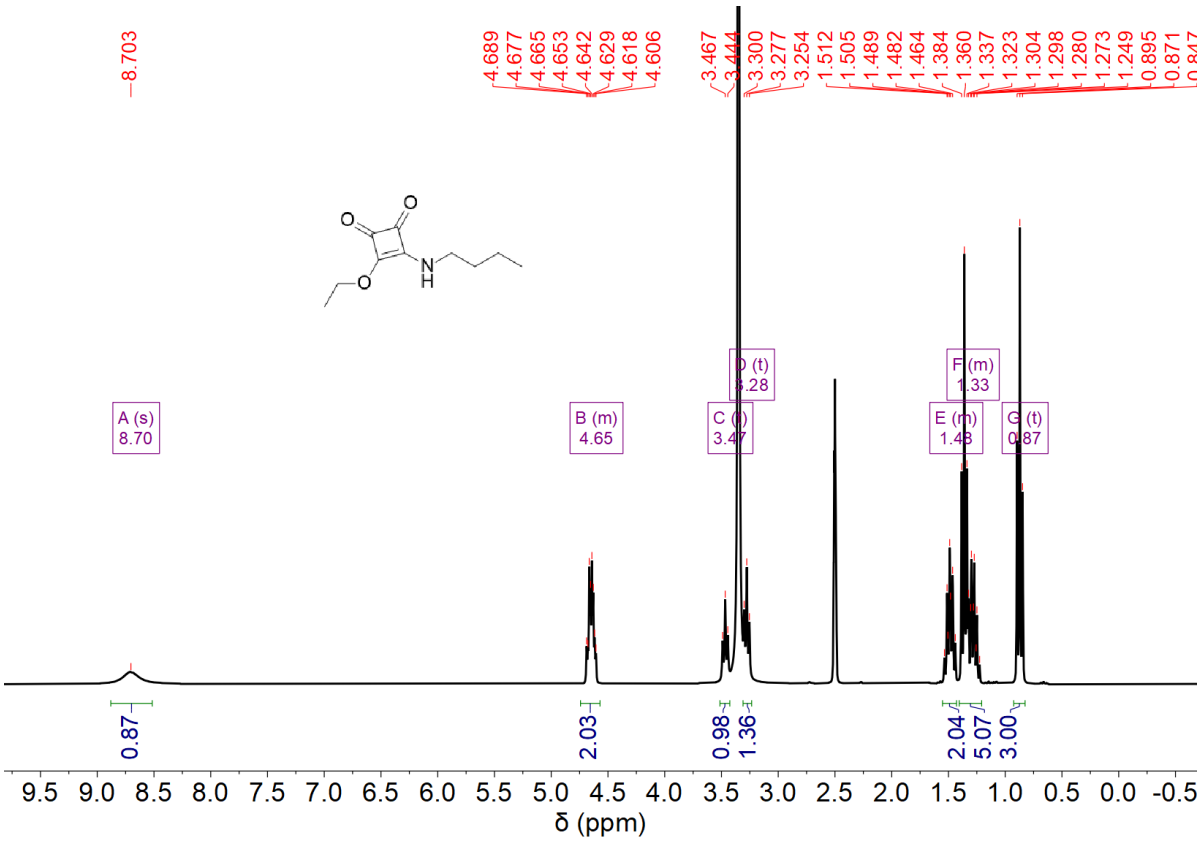

Figure S12. ^{1}H NMR (300 MHz, DMSO-d_6) spectrum of **ES7**.

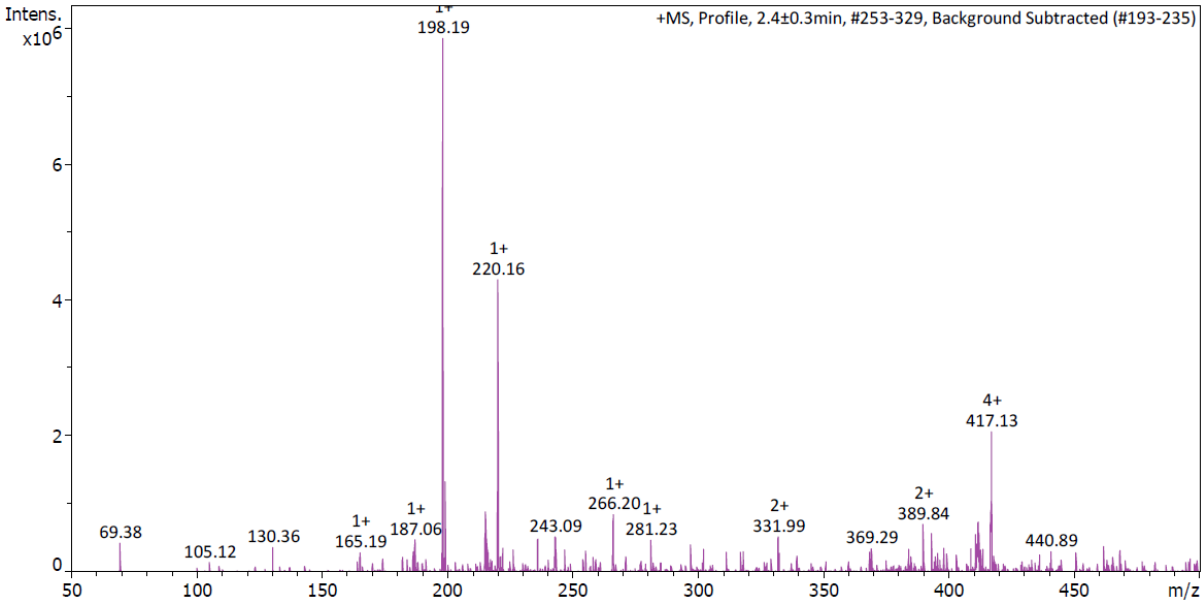

Figure S13. LR-MS (ESI+) of **ES7**.

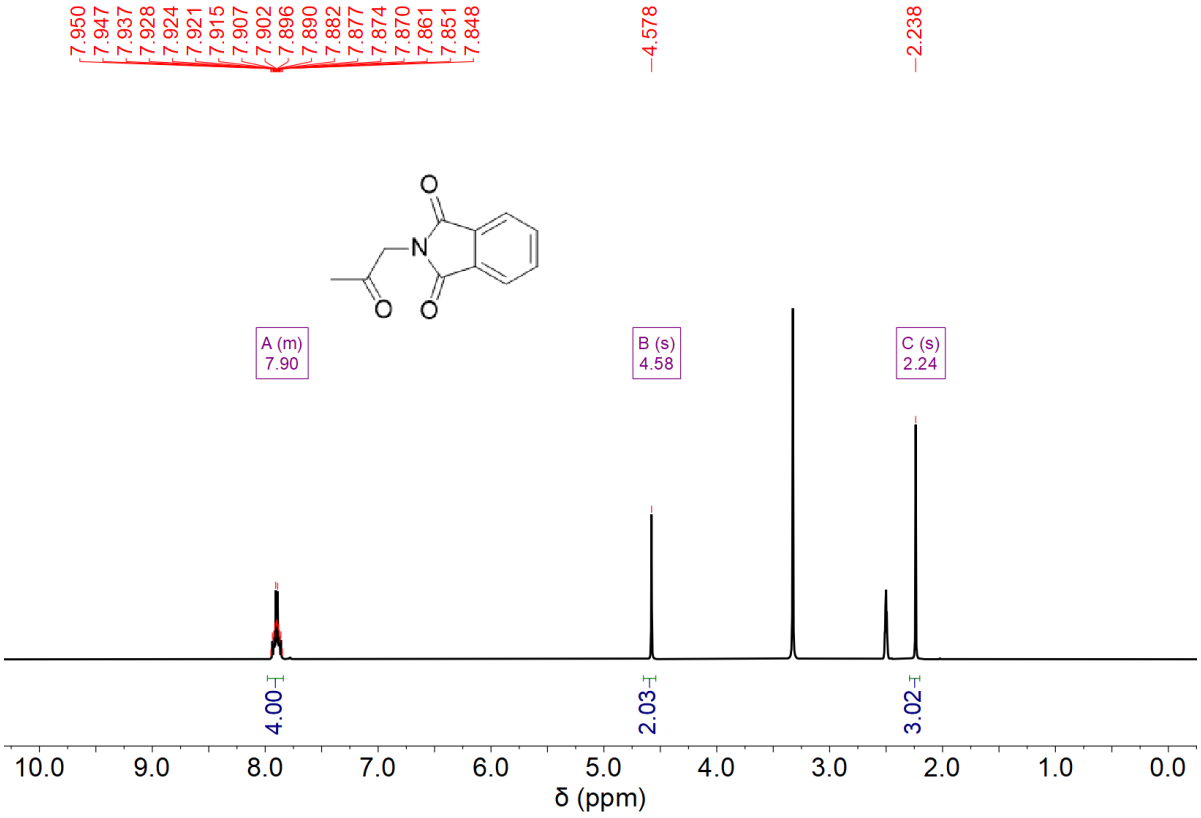

Figure S14. ^{1}H NMR (300 MHz, DMSO-d_6) spectrum of **I1**.

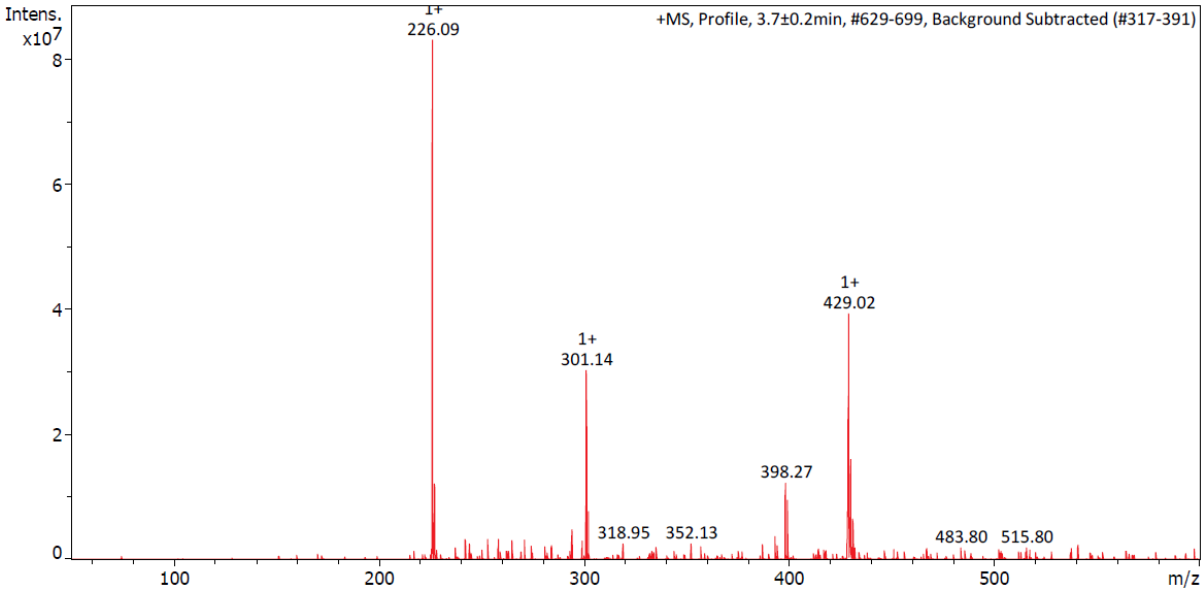

Figure S15. LR-MS (ESI+) of **I1**.

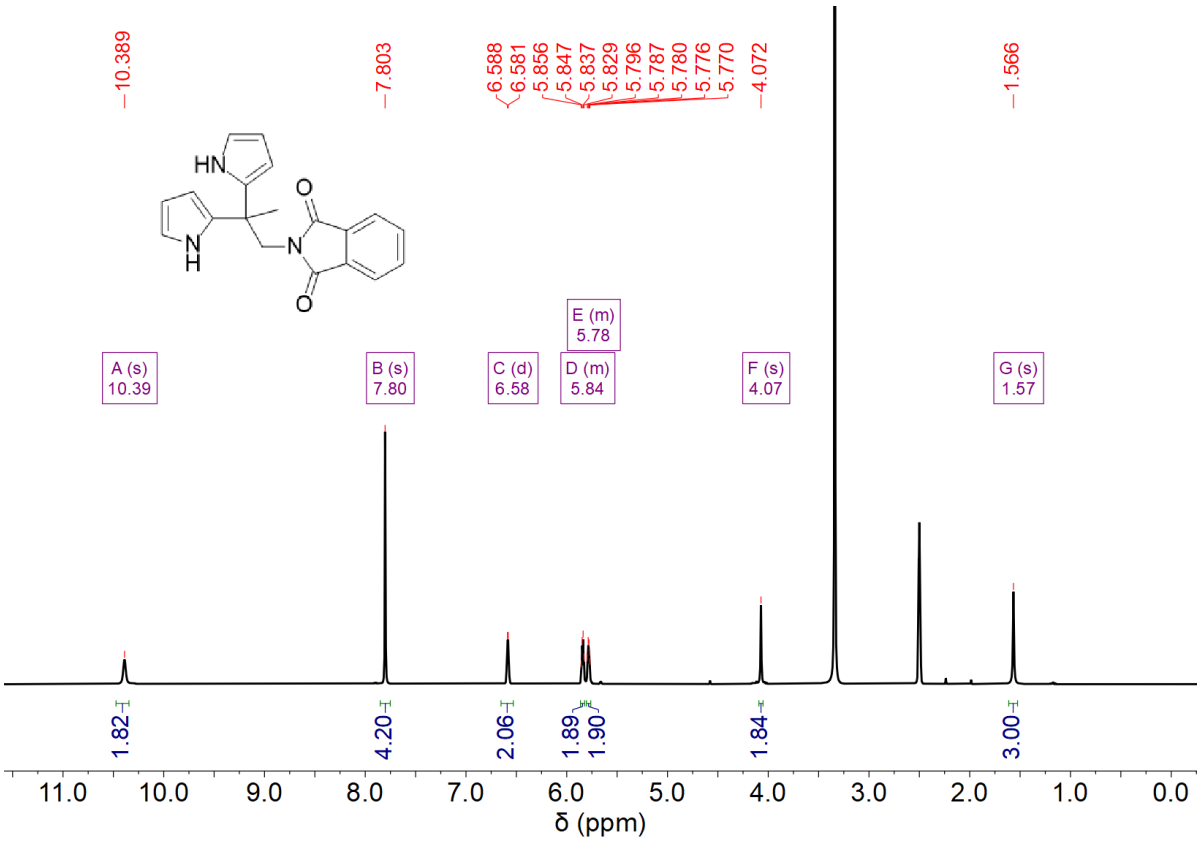

Figure S16. ^{1}H NMR (300 MHz, DMSO-d_6) spectrum of **I2**.

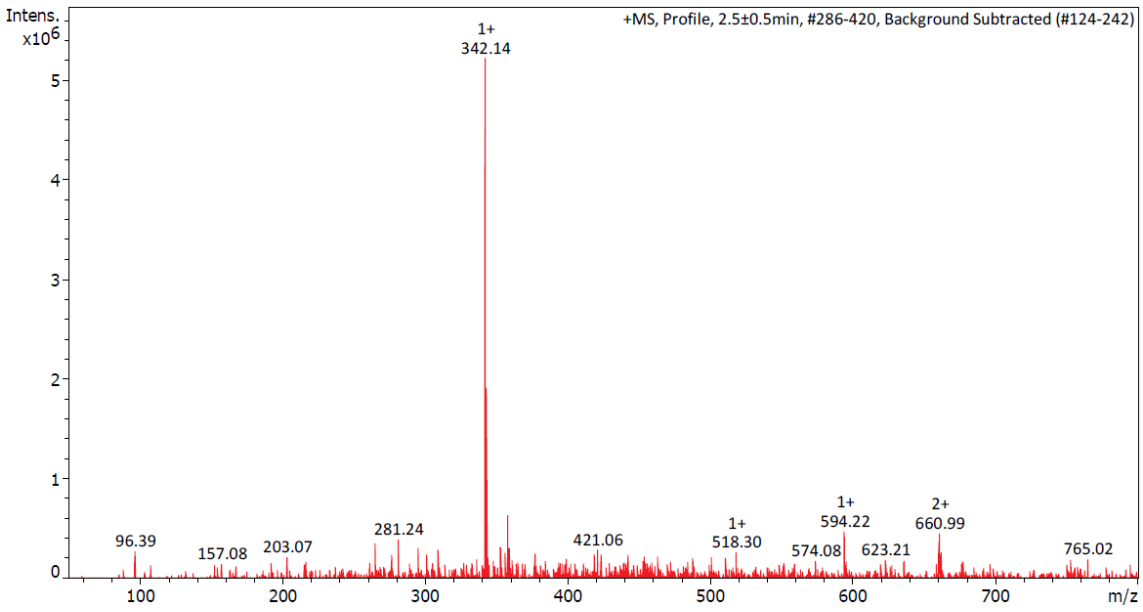

Figure S17. LR-MS (ESI+) of **I2**.

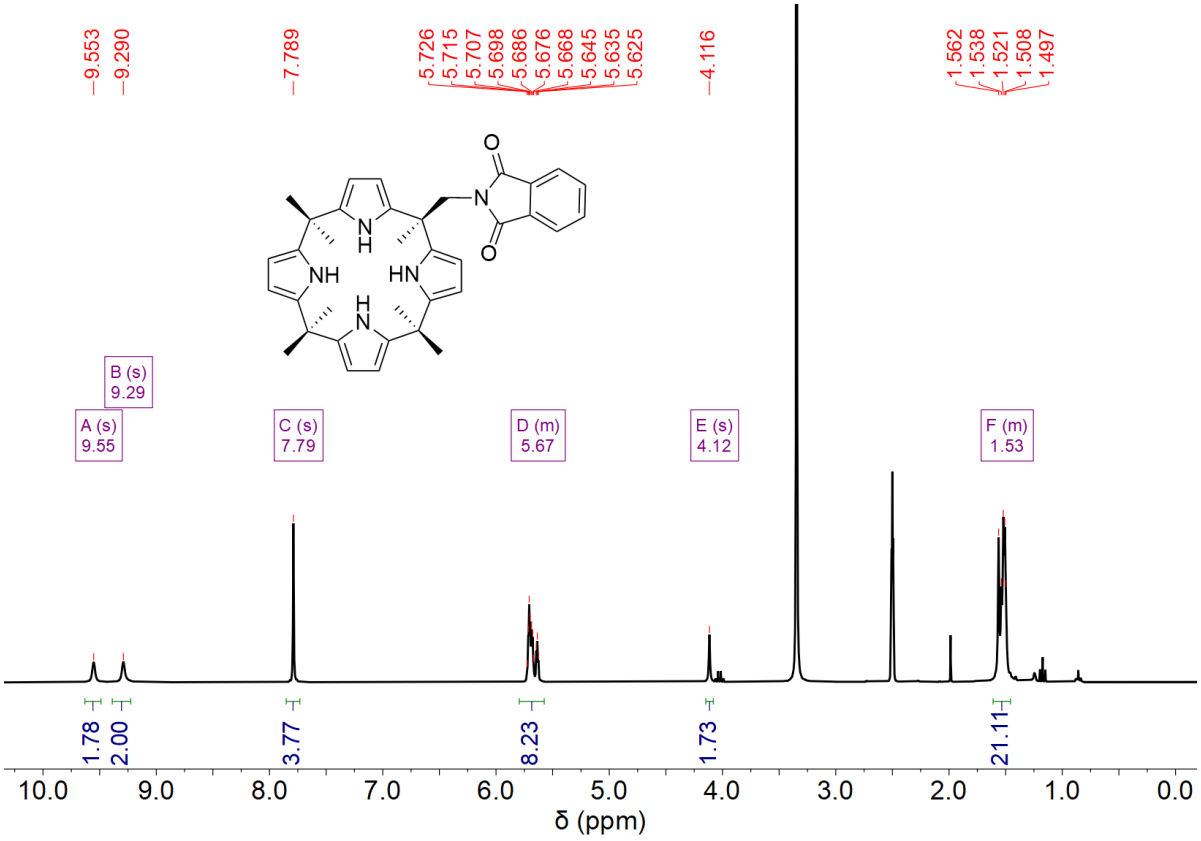

Figure S18. ^{1}H NMR (300 MHz, DMSO-d_6) spectrum of **I3**.

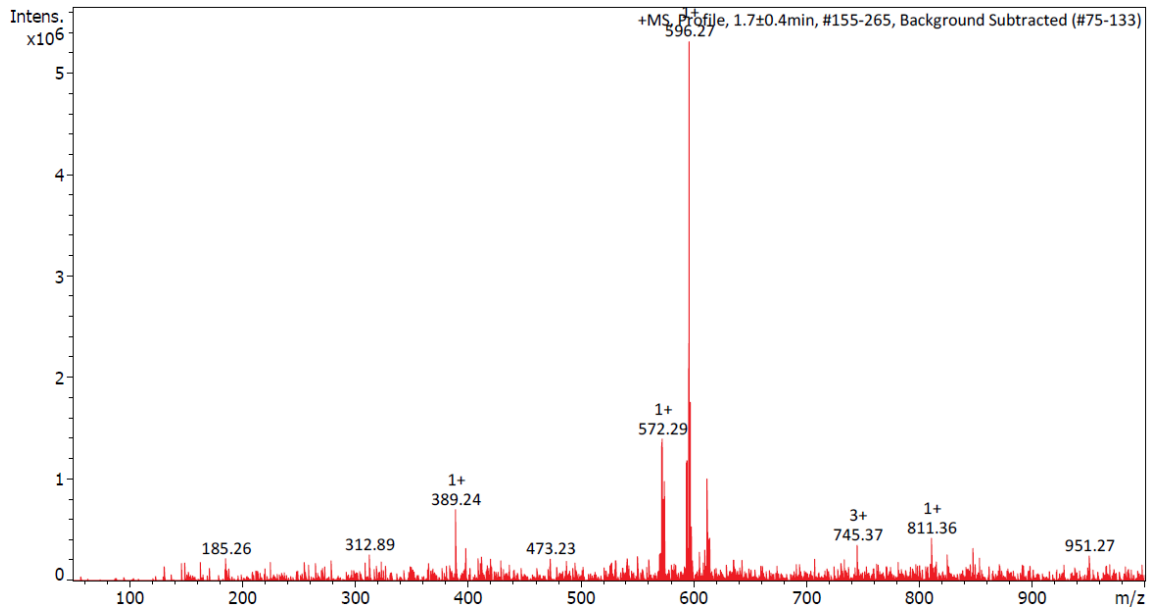

Figure S19. LR-MS (ESI+) of **I3**.

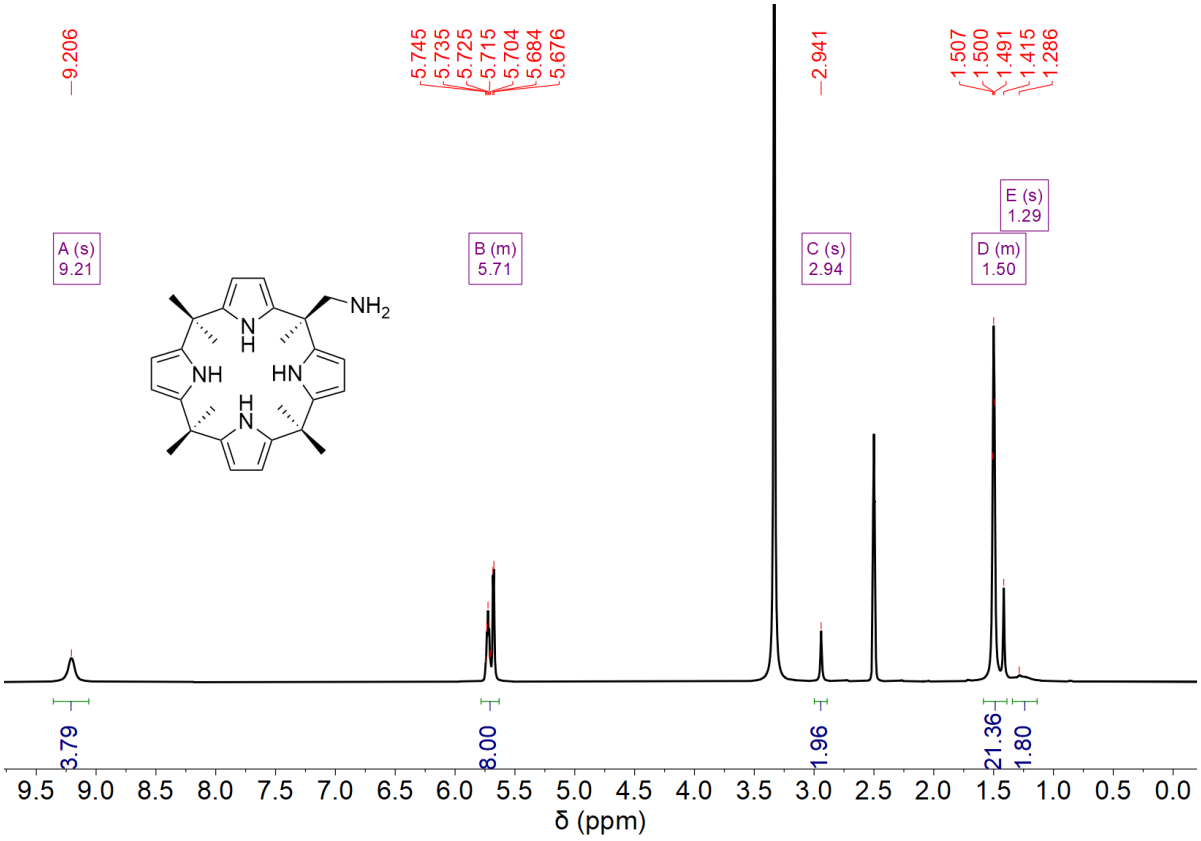

Figure S20. ^{1}H NMR (300 MHz, DMSO-d_6) spectrum of **I4**.

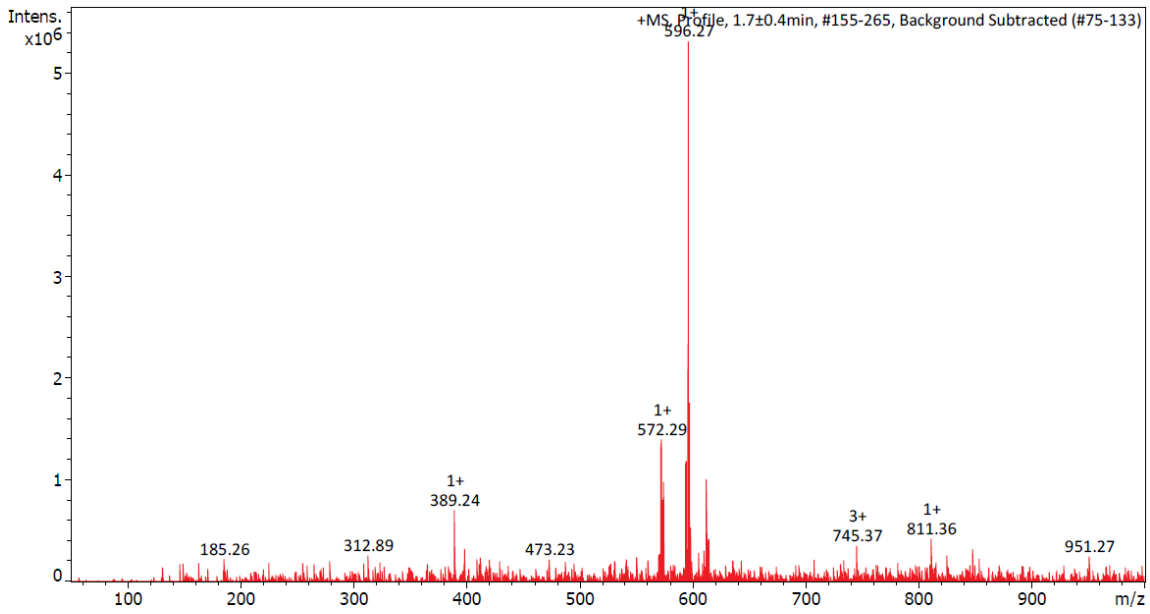

Figure S21. LR-MS (ESI+) of **I4**.

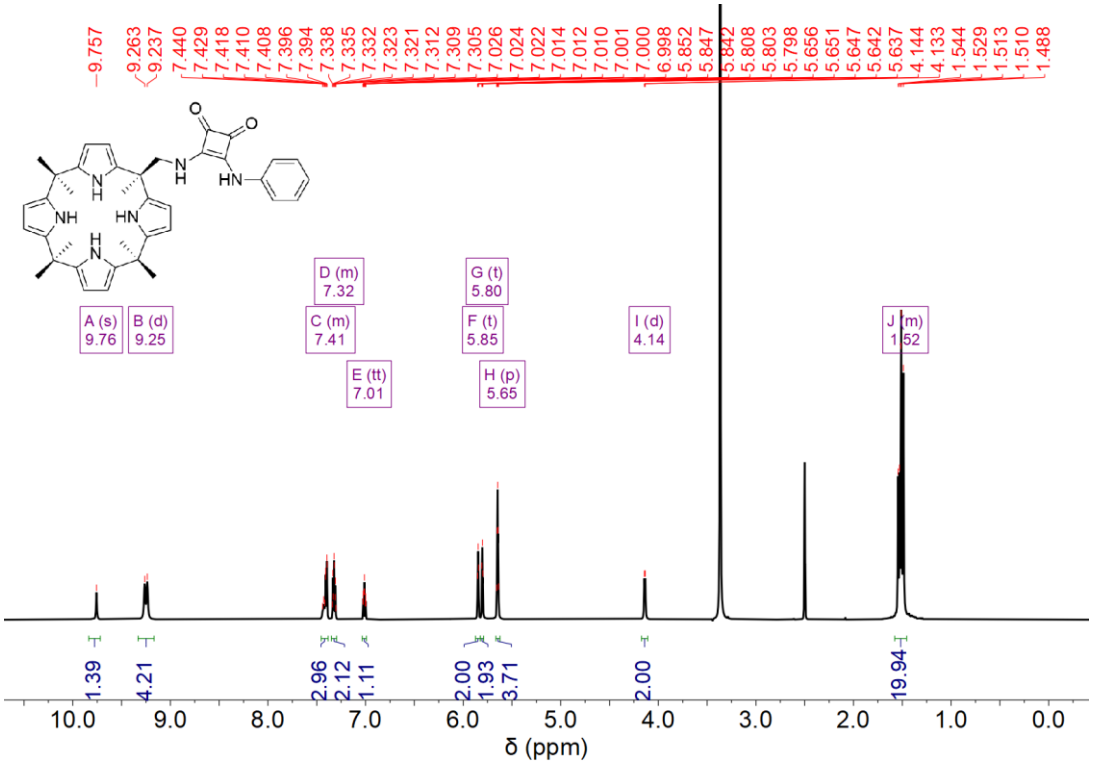

Figure S22. ^{1}H NMR (600 MHz, DMSO-d_6) spectrum of **1**.

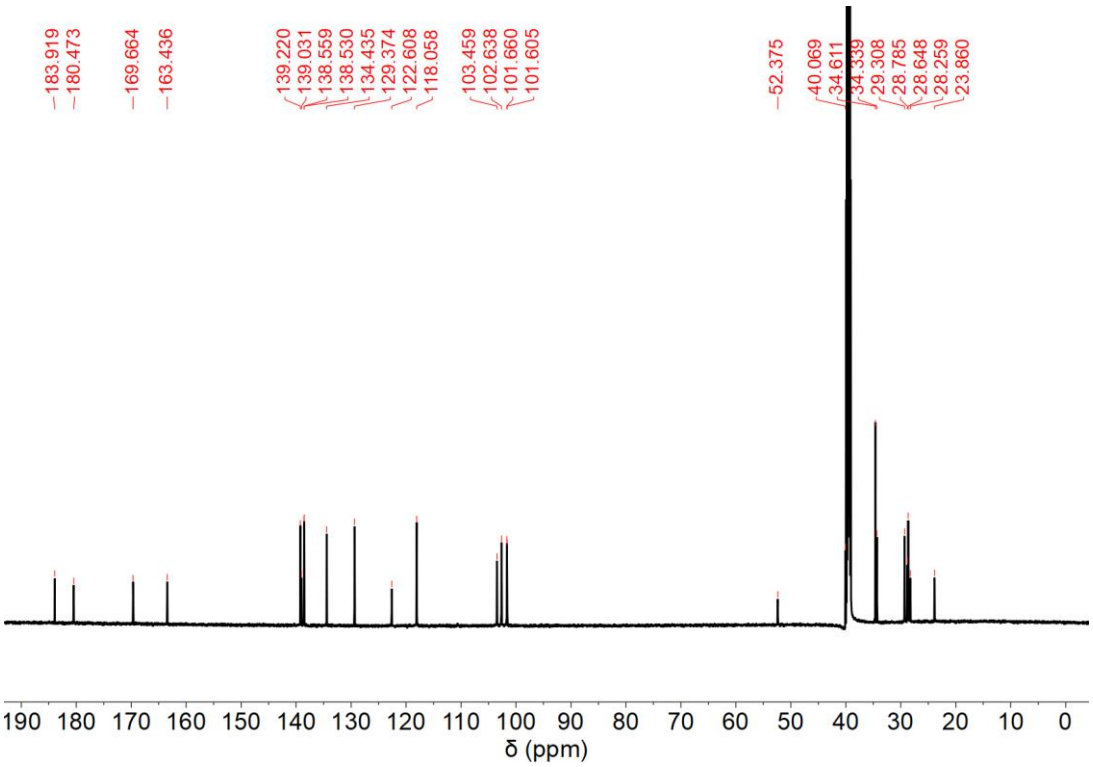

Figure S23. ^{13}C NMR (151 MHz, DMSO-d_6) spectrum of **1**.

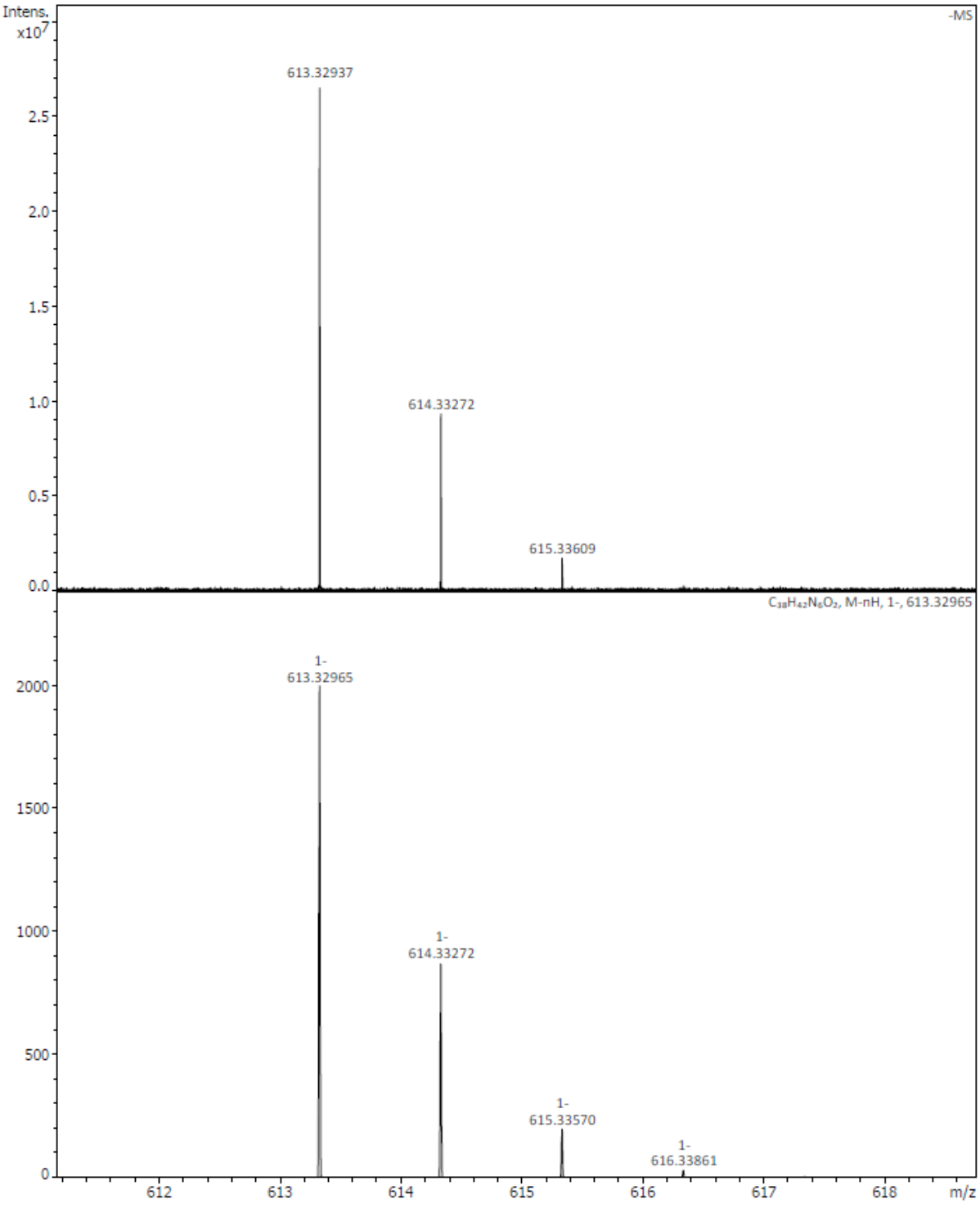

Figure S24. HR-MS (ESI+) of **1**.

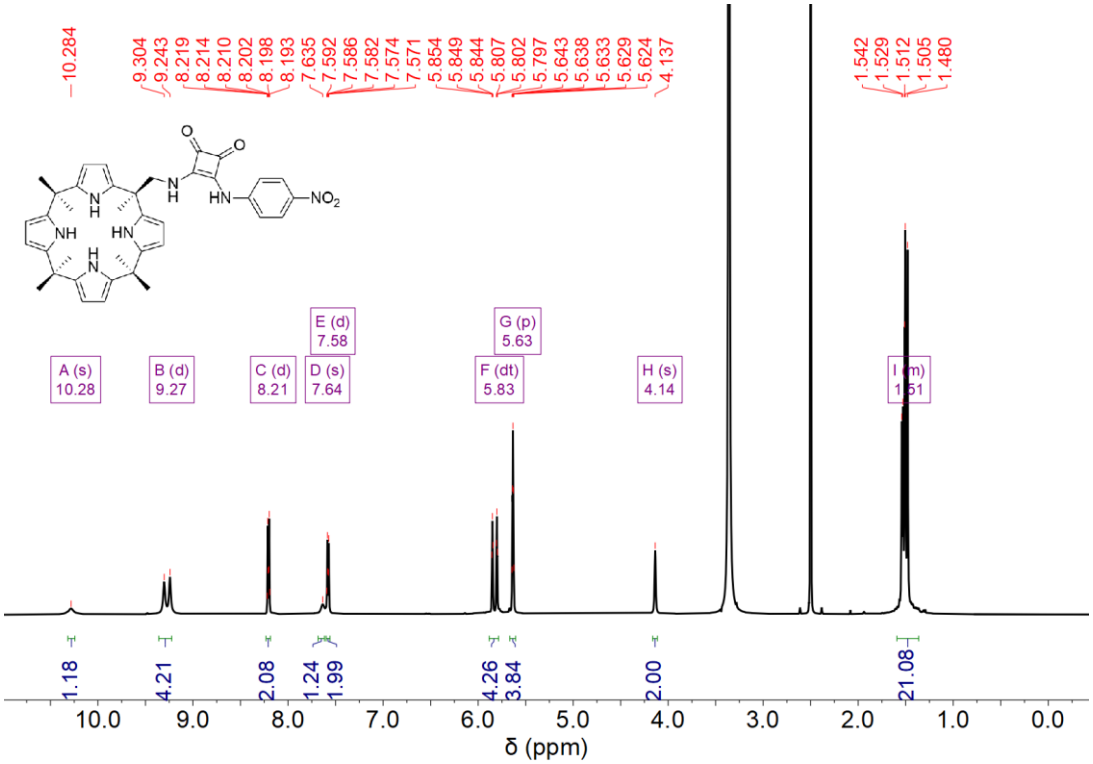

Figure S25. ^{1}H NMR (600 MHz, DMSO-d_6) spectrum of **2**.

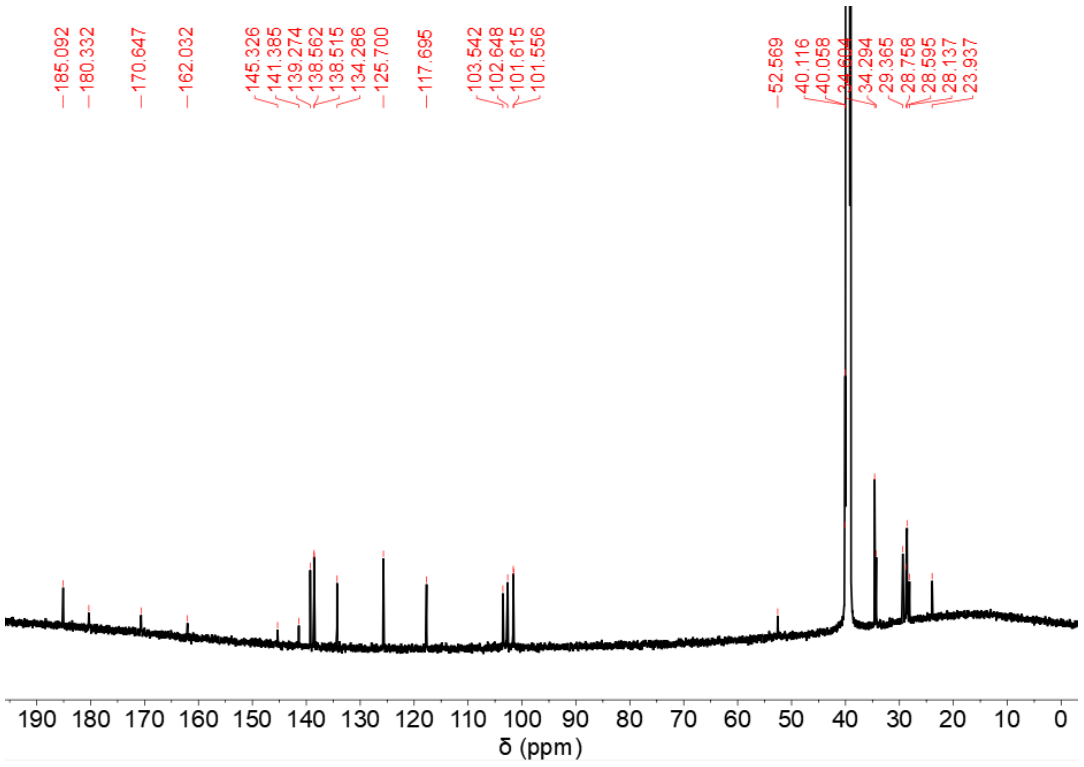

Figure S26. ^{13}C NMR (151 MHz, DMSO-d_6) spectrum of **2**.

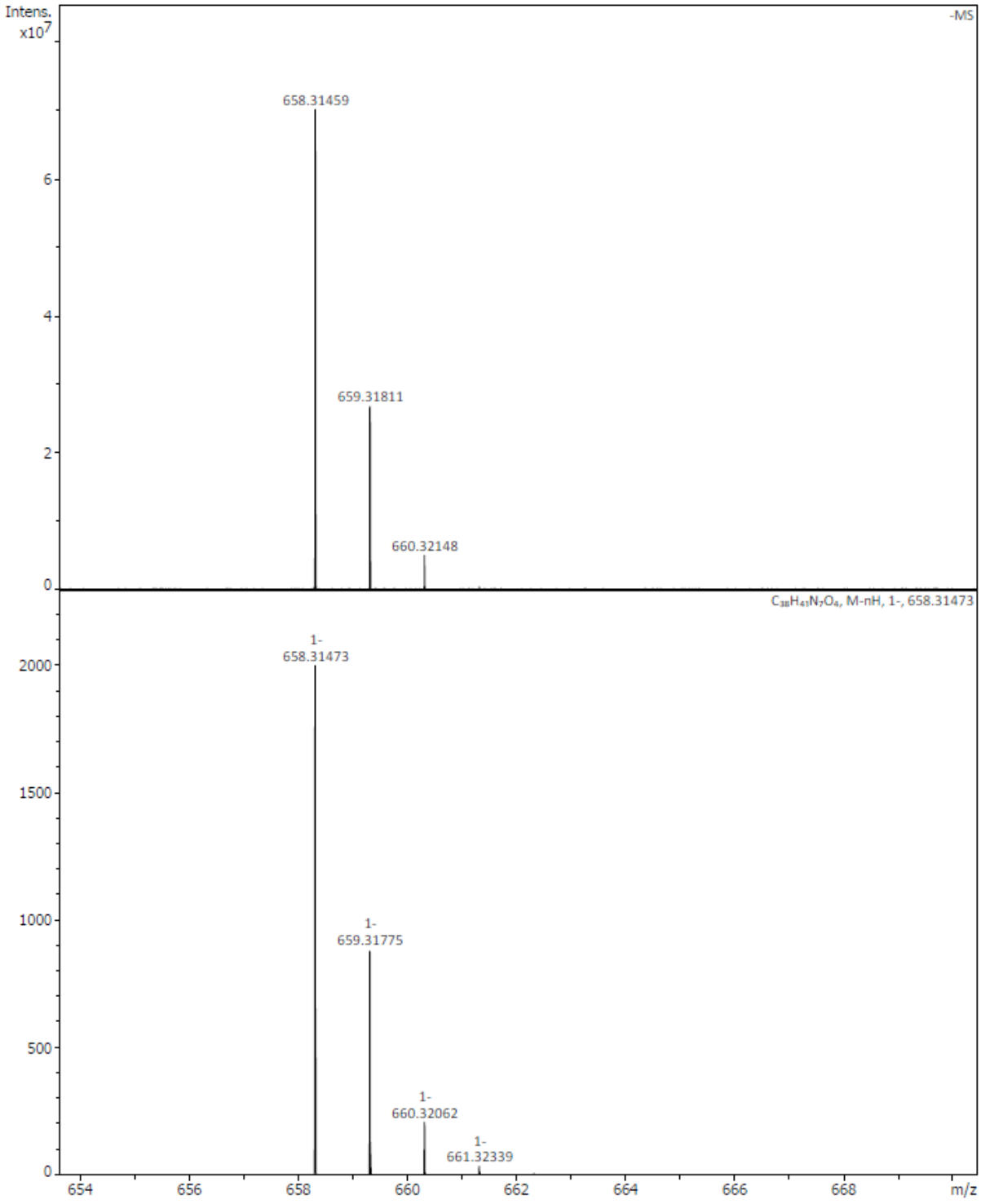

Figure S27. HR-MS (ESI−) of **2**.

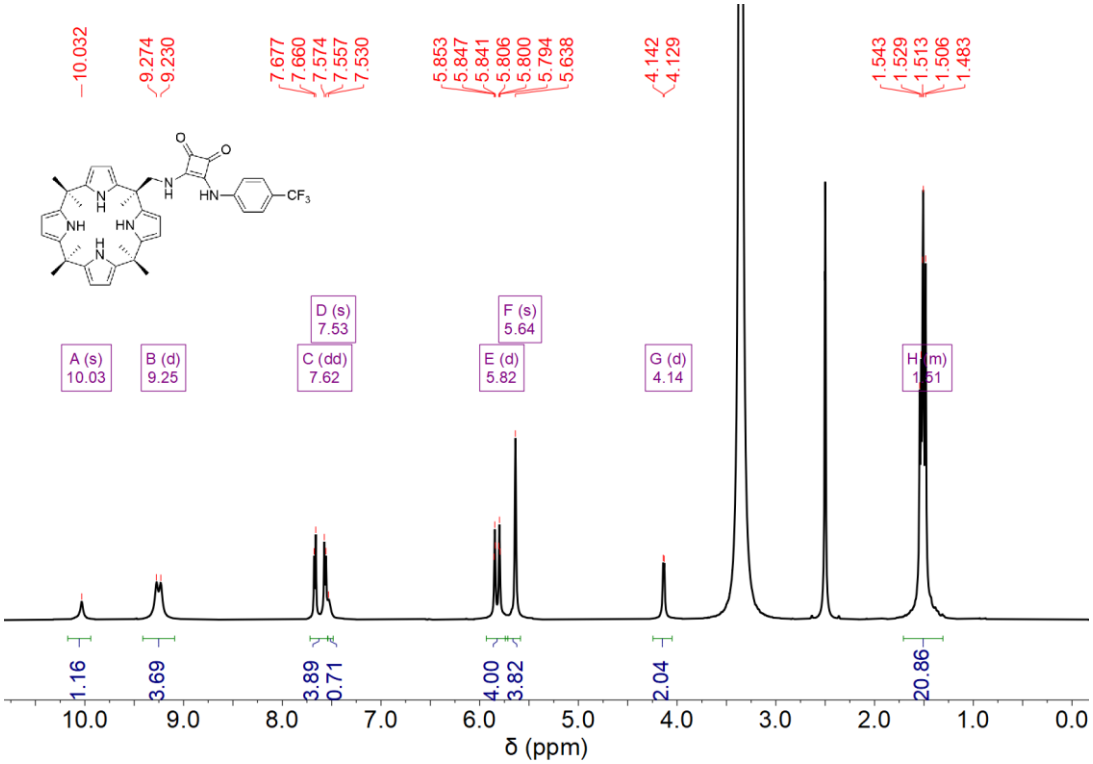

Figure S28. ^{1}H NMR (500 MHz, DMSO-d_6) spectrum of **3**.

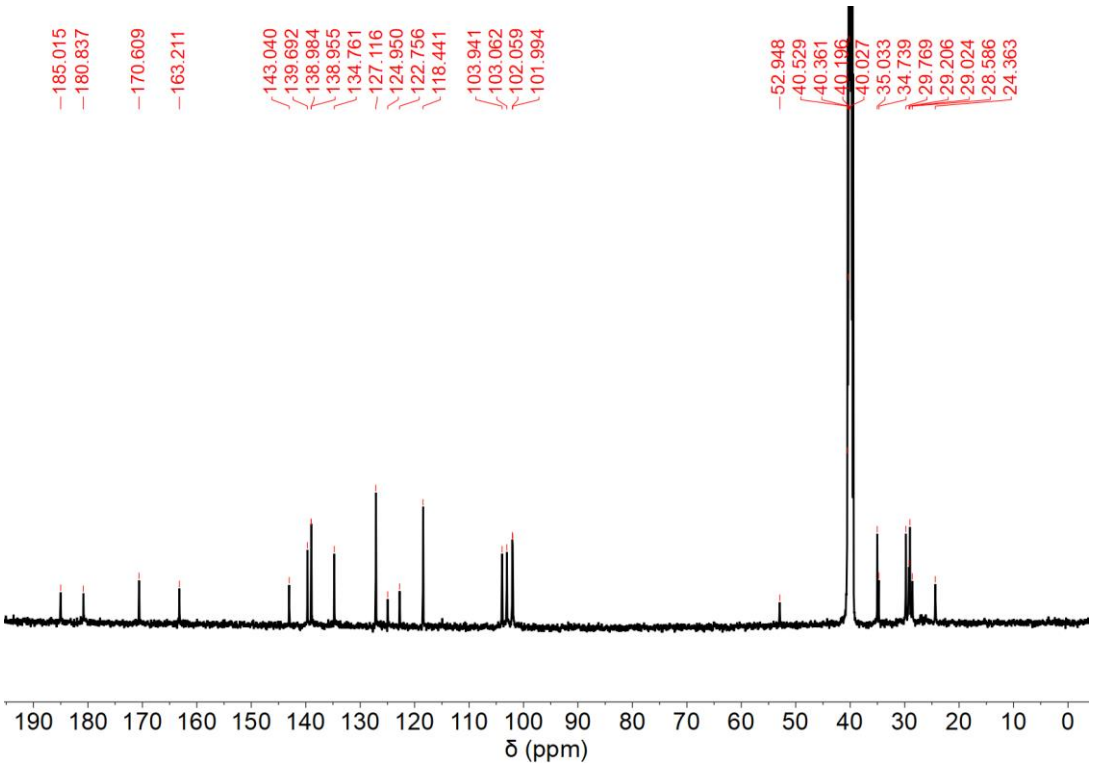

Figure S29. ^{13}C NMR (126 MHz, DMSO-d_6) spectrum of **3**.

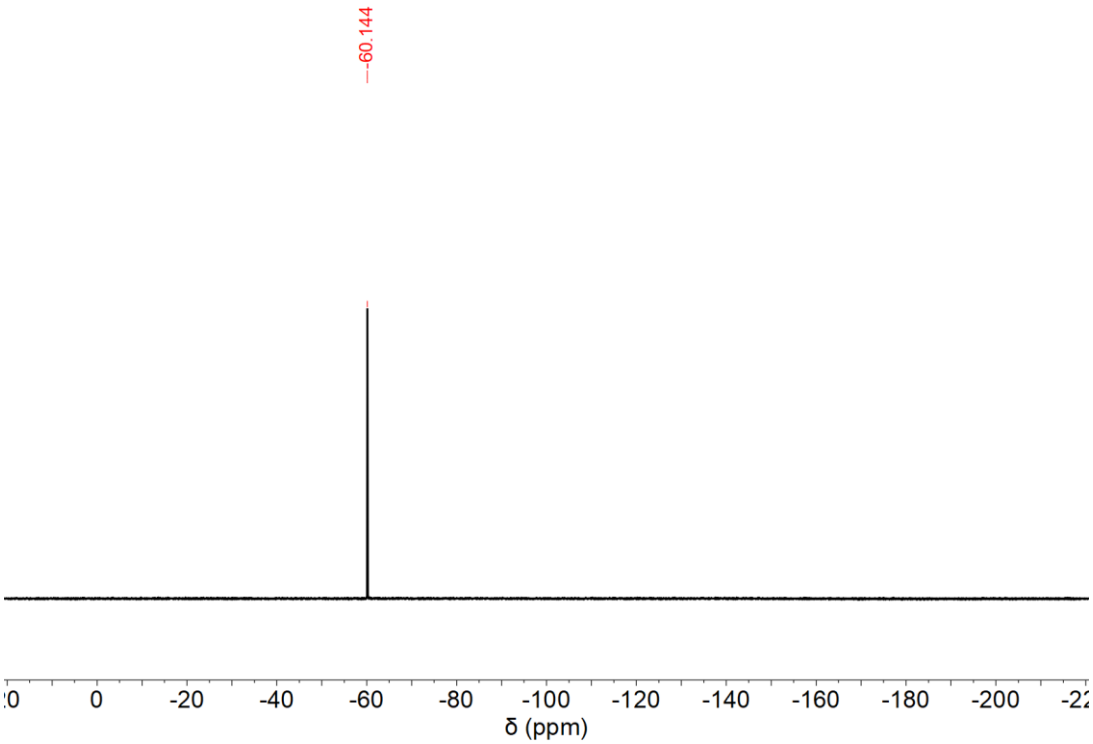

Figure S30. ^{19}F NMR (471 MHz, DMSO-d_6) spectrum of **3**.

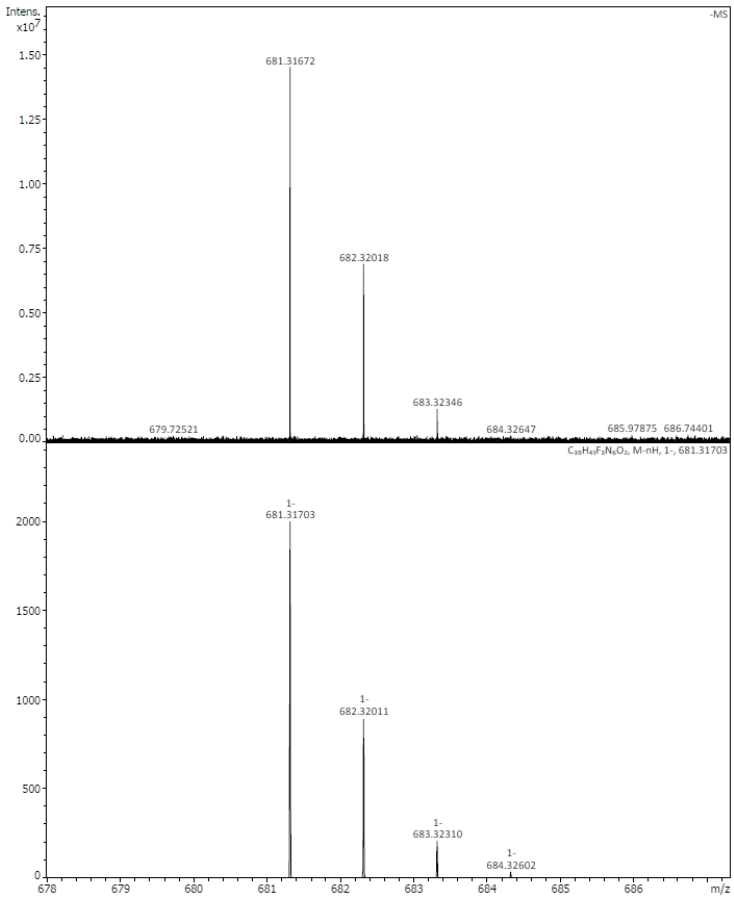

Figure S31. HR-MS (ESI−) of **3**.

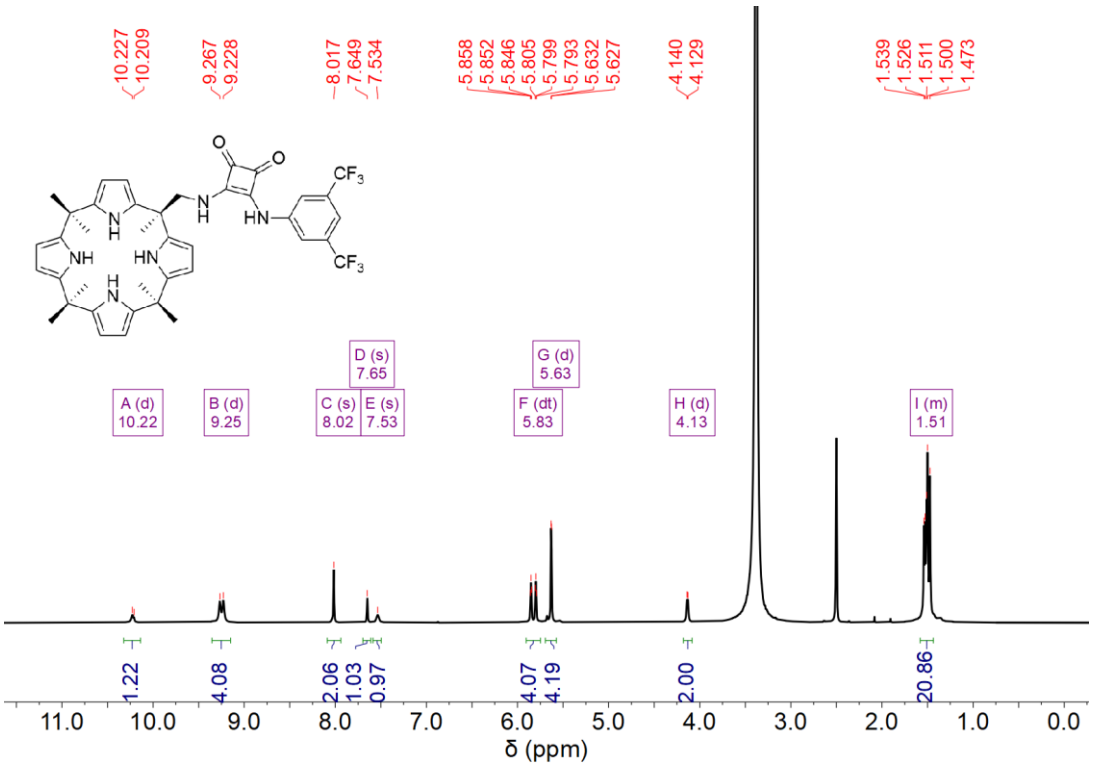

Figure S32. ^{1}H NMR (500 MHz, DMSO-d_6) spectrum of **4**.

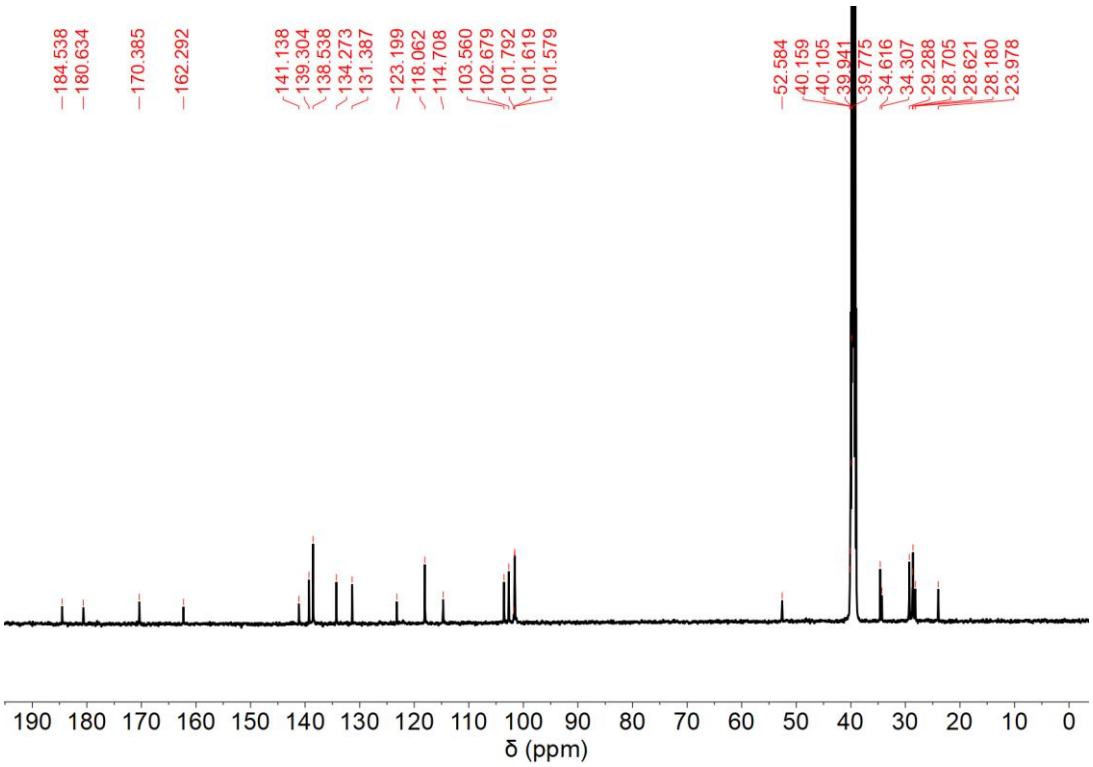

Figure S33. ^{13}C NMR (126 MHz, DMSO-d_6) spectrum of **4**.

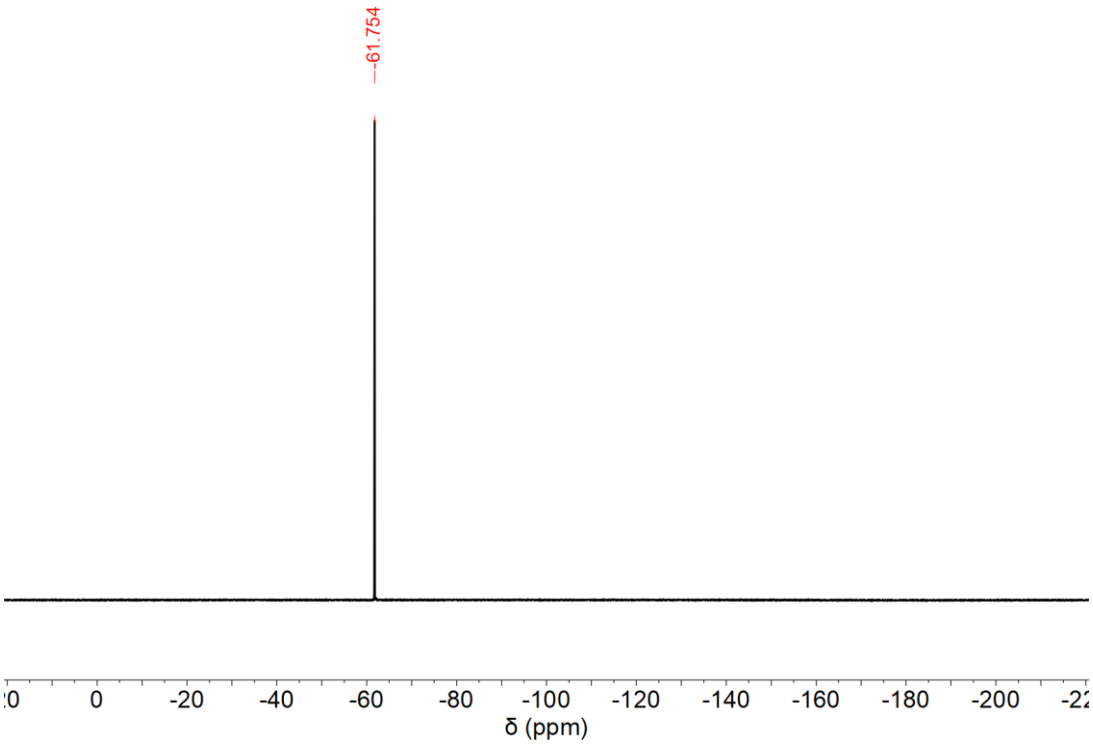

Figure S34. ^{19}F NMR (471 MHz, DMSO-d_6) spectrum of **4**.

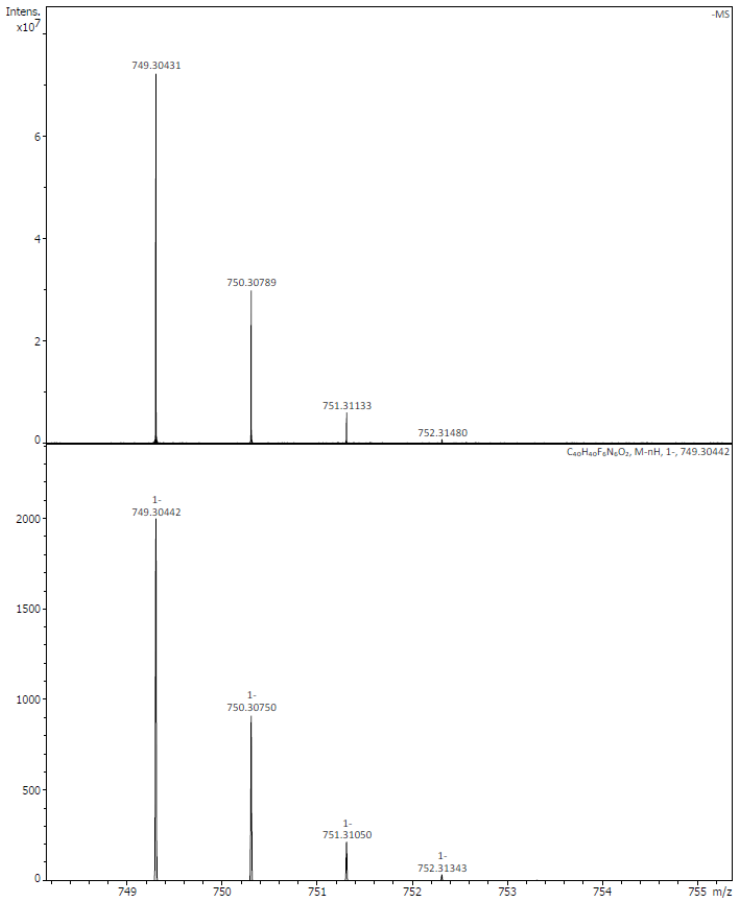

Figure S35. HR-MS (ESI−) of **4**.

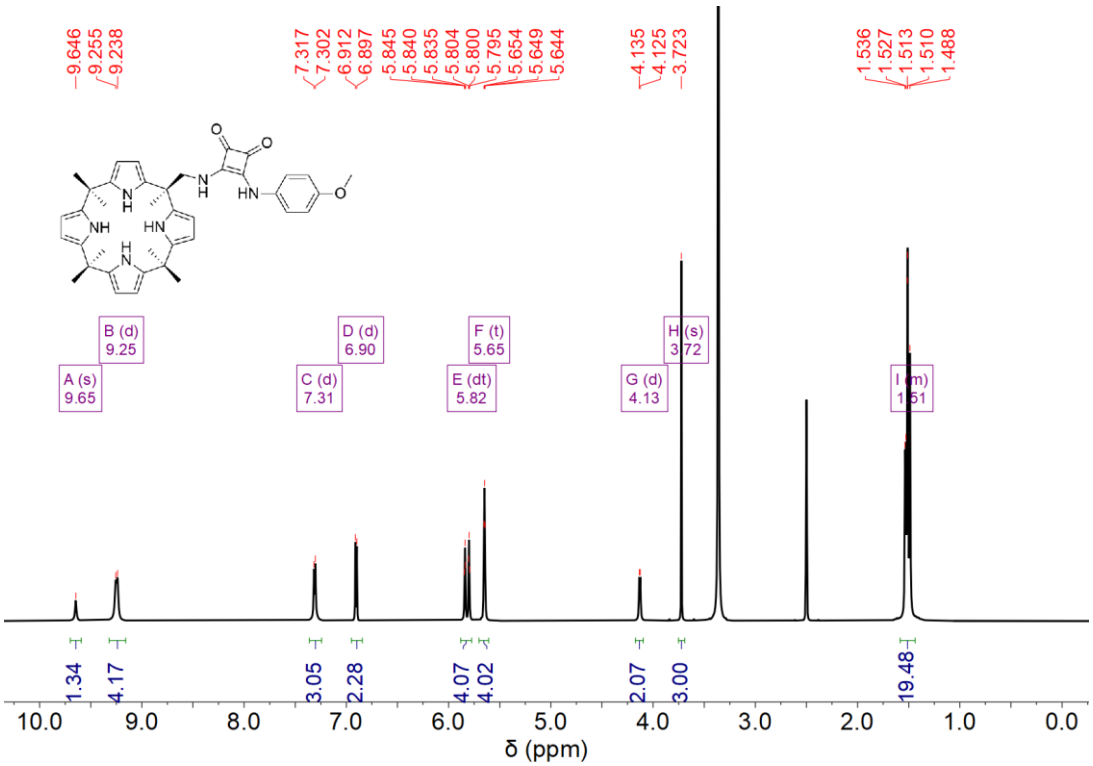

Figure S36. ^{1}H NMR (600 MHz, DMSO-d_6) spectrum of **5**.

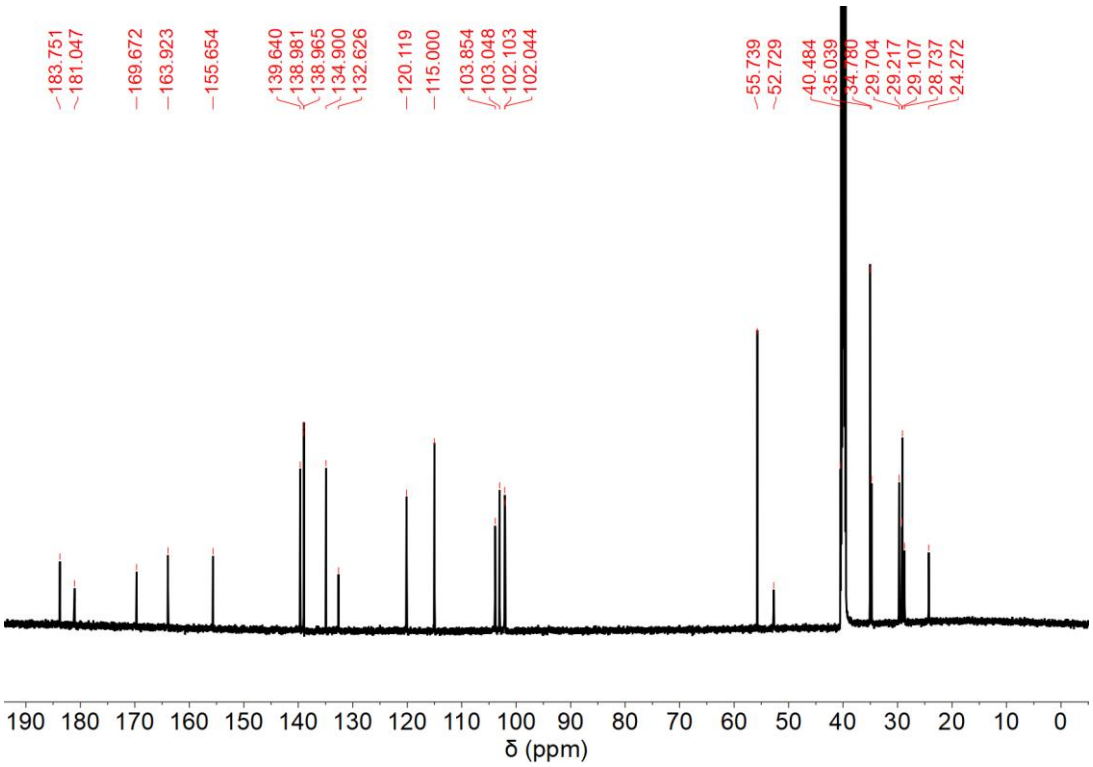

Figure S37. ^{13}C NMR (151 MHz, DMSO-d_6) spectrum of **5**.

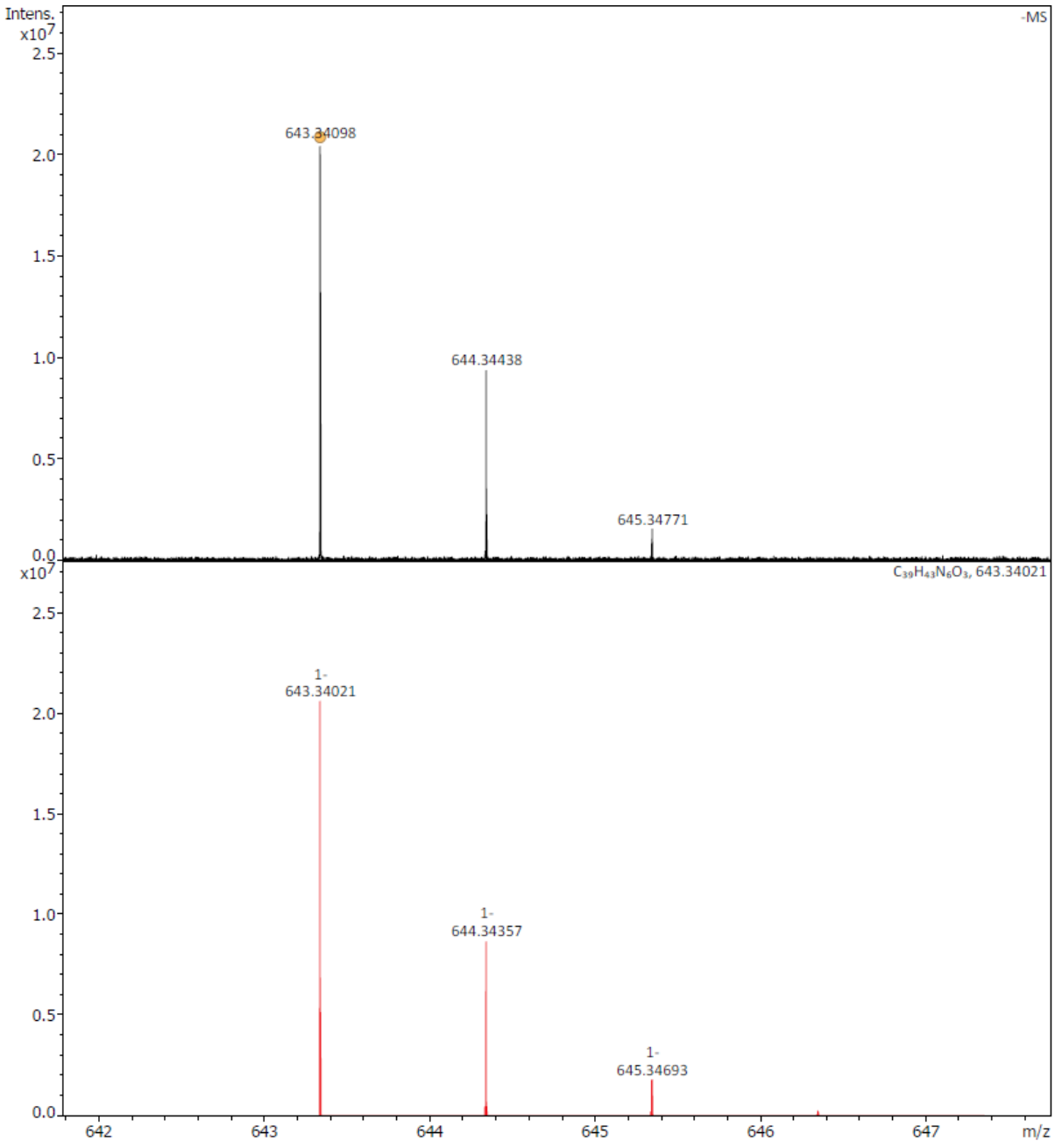

Figure S38. HR-MS (ESI−) of **5**.

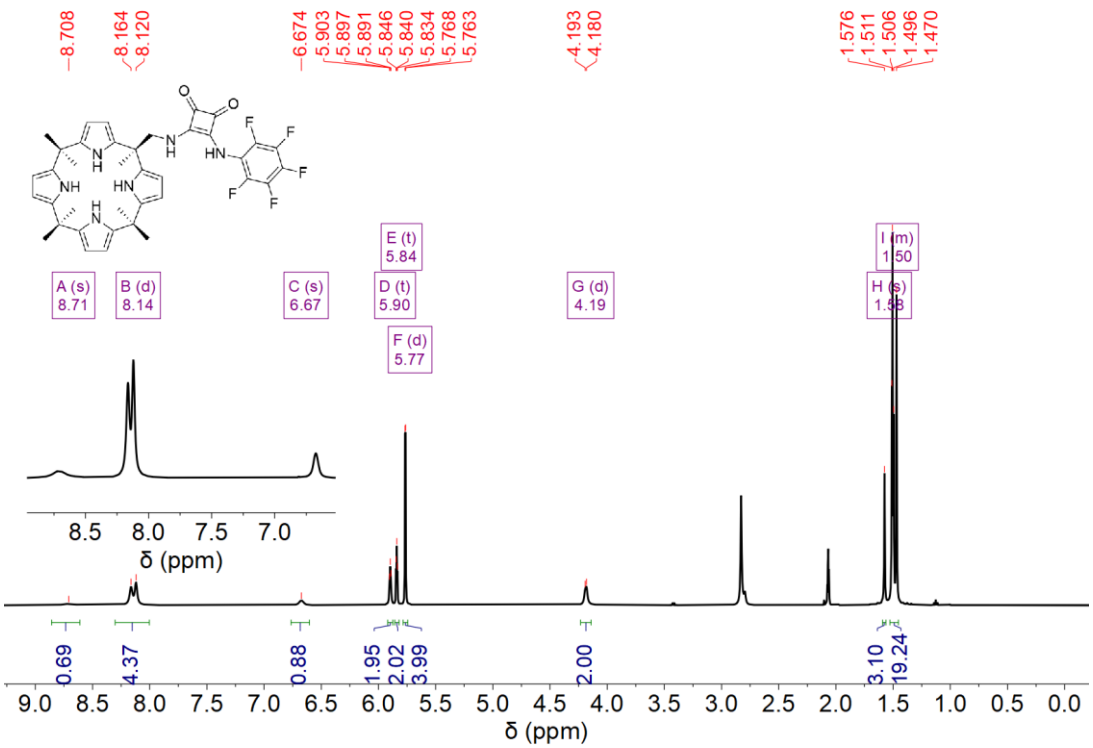

Figure S39. ^{1}H NMR (500 MHz, acetone-d_6) spectrum of **6**.

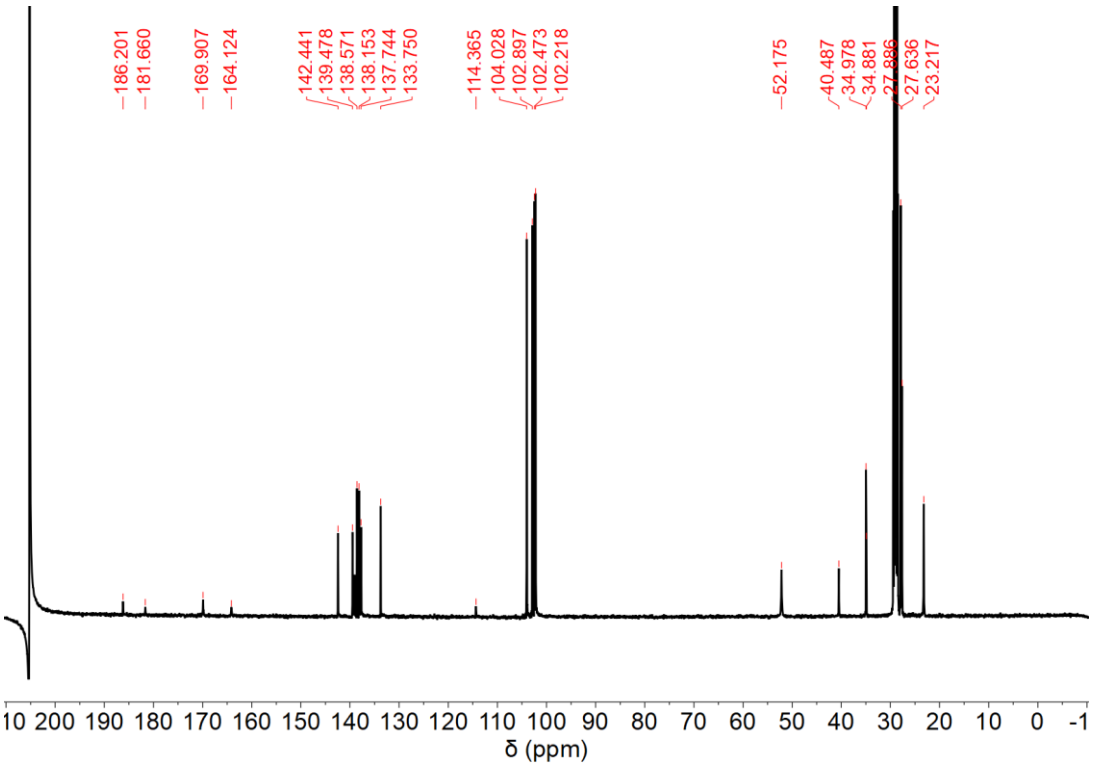

Figure S40. ^{13}C NMR (126 MHz, acetone-d_6) spectrum of **6**.

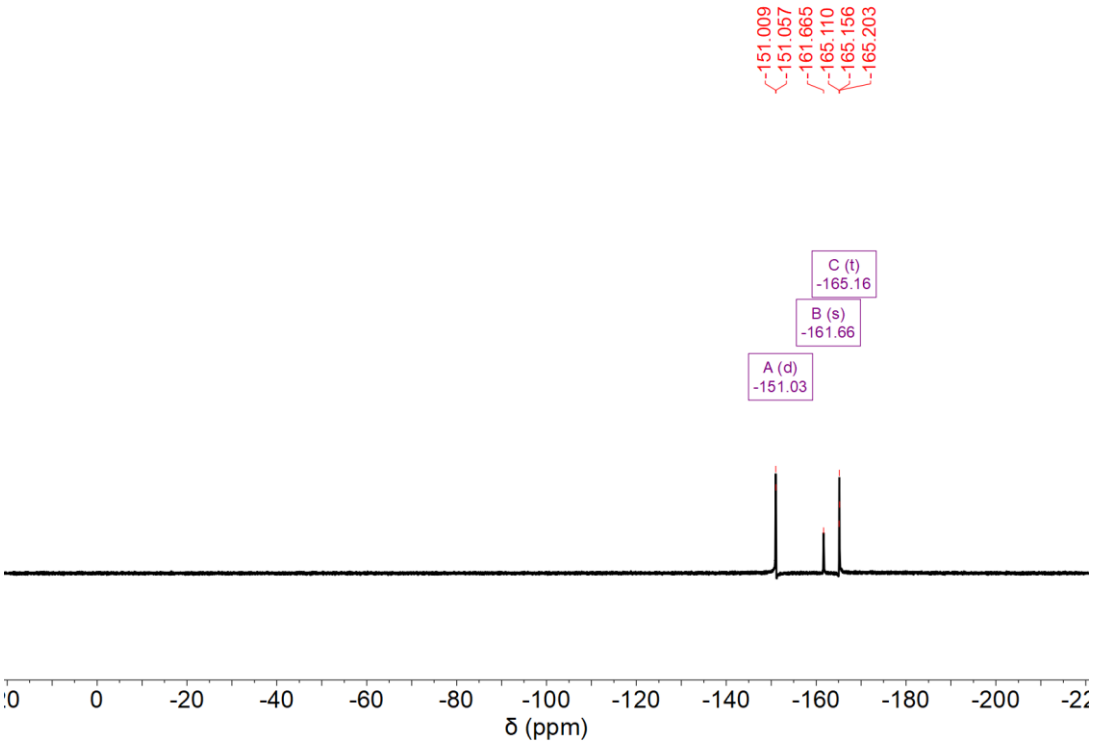

Figure S41. ^{19}F NMR (471 MHz, acetone-d_6) spectrum of **6**.

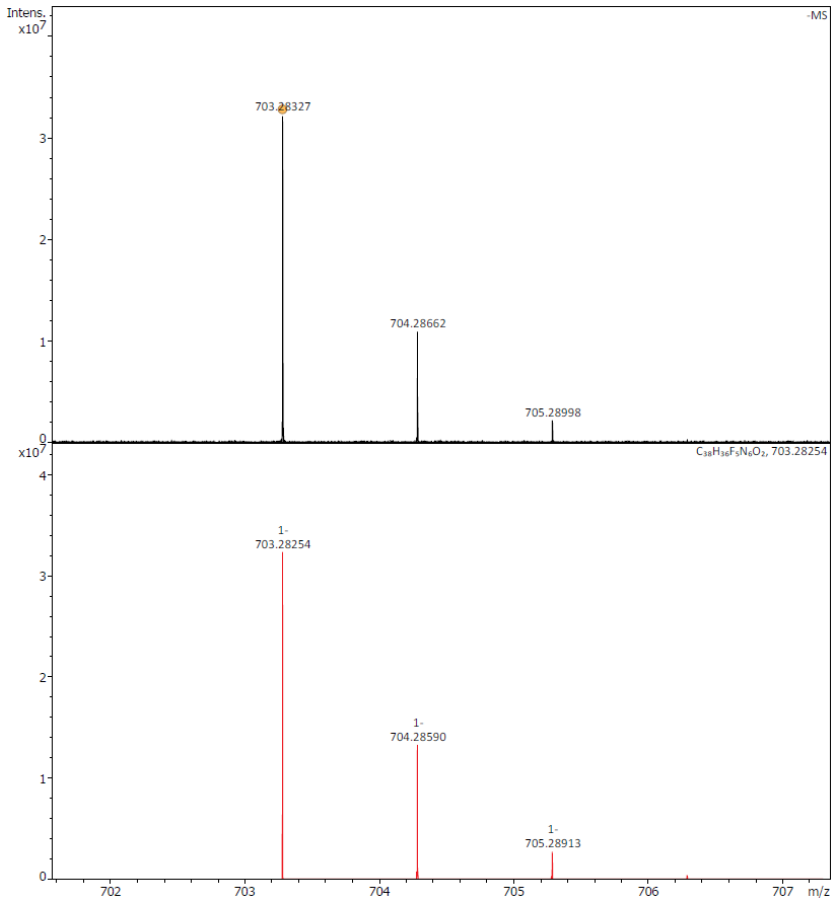

Figure S42. HR-MS (ESI−) of **6**.

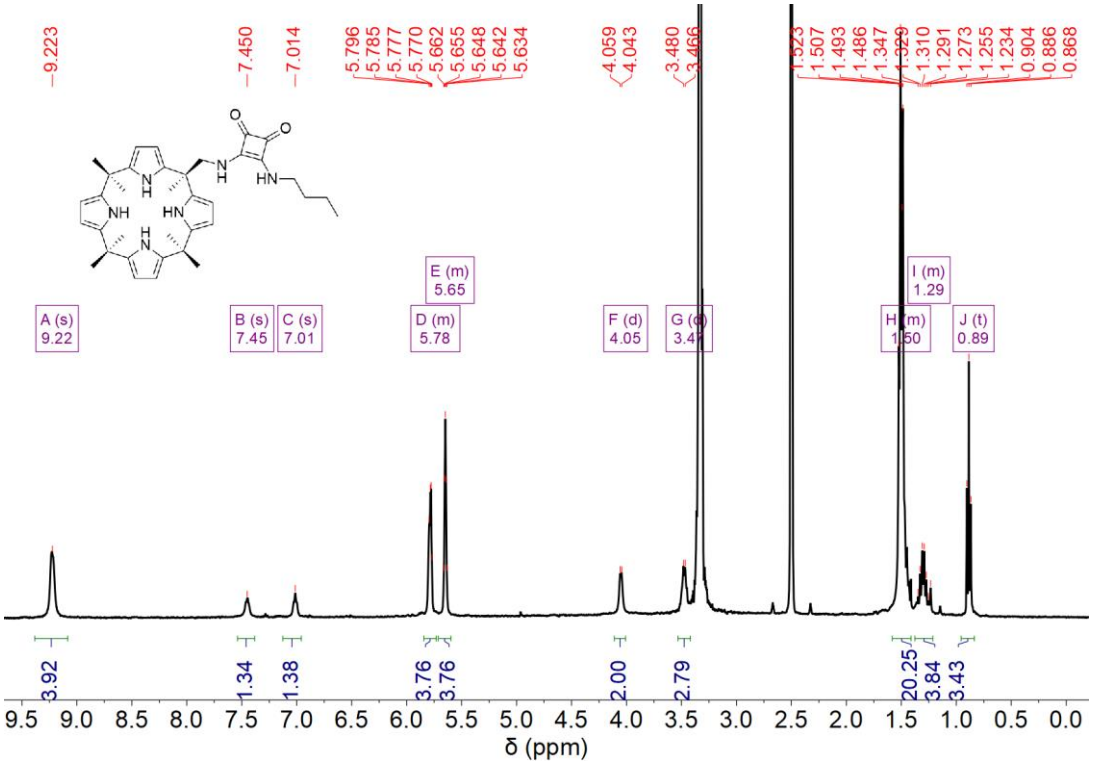

Figure S43. ^{1}H NMR (300 MHz, DMSO-d_6) spectrum of **7**.

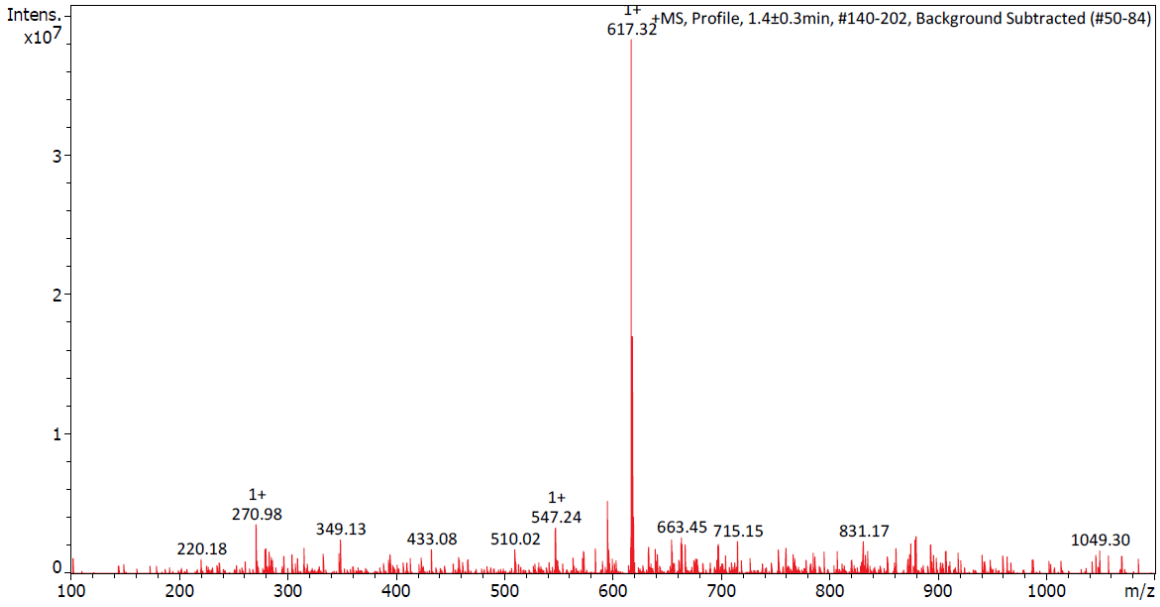

Figure S44. LR-MS (ESI+) of **7**.

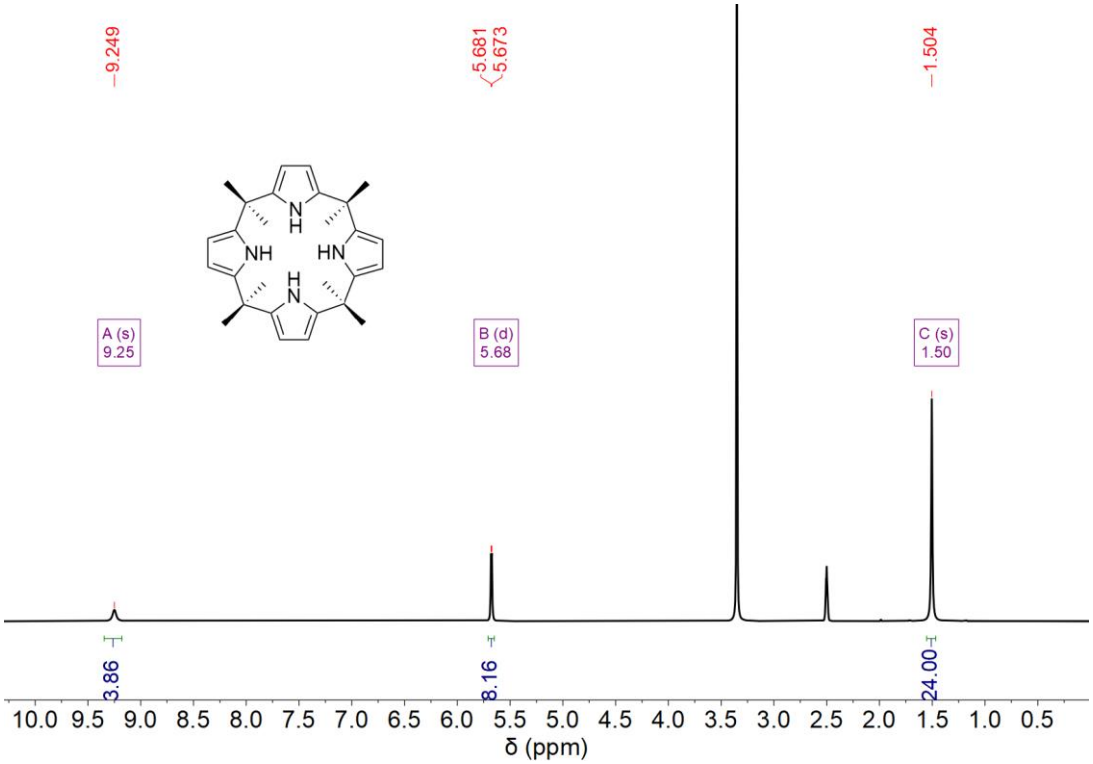

Figure S45. ^{1}H NMR (300 MHz, DMSO-d_6) spectrum of OMCP **8**.

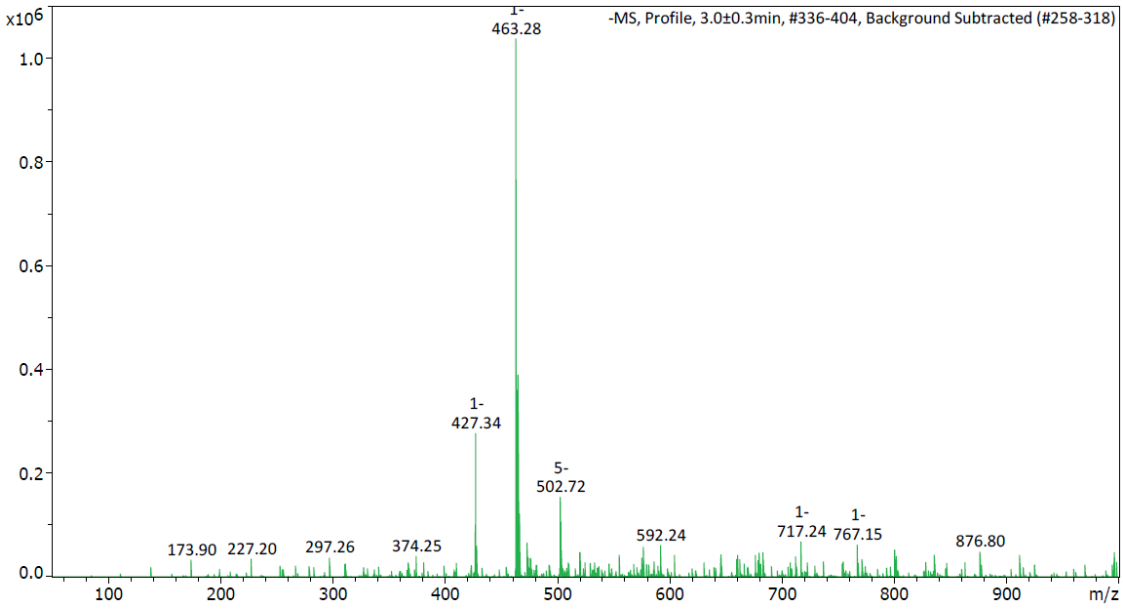

Figure S46. LR-MS (ESI+) of OMCP **8**.

Experimental procedures

Binding studies

A 2.5 mM stock solution of the compound ('host') was prepared in DMSO-d_6/0.5 % H_2O, which was used to prepare the salt solutions. Tetrabutylammonium chloride (TBACl) was purchased

commercially from Sigma Aldrich and dried for a minimum of 48 h in a desiccator under high vacuum before use.

A series of 0.15, 0.03, and 1 M stock solutions of TBACl were made in the host solution. The host solution (600 µL) was added into an NMR tube before adding aliquots of the TBACl solution and collecting a spectrum for each titre. Titres were added from 0 – 100 equivalents of chloride.

The peak shifts of the pyrrolic N–H, squaramide N–H, and methylene $–CH_2$ protons were plotted against the chloride concentration and fit using BindFit v0.5 to both a 1:1 and 1:2 binding model.[1]

Preferred binding models were calculated by performing a covariance of fit on the output data from Bindfit. The 1:2 binding model was determined as the preferred binding for all compounds.[2]

Transport studies

Transport studies were performed using an Orion Chloride Selective electrode from ThermoFisher Scientific, which was calibrated using five NaCl stock solutions ranging from 1×10^{-5} M to 1×10^{-2} M.

General Vesicle Preparation

Vesicles were prepared according to the method outlined in 'Supramolecular methods: the chloride/nitrate transmembrane exchange assay'.[3] POPC lipids from Corden Pharma were dissolved in chloroform to make a 1 g in 35 mL solution. In a pre-weighed round bottom flask, 4 mL of the POPC solution was added and gently removed under reduced pressure, ensuring a smooth lipid cake. The lipids were dried in a desiccator under vacuum overnight before rehydration with 4 mL of internal solution. The lipid suspension was frozen in liquid nitrogen and thawed in water, repeating nine times. The suspension of lipids was extruded by passing through a 200 nm polycarbonate membrane 25 times. The external solution of the extruded vesicles was exchanged with the final external solution to be used for transport studies, either through dialysis or size-exclusion chromatography. The vesicles were then diluted to either a known concentration or to a known volume and the correct volume to add for each experiment was calculated.

ISE Cl^-/NO_3^- Exchange Assay

Vesicles were prepared with an internal solution of sodium chloride (487 mM) in a sodium phosphate buffer (5 mM) at pH 7.20. An external solution of sodium nitrate (487 mM) was made in the same phosphate salt buffer solution. Vesicles were dialysed in sodium nitrate solution overnight, before diluting to 10 mL with fresh sodium nitrate external solution.

For each run, vesicles were diluted to a final concentration of 1 mM in 5 mL external solution. The compound was added at t = 0 s and data was collected for 300 s. At t = 300 s, 50 µL of Triton X-100 (10 % *v/v* in H_2O) detergent was added to lyse the vesicles and release any remaining internal chloride. At t = 420 s, data collection was stopped, and the final reading taken as 100 % efflux. Reported concentrations and error for each complex were repeated in duplicates.

Hill plot analysis was conducted on the results by plotting the percentage chloride efflux at t = 270 s against the receptor concentration in mol %. The graphed data was fitted to the Hill equation using OriginPro 8.6 (**Equation S1**).

$$y = START + (END - START)\frac{x^n}{k^n + x^n}$$

Equation S1: The Hill equation.

Where *y* represents the chloride efflux, START is the efflux value at *t* = 0 s, END is the 100% efflux value obtained from lysing the vesicles, *x* is the transporter concentration (in mol%, with respect to lipid concentration), *k* is a derived parameter, and *n* is the Hill coefficient.

A derived equation (**Equation S2**) was used to calculate the EC_{50}.

$$EC_{50} = k * (\frac{50}{END - START - 50})^{\frac{1}{n}}$$

Equation S2: Derived Hill function used to calculate EC_{50} values when chloride efflux did not reach 100 % over the duration of the ISE assay.

Where *k* and *n* are the derived parameters from the original Hill equation, END is the percentage chloride efflux at *t* = 300 s, and START is the efflux at *t* = 0 s.

Cationophore Coupled Transport

Vesicles were prepared with an internal solution of potassium chloride (300 mM) in a buffer solution of potassium phosphate salts (5 mM), adjusted to pH 7.20. Two external solutions

were made in the potassium phosphate buffer; potassium nitrate (333 mM) and potassium gluconate (300 mM), both adjusted to pH 7.20. After extrusion, vesicles were filtered through a column containing Sephadex G-25 Coarse, eluting with the potassium gluconate solution. The vesicles were collected and diluted to 10 mM with the same potassium gluconate solution. Cationophore-coupled transport for the complexes was tested at the calculated EC_{50} concentrations from the Cl^-/NO_3^- exchange assay.

For each experiment, 0.5 mL of vesicles were added to 4.5 mL of either potassium nitrate or potassium gluconate external solution. 10 µL of a cationophore (valinomycin or monensin) in DMSO was added to a final concentration of 0.1 mol % at t = −30 s. 100 µL of the compound in DMSO was added at t = 0 s, before collecting data for 300 s. At t = 300 s, 50 µL of Triton X-100 (10 % v/v in H_2O) detergent was added to lyse the vesicles and release any remaining internal chloride. At t = 420 s, data collection was stopped, and the final reading taken as 100 % efflux. Experiments were performed in duplicate.

HPTS Assay

An external solution of potassium chloride (100 mM) and HEPES (5 mM) was made, adjusted to pH 7.00. Vesicles were prepared with an internal solution containing 1 mM HPTS dissolved in the external solution.[4] After extrusion, vesicles were filtered through a column containing Sephadex G-25 Coarse, eluting with the potassium chloride external solution. The vesicles were collected and diluted to 10 mL with fresh external solution. For each experiment, HPTS vesicles were diluted to 0.1 mM in a final volume of 2.5 mL external solution in a cuvette. Experiments were performed in triplicates simultaneously.

Every addition of solution into the lipids were staggered by 10 s between each cuvette. At the start of each run, a pH gradient was induced in each cuvette by adding 25 µL of 0.5 M sodium hydroxide. After 30 s, the compound was added as a 5 µL DMSO solution before collecting data for 200 s. At t = 200 s, 25 µL Triton X-100 (10 % v/v in H_2O) was added before stopping at t = 240 s, with the final reading taken as 100 % proton efflux.

Ionophore-coupled studies required the further addition of either valinomycin or carbonyl cyanide *m*-chlorophenyl hydrazone (CCCP) to a final concentration of 0.1 or 1 mol % respectively. The cationophores were added prior to the base pulse and allowed to evenly

distribute throughout the lipids first. For fatty acid-free conditions, 1 mol % bovine serum albumin (BSA) was incorporated into the HPTS vesicles prior to dilution in cuvettes. Oleic acid (OA) was added to a final concentration of either 2 mol % or 4 mol % to restore the fatty acid flip-flop mechanism after sequestration by BSA. Transporters were added to the lipids at a concentration corresponding to approximately 50 % efflux.

Proton efflux was studied by using an HPTS ratiometric fluorescent probe, detecting the emission of HPTS at 510 nm. As HPTS is fluorescent in its acidic and basic form, a ratio (*R*) can be interpreted by exciting the vesicles at 403 nm and 460 nm respectively. Fractional fluorescence intensity (I_F) can then be calculated using the following equation:

$$I_F = \frac{R_t - R_0}{R_d - R_0}$$

Equation S3: HPTS fractional fluorescence intensity (I_F) based on fluorescence ratios at the start (R_0), end (R_d), and any chosen time point (R_t).

Data analysis was conducted via Hill analysis on OriginPro 8.6, plotting I_F against the receptor concentration in mol %. A modified Hill equation was used for this analysis:

$$y = y_0 + (y_{max} - y_0) * \frac{x^n}{k^n + x^n}$$

Equation S4: Modified Hill equation used to analyse the data from the HPTS assay.

Where y_{max} is the maximum value of I_F, y_0 is the value at t = 200 s for a DMSO blank experiment, k is the EC_{50} concentration, and n is the Hill coefficient.

Anion Selectivity Assay

Vesicles were prepared with an internal solution of NaCl (300 mM) and HPTS (1 mM) in a buffer solution of HEPES (10 mM), adjusted to pH 7.00. Five external solutions were made in an isotonic buffer, containing NaCl, NaBr, $NaNO_3$, NaI, or $NaClO_4$. After extrusion, vesicles were filtered through a Sephadex G-25 Coarse column, eluting with NaCl. Anion exchange was induced by adding 5 µL of the transporter in DMSO to the solution. Anion exchange was continued for as long as required for all anions to reach a plateau in activity. Note that NaI contains iodine impurities which may act as transporter for I^-. Conversion of I_F values were done according to the published method.[5]

Crystallography

Suitable crystals of compound **6** were grown from a DMSO solution of the compound. A suitable crystal was selected and mounted on a Rigaku XtaLAB Synergy-DW Custom diffractometer (FR-X rotating-anode source, Rigaku HyPix-6000HE detector), outputting confocal mirror-monochromated Cu-Kα radiation (λ = 1.54184 Å). The crystal was kept at 100 K during collection.

Table S1. Crystal and data refinement parameters for the X-ray studies of compound **6**.

Crystallographic details	**Compound 6**
Empirical formula	$C_{46}H_{61}F_5N_6O_6S_4$
Formula weight	1017.24
Temperature/K	100(2)
Crystal system	triclinic
Space group	P-1
a/Å	10.1261(2)
b/Å	14.3953(4)
c/Å	18.7947(4)
α/°	89.294(2)
β/°	82.002(2)
γ/°	69.514(2)
Volume/Å^3	2539.49(11)
Z	2
ρ_{calc}g/cm^3	1.330
μ/mm^{-1}	2.316
F(000)	1072.0
Crystal size/mm^3	0.13 × 0.1 × 0.04
Radiation	CuKα (λ = 1.54184)
2Θ range for data collection/°	4.752 to 145.074
Index ranges	-12 ≤ h ≤ 12, -17 ≤ k ≤ 17, -23 ≤ l ≤ 20
Reflections collected	56016
Independent reflections	9794 [R_{int} = 0.0506, R_{sigma} = 0.0267]
Data/restraints/parameters	9794/0/643
Goodness-of-fit on F^2	0.965
Final R indexes [I>=2σ (I)]	R_1 = 0.0439, wR_2 = 0.1221
Final R indexes [all data]	R_1 = 0.0510, wR_2 = 0.1268
Largest diff. peak/hole / e Å^{-3}	1.44/-0.66

Binding Data and Fittings

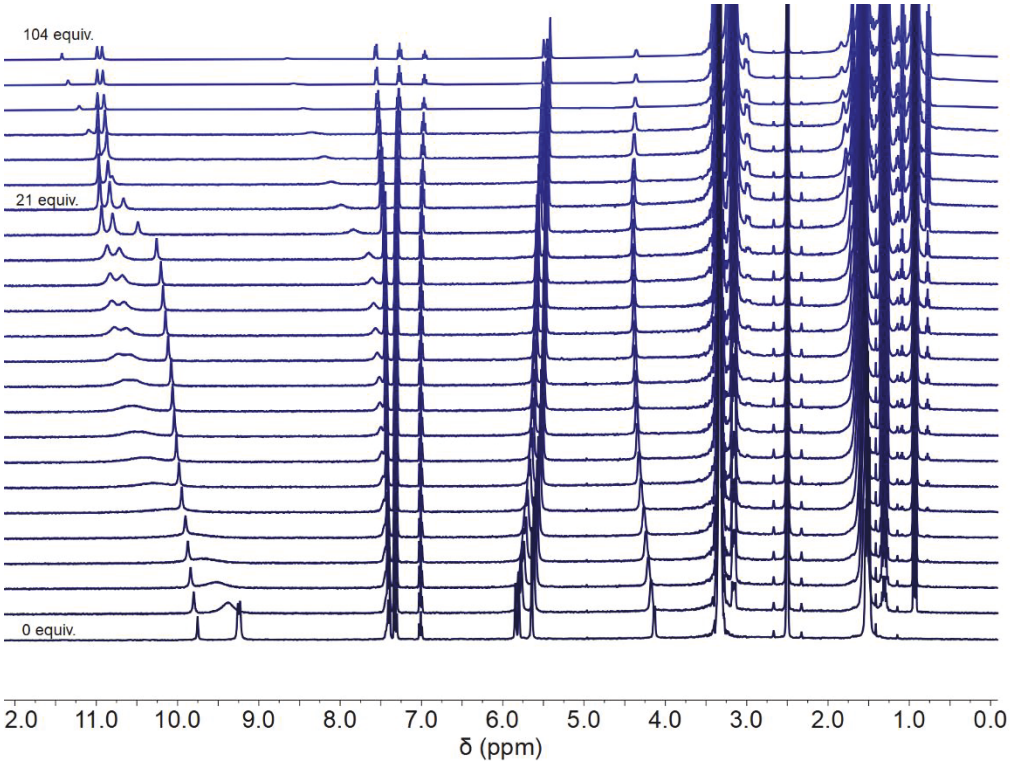

Figure S47. Stack plot of ^{1}H NMR titration of **1** (2.5 mM) with TBACl in DMSO-d_6/0.5 % H_2O at 298 K. Concentrations are normalised against dilution factors. Available at http://app.supramolecular.org/bindfit/view/bd286361-f7db-4725-a2f7-e28b537060cc

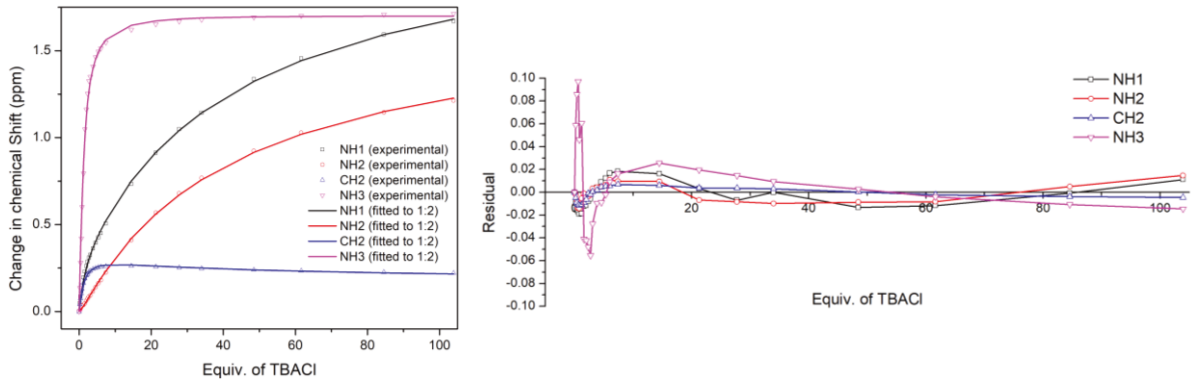

Figure S48. Fitted binding isotherm of **1** with TBACl showing the change in chemical shift of the squaramide N–H, methylene –CH_2, and calix[4]pyrrole N–H protons fitted to the 1:2 binding model (left). Residual plot showing the random error obtained from the binding isotherm fitting (right).

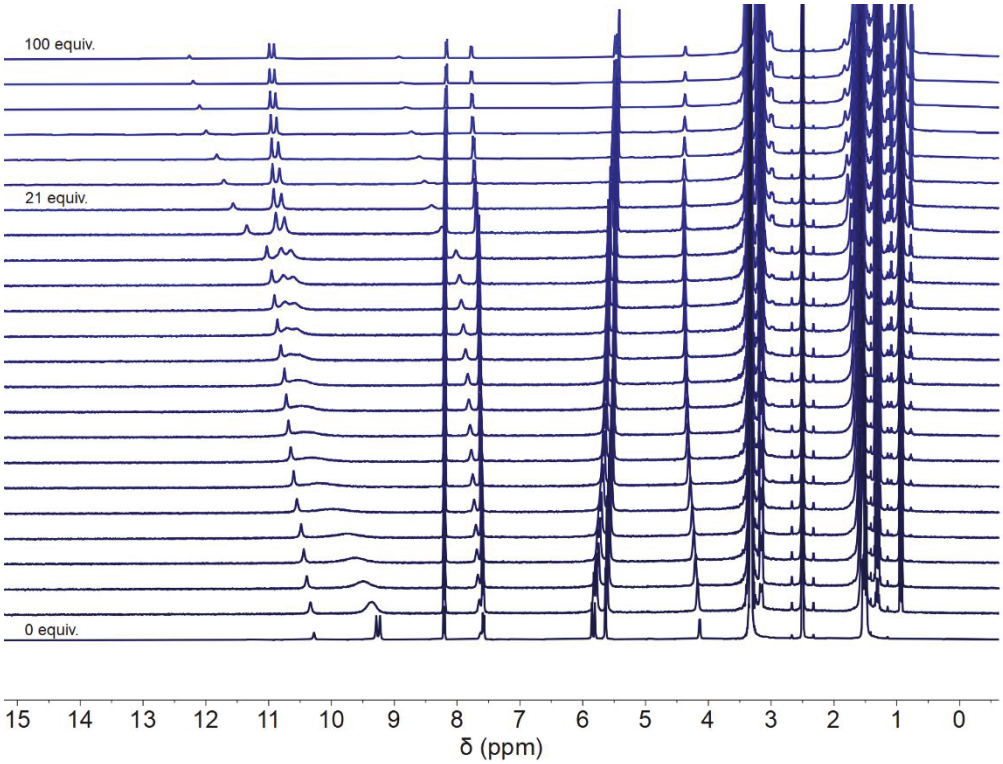

Figure S49. Stack plot of ^{1}H NMR titration of **2** (2.5 mM) with TBACl in DMSO-d_6/0.5 % H_2O at 298 K. Concentrations are normalised against dilution factors. Available at http://app.supramolecular.org/bindfit/view/cf229bac-7a72-4258-b604-2025bffb5cfa

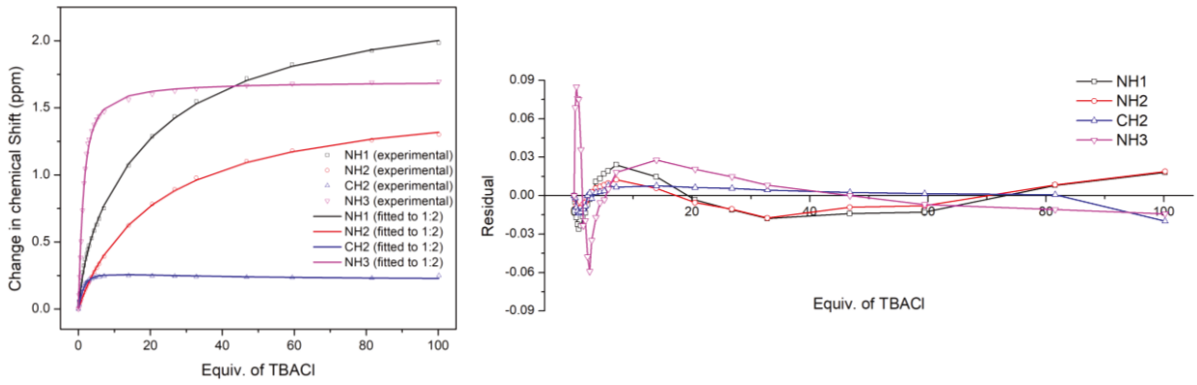

Figure S50. Fitted binding isotherm of **2** with TBACl showing the change in chemical shift of the squaramide N–H, methylene –CH_2, and calix[4]pyrrole N–H protons fitted to the 1:2 binding model (left). Residual plot showing the random error obtained from the binding isotherm fitting (right).

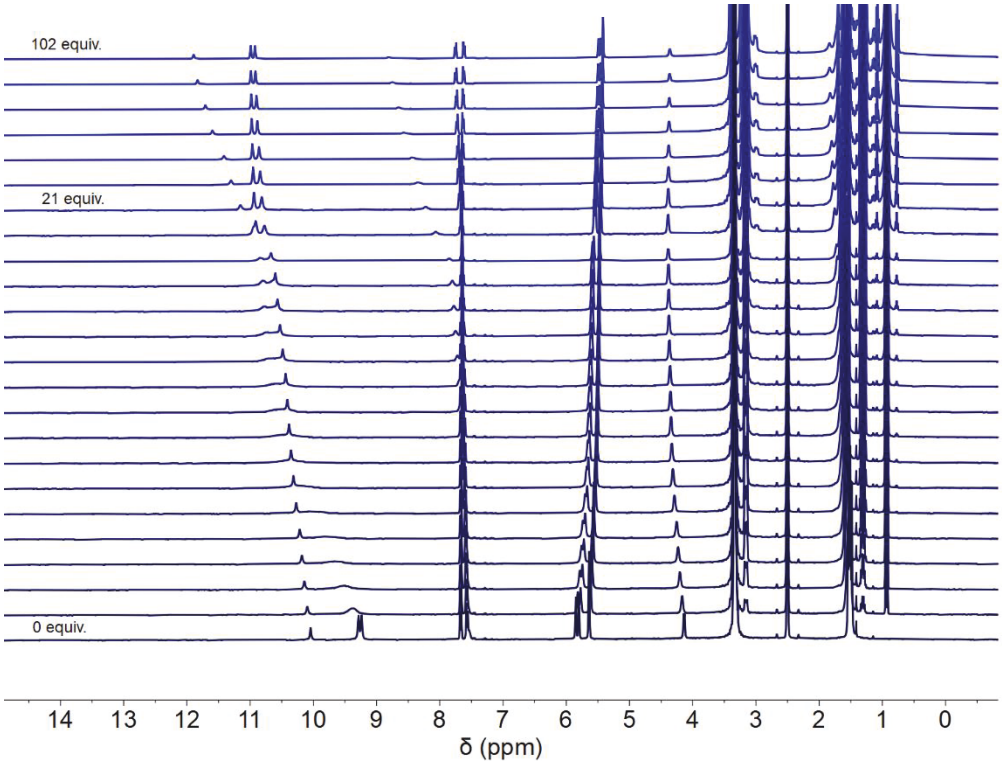

Figure S51. Stack plot of ^{1}H NMR titration of **3** (2.5 mM) with TBACl in DMSO-d_6/0.5 % H_2O at 298 K. Concentrations are normalised against dilution factors. Available at http://app.supramolecular.org/bindfit/view/822dc79b-ad9e-47bb-9d9f-6a9cc739876d

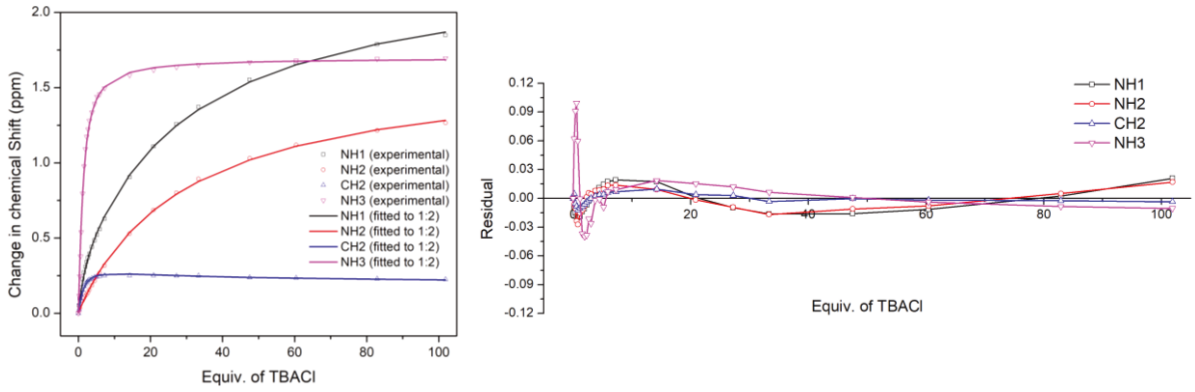

Figure S52. Fitted binding isotherm of **3** with TBACl showing the change in chemical shift of the squaramide N–H, methylene –CH_2, and calix[4]pyrrole N–H protons fitted to the 1:2 binding model (left). Residual plot showing the random error obtained from the binding isotherm fitting (right).

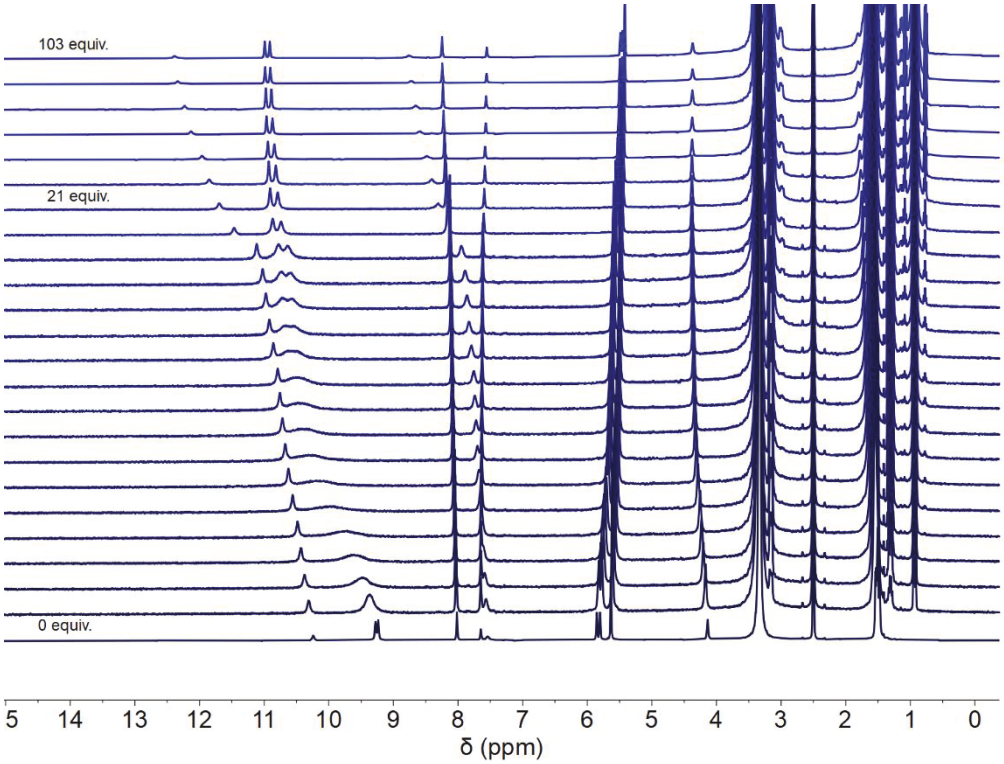

Figure S53. Stack plot of ^{1}H NMR titration of **4** (2.5 mM) with TBACl in DMSO-d_6/0.5 % H_2O at 298 K. Concentrations are normalised against dilution factors. Available at http://app.supramolecular.org/bindfit/view/291b8cbd-683f-42a4-9f72-e89d1c83880c

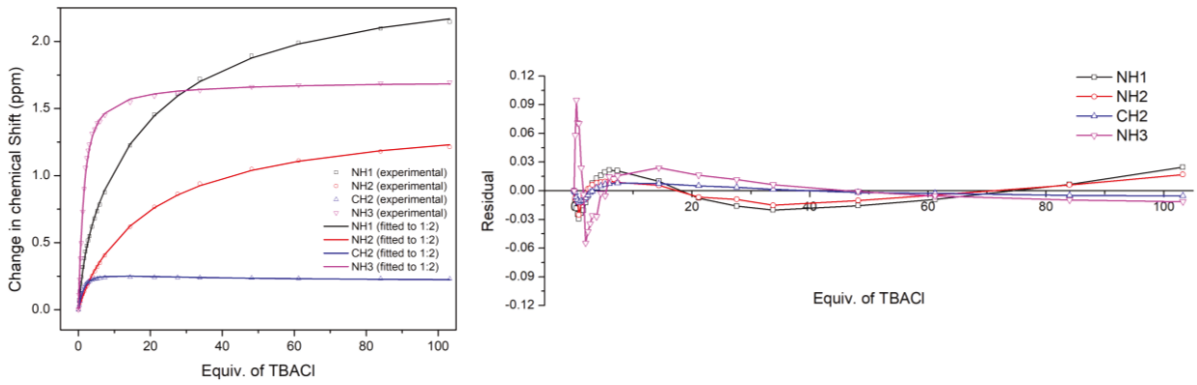

Figure S54. Fitted binding isotherm of **4** with TBACl showing the change in chemical shift of the squaramide N–H, methylene –CH_2, and calix[4]pyrrole N–H protons fitted to the 1:2 binding model (left). Residual plot showing the random error obtained from the binding isotherm fitting (right).

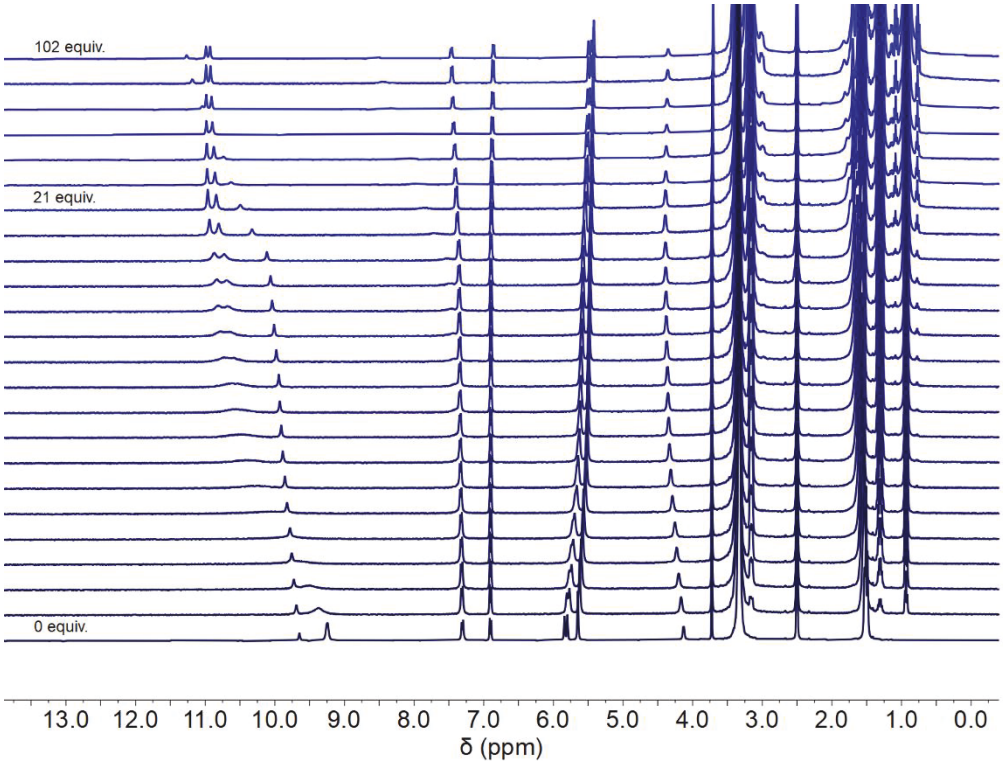

Figure S55. Stack plot of ^{1}H NMR titration of **5** (2.5 mM) with TBACl in DMSO-d_6/0.5 % H_2O at 298 K. Concentrations are normalised against dilution factors.

http://app.supramolecular.org/bindfit/view/fdb82547-a806-4002-841f-3105b4caa489

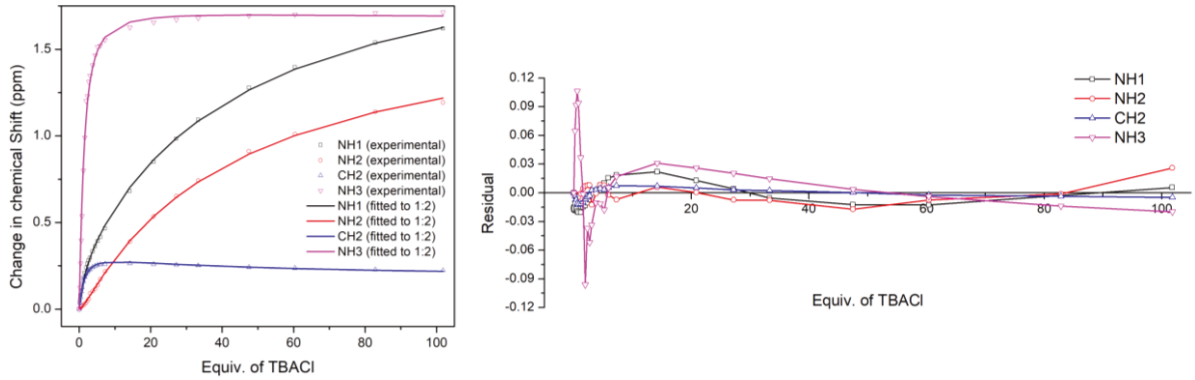

Figure S56. Fitted binding isotherm of **5** with TBACl showing the change in chemical shift of the squaramide N–H, methylene –CH_2, and calix[4]pyrrole N–H protons fitted to the 1:2 binding model (left). Residual plot showing the random error obtained from the binding isotherm fitting (right).

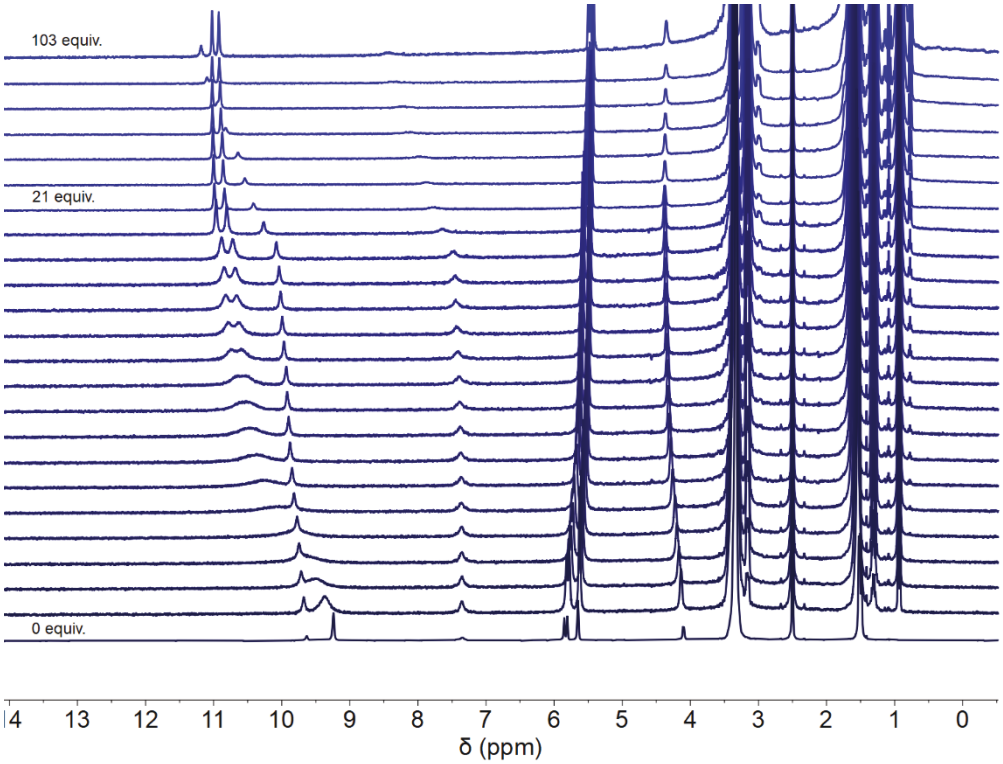

Figure S57. Stack plot of ^{1}H NMR titration of **6** (2.5 mM) with TBACl in DMSO-d_6/0.5 % H_2O at 298 K. Concentrations are normalised against dilution factors. Available at http://app.supramolecular.org/bindfit/view/197b6f84-4662-43f9-98a8-3bbd64d36aa7

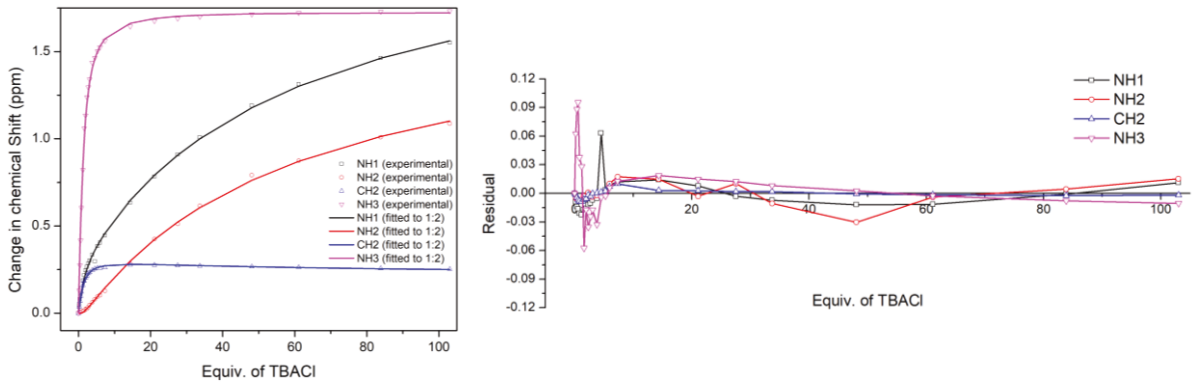

Figure S58. Fitted binding isotherm of **6** with TBACl showing the change in chemical shift of the squaramide N–H, methylene –CH_2, and calix[4]pyrrole N–H protons fitted to the 1:2 binding model (left). Residual plot showing the random error obtained from the binding isotherm fitting (right).

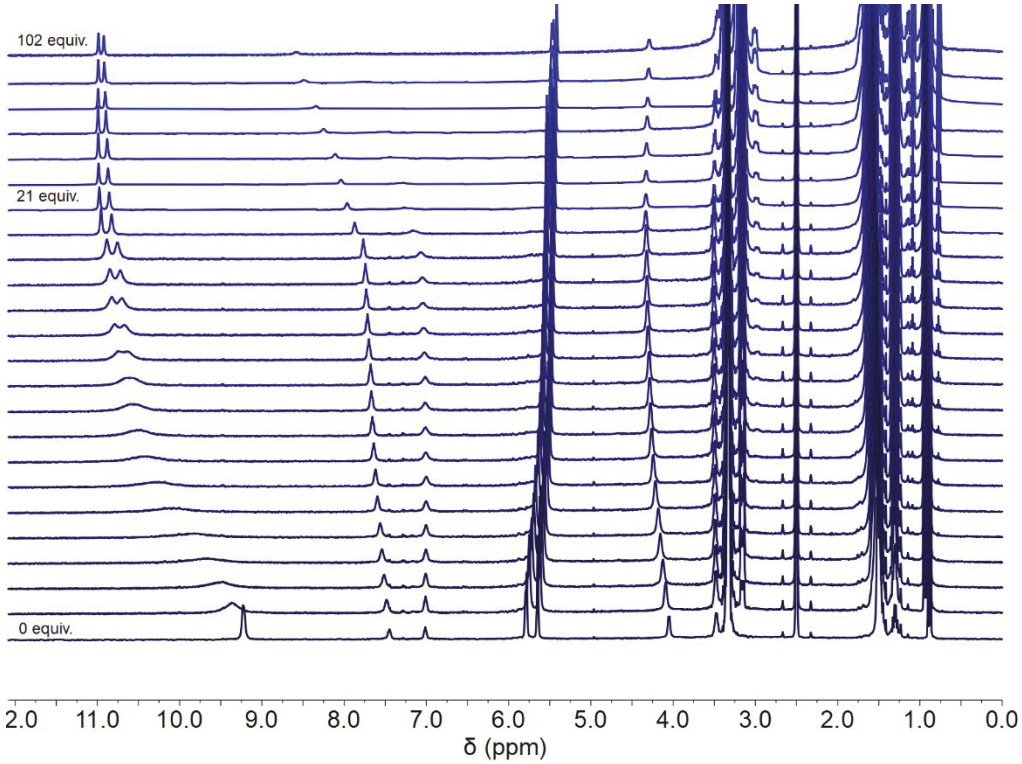

Figure S59. Stack plot of ^{1}H NMR titration of **7** (2.5 mM) with TBACl in DMSO-d_6/0.5 % H_2O at 298 K. Concentrations are normalised against dilution factors. Available at http://app.supramolecular.org/bindfit/view/eff8d04e-dd7e-49c9-a420-8a7a25fbfbb7

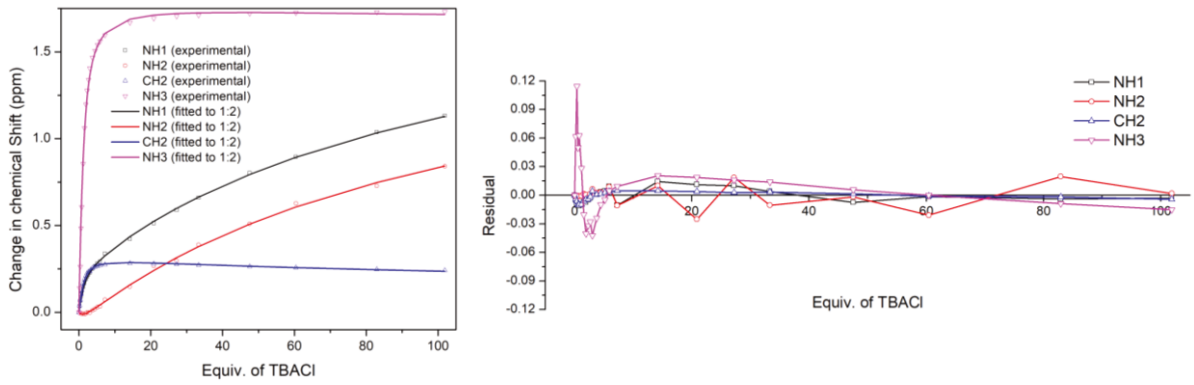

Figure S60. Fitted binding isotherm of **7** with TBACl showing the change in chemical shift of the squaramide N–H, methylene –CH_2, and calix[4]pyrrole N–H protons fitted to the 1:2 binding model (left). Residual plot showing the random error obtained from the binding isotherm fitting (right).

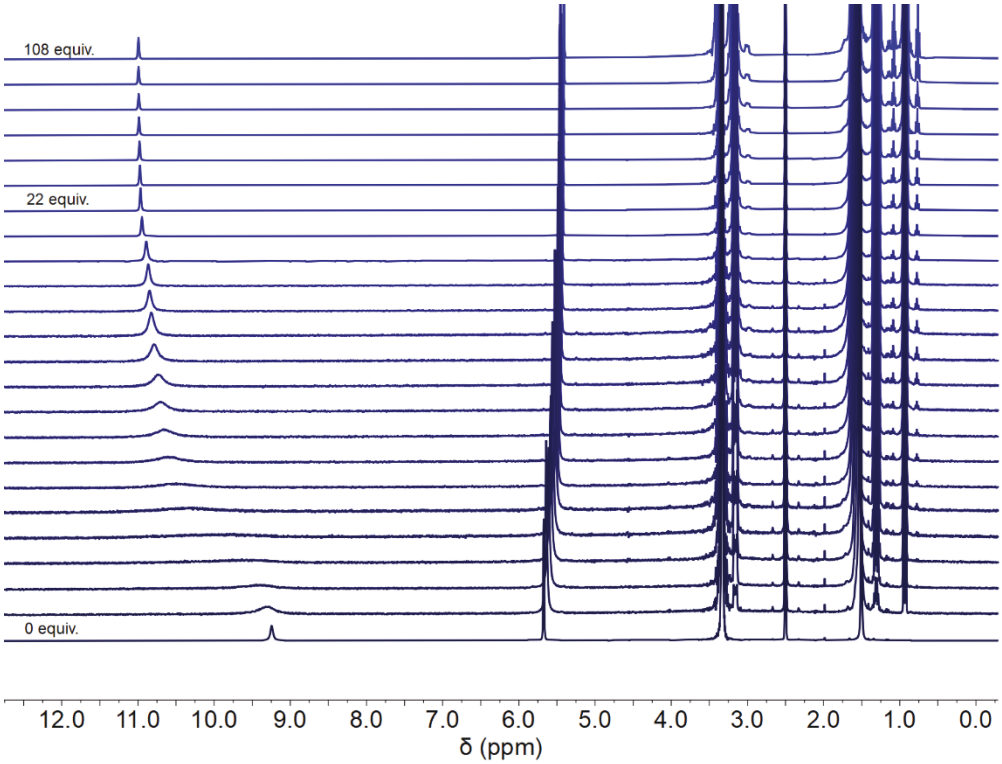

Figure S61. Stack plot of ^{1}H NMR titration of OMCP **8** (2.5 mM) with TBACl in DMSO-d_6/0.5 % H_2O at 298 K. Concentrations are normalised against dilution factors. Available at http://app.supramolecular.org/bindfit/view/c1e3453f-703a-4d8d-bd8e-23dab2810eed

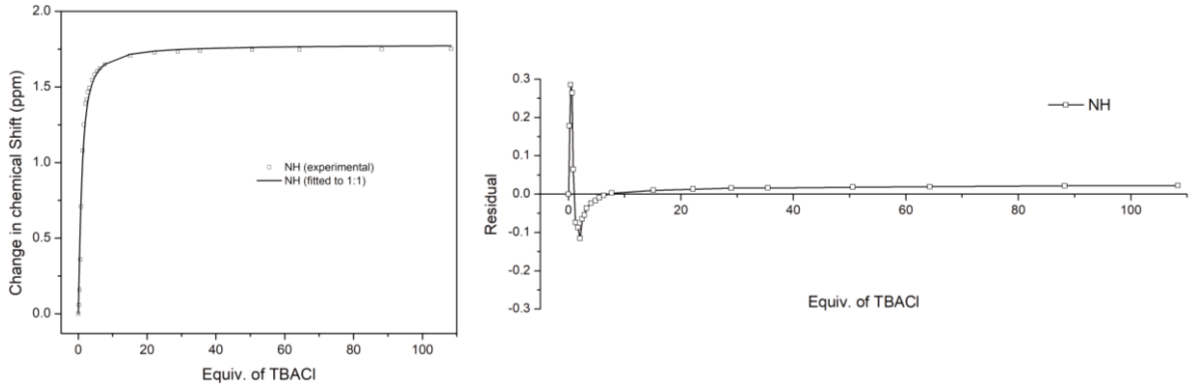

Figure S62. Fitted binding isotherm of OMCP **8** with TBACl showing the change in chemical shift of the squaramide N–H, methylene –CH_2, and calix[4]pyrrole N–H protons fitted to the 1:2 binding model (left). Residual plot showing the random error obtained from the binding isotherm fitting (right).

Covariance of Fit Calculations

Table S2: Binding constants (K_a) for compounds **1**–**8** with TBACl in DMSO-d_6/0.5% H_2O at 298 K, calculated using 1:1 and 1:2 binding models, and the covariance of fit (cov_{fit}) for both models. Errors are < 6 % for **1**–**8** and 23 % for **8**.

Compound	Compound Binding Constants (M^{-1})				
	1:1 (K_{11})	cov_{fit}	1:2	cov_{fit}	F cov_{fit}
1	186	5.10×10^{-2}	K_{11}: 549 K_{12}: 9.28	5.13×10^{-4}	99
2	127	4.47×10^{-2}	K_{11}: 510 K_{12}: 16.4	7.85×10^{-4}	57
3	140	4.77×10^{-2}	K_{11}: 518 K_{12}: 12.7	4.84×10^{-4}	98
4	117	4.47×10^{-2}	K_{11}: 491 K_{12}: 17.7	5.80×10^{-4}	77
5	193	4.90×10^{-2}	K_{11}: 513 K_{12}: 8.96	7.85×10^{-4}	62
6	222	3.97×10^{-2}	K_{11}: 529 K_{12}: 6.77	3.38×10^{-4}	117
7	388	4.53×10^{-2}	K_{11}: 568 K_{12}: 3.67	3.74×10^{-4}	121
8	740				

Transport data

ISE Cl^-/NO_3^- Exchange

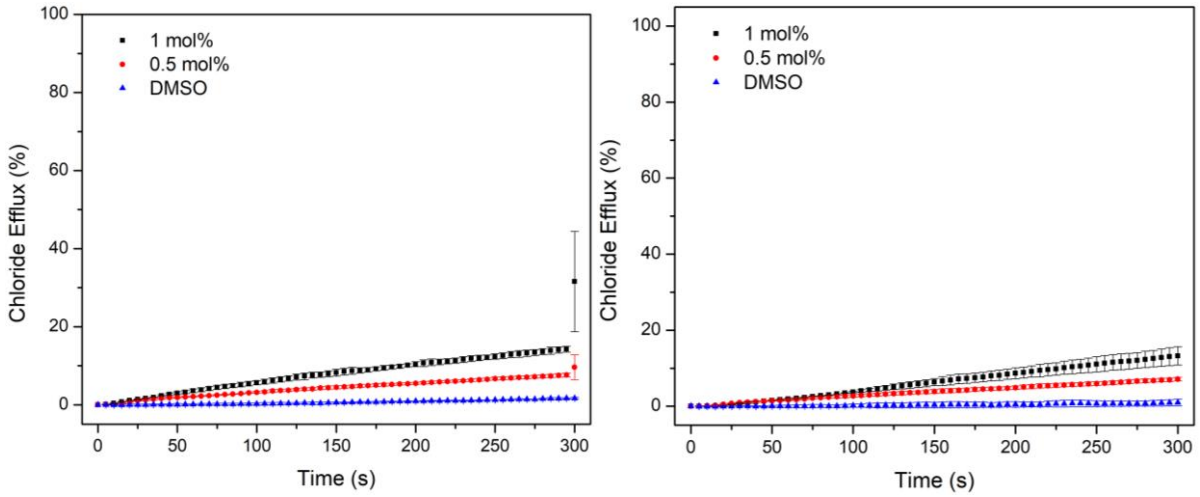

Figure S63. Chloride transport facilitated by **1** in the Cl^-/NO_3^- exchange assay with a NaCl (left) and CsCl (right) internal solution. Each data point is the average of three repeats with error bars showing the standard deviation. DMSO was used as a control.

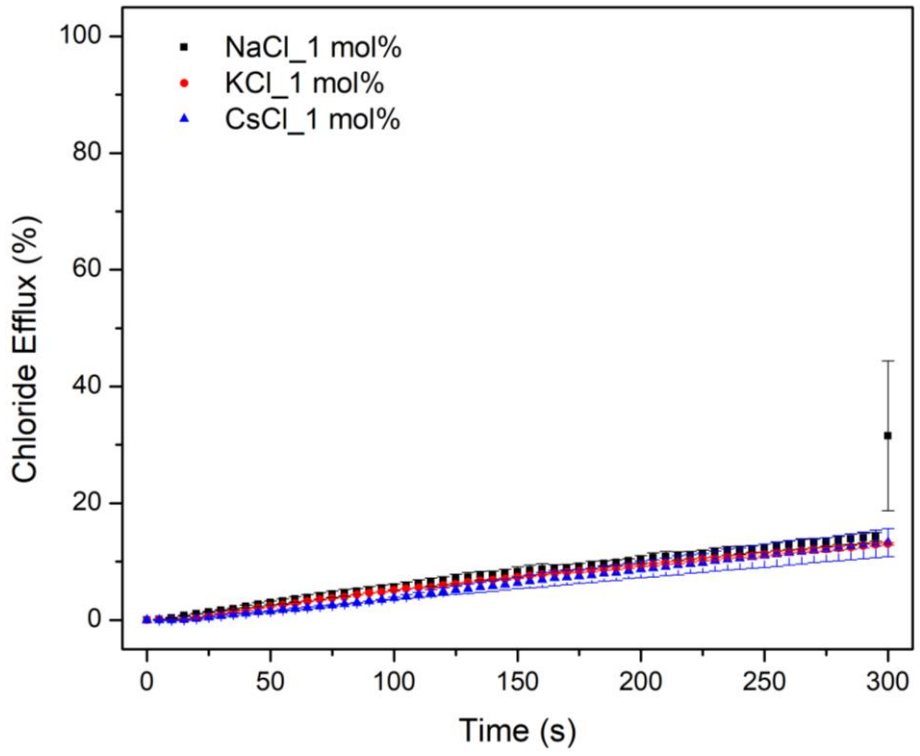

Figure S64. Comparison of the Cl^- transport by **1** (1 mol%) in the Cl^-/NO_3^- exchange assay with a NaCl (black), KCl (red), and CsCl (blue) internal solution.

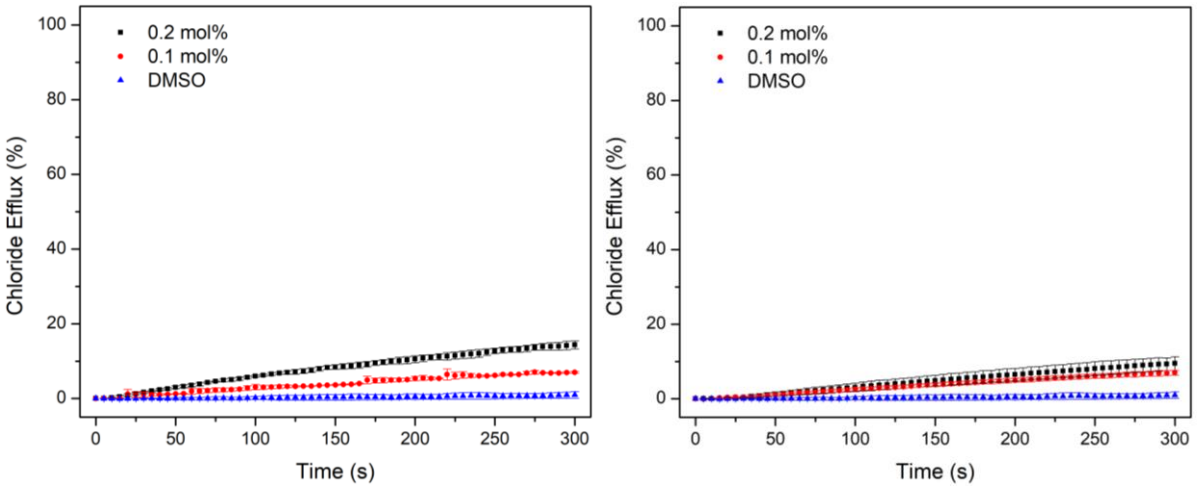

Figure S65. Chloride transport facilitated by **2** in the Cl^-/NO_3^- exchange assay with a NaCl (left) and CsCl (right) internal solution. Each data point is the average of three repeats with error bars showing the standard deviation. DMSO was used as a control.

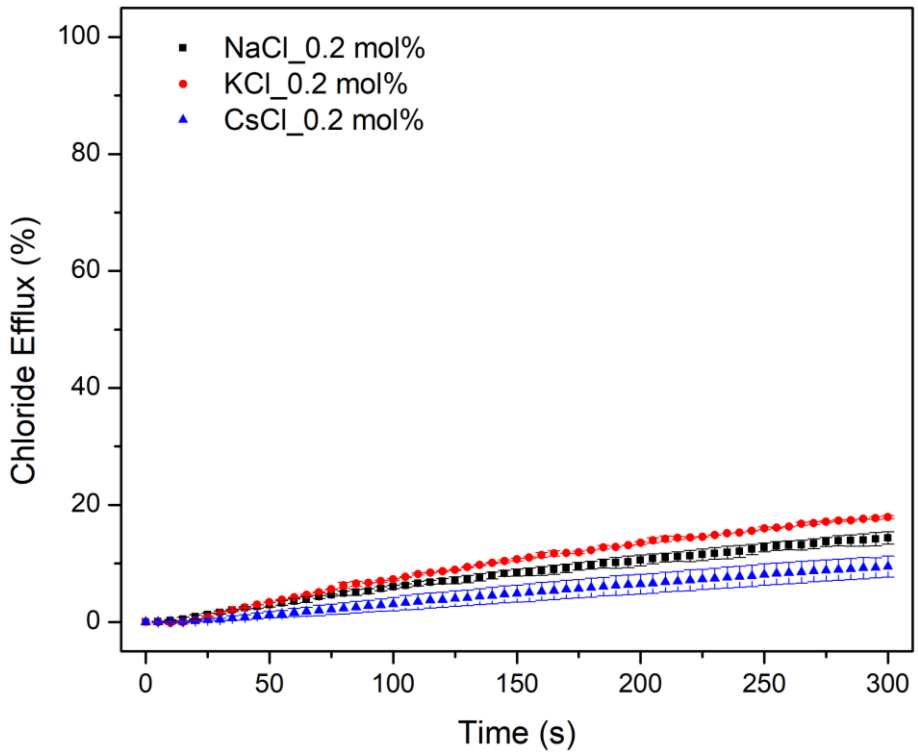

Figure S66. Comparison of the Cl^- transport by **2** (0.2 mol%) in the Cl^-/NO_3^- exchange assay with a NaCl (black), KCl (red), and CsCl (blue) internal solution.

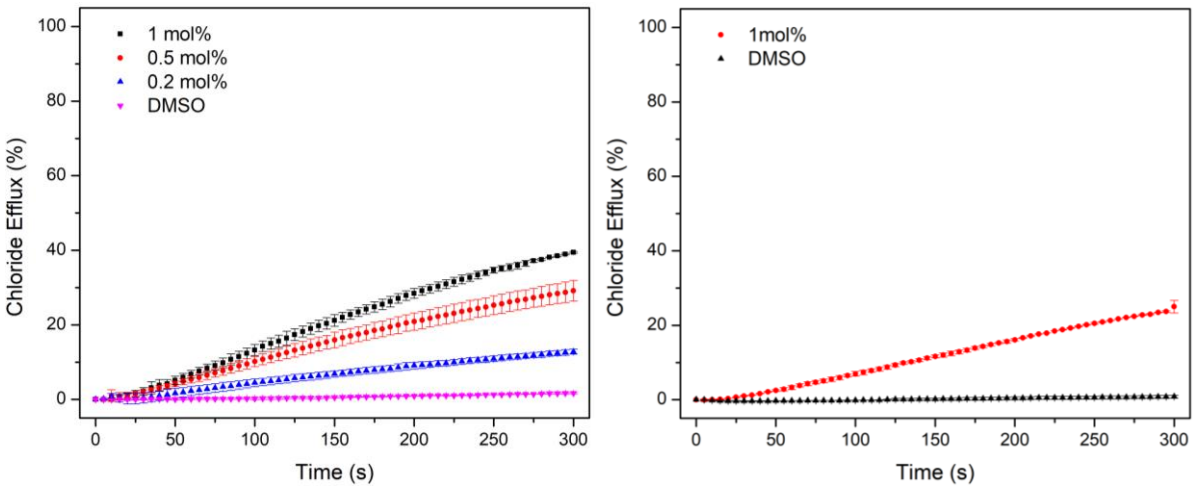

Figure S67. Chloride transport facilitated by **3** in the Cl^-/NO_3^- exchange assay with a NaCl (left) and CsCl (right) internal solution. Each data point is the average of three repeats with error bars showing the standard deviation. DMSO was used as a control.

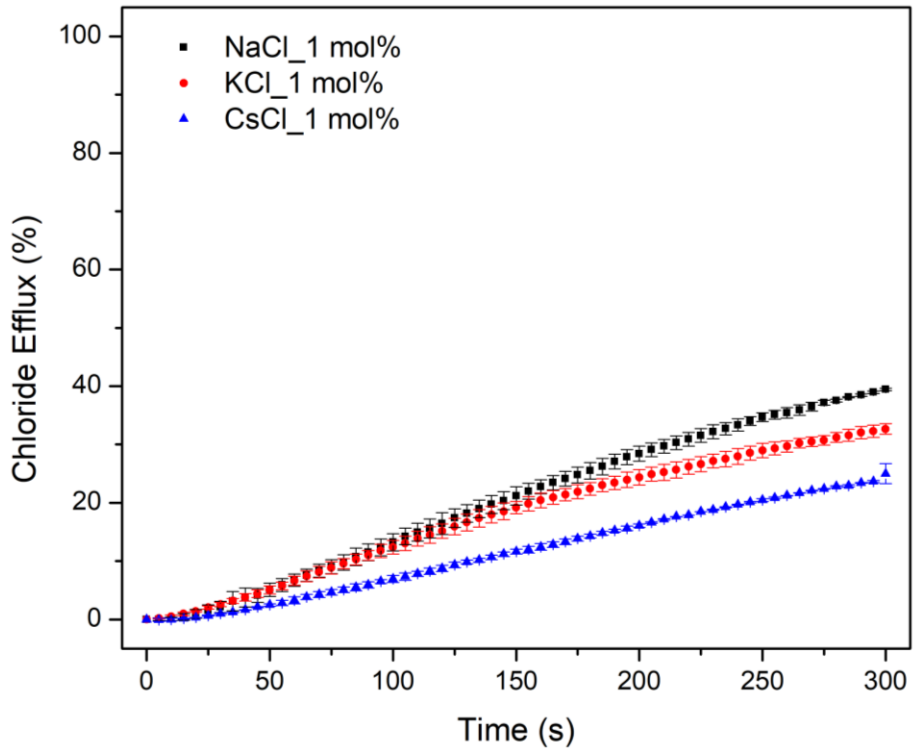

Figure S68. Comparison of the Cl^- transport by **3** (1 mol%) in the Cl^-/NO_3^- exchange assay with a NaCl (black), KCl (red), and CsCl (blue) internal solution.

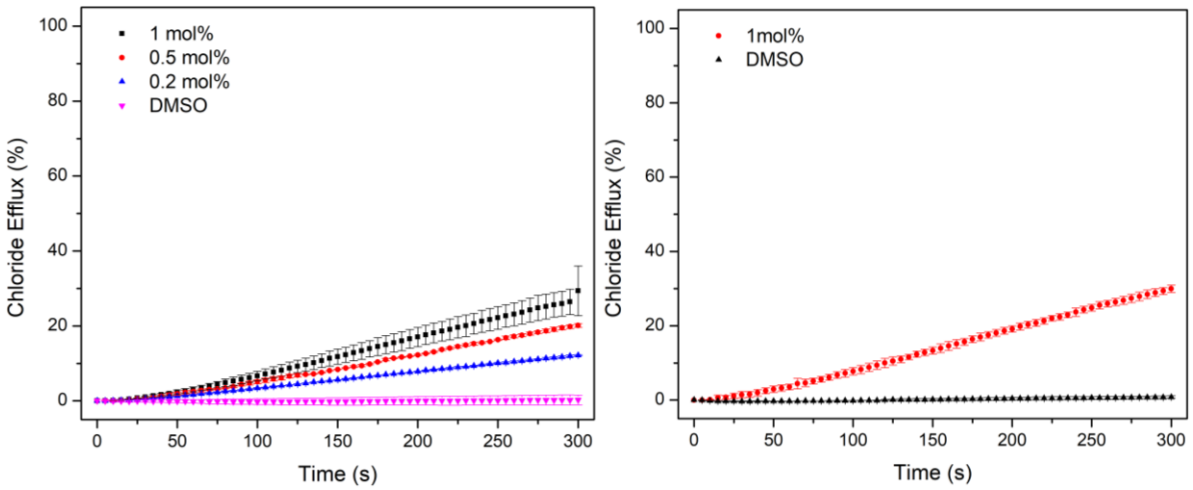

Figure S69. Chloride transport facilitated by **4** in the Cl^-/NO_3^- exchange assay with a NaCl (left) and CsCl (right) internal solution. Each data point is the average of three repeats with error bars showing the standard deviation. DMSO was used as a control.

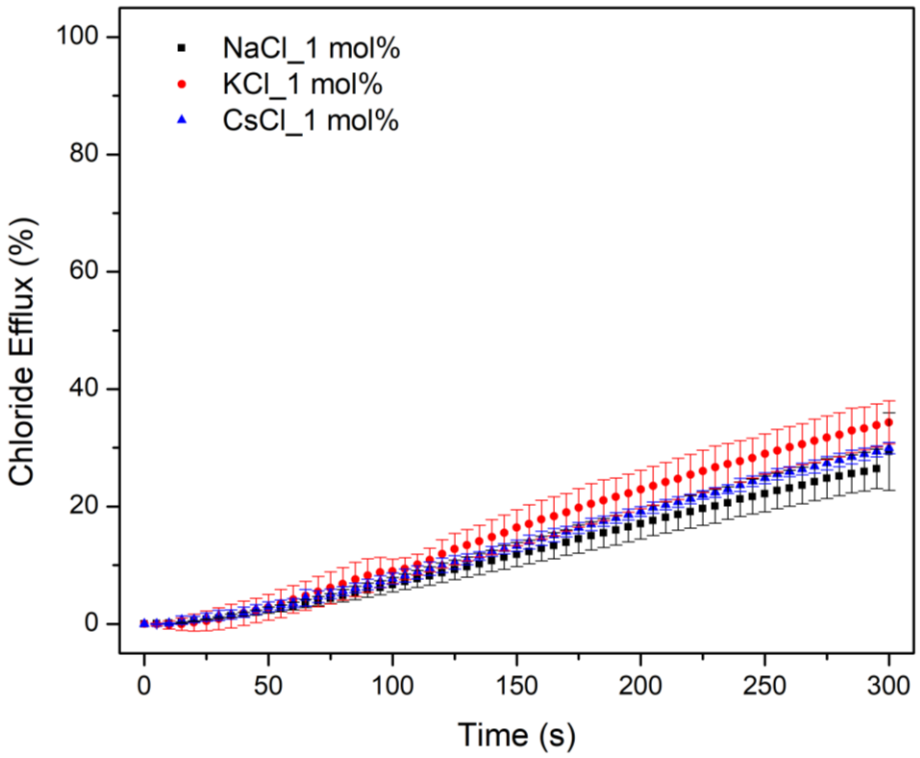

Figure S70. Comparison of the Cl^- transport by **4** (1 mol%) in the Cl^-/NO_3^- exchange assay with a NaCl (black), KCl (red), and CsCl (blue) internal solution.

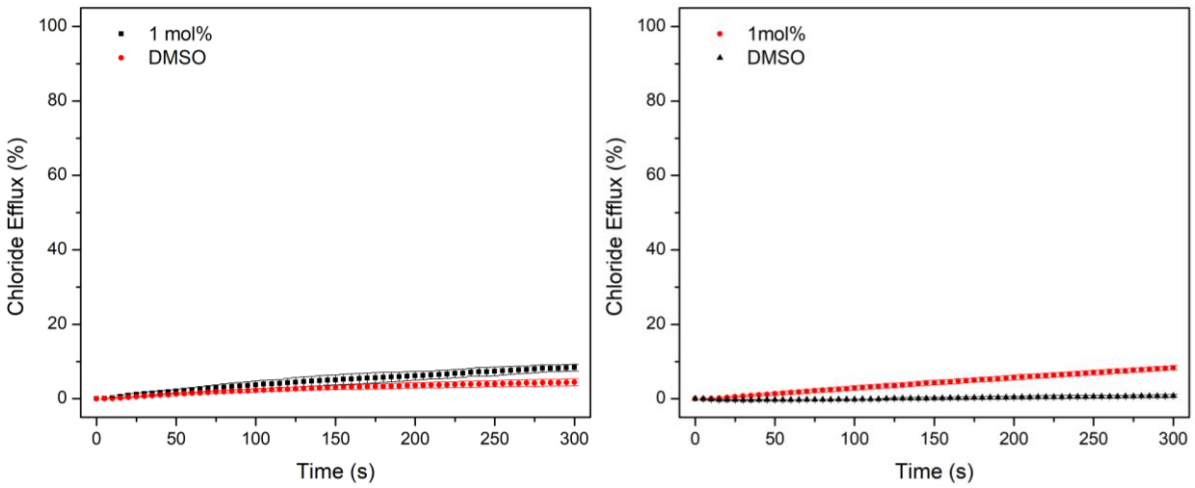

Figure S71. Chloride transport facilitated by **5** in the Cl^-/NO_3^- exchange assay with a NaCl (left) and CsCl (right) internal solution. Each data point is the average of three repeats with error bars showing the standard deviation. DMSO was used as a control.

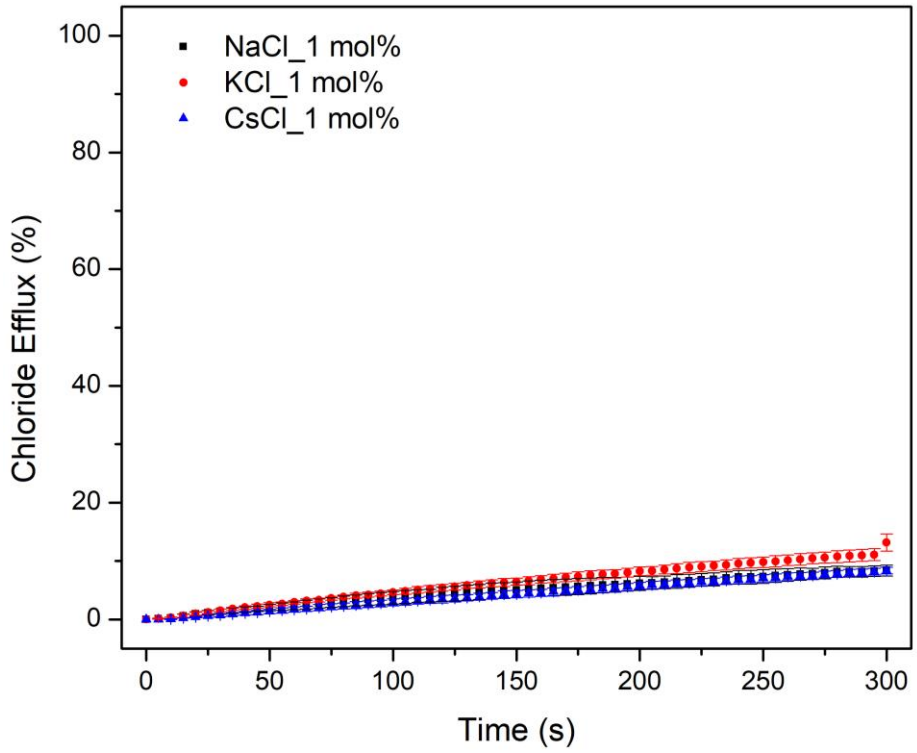

Figure S72. Comparison of the Cl^- transport by **5** (1 mol%) in the Cl^-/NO_3^- exchange assay with a NaCl (black), KCl (red), and CsCl (blue) internal solution.

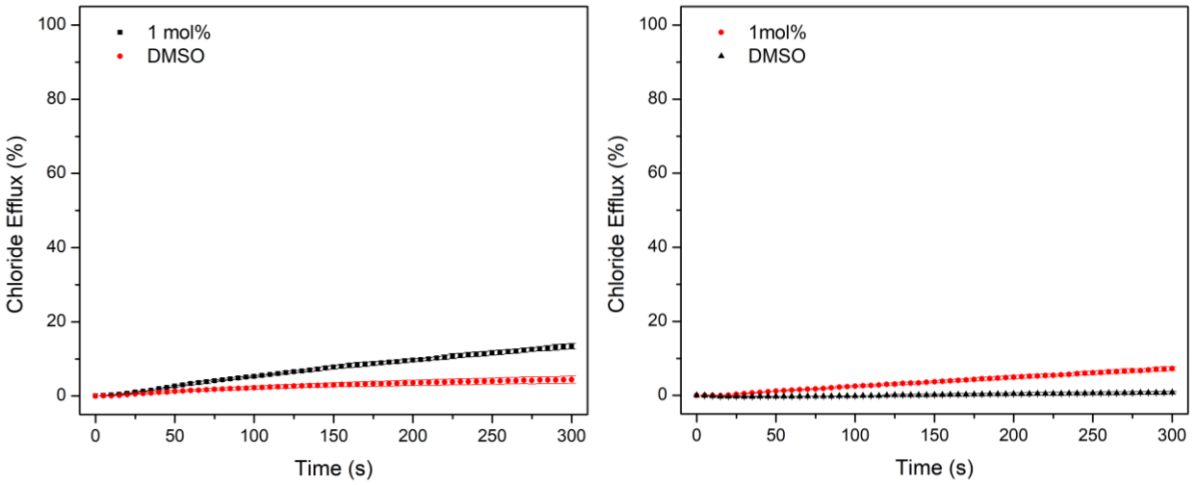

Figure S73. Chloride transport facilitated by **6** in the Cl^-/NO_3^- exchange assay with a NaCl (left) and CsCl (right) internal solution. Each data point is the average of three repeats with error bars showing the standard deviation. DMSO was used as a control.

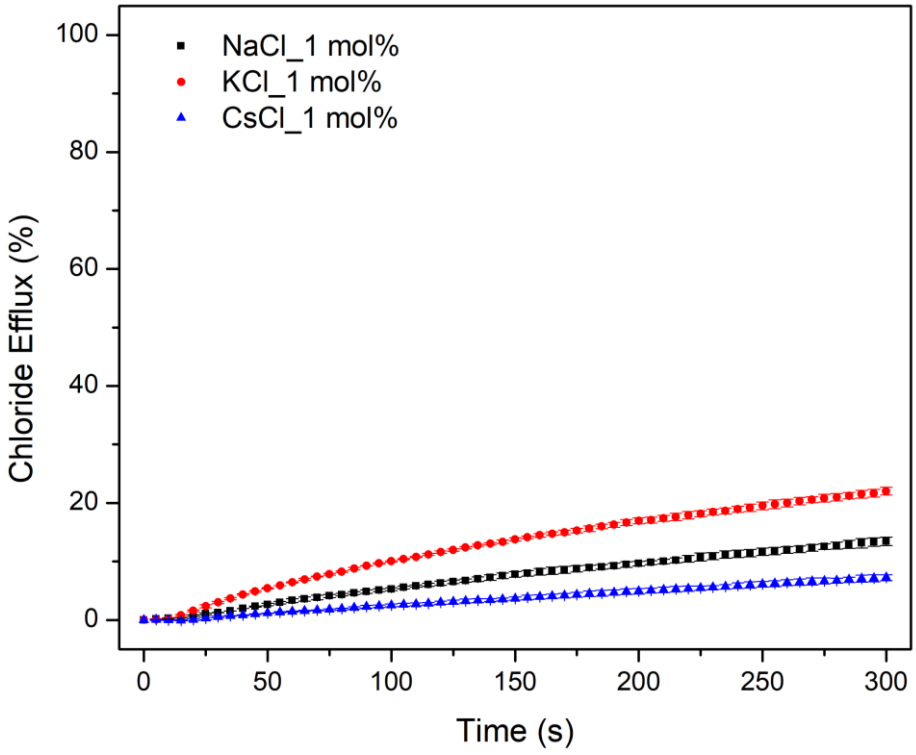

Figure S74. Comparison of the Cl^- transport by **6** (1 mol%) in the Cl^-/NO_3^- exchange assay with a NaCl (black), KCl (red), and CsCl (blue) internal solution.

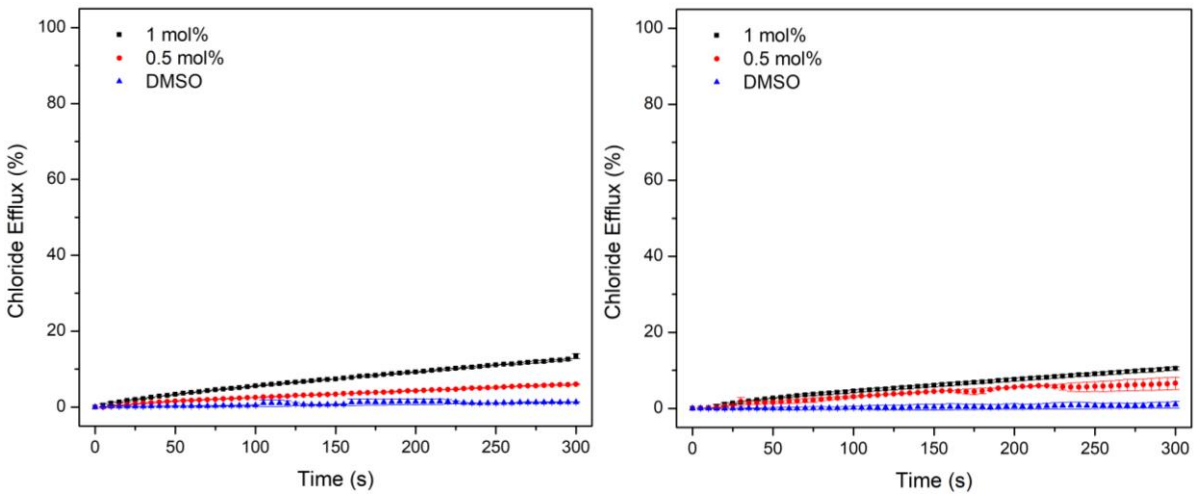

Figure S75. Chloride transport facilitated by **7** in the Cl^-/NO_3^- exchange assay with a NaCl (left) and CsCl (right) internal solution. Each data point is the average of three repeats with error bars showing the standard deviation. DMSO was used as a control.

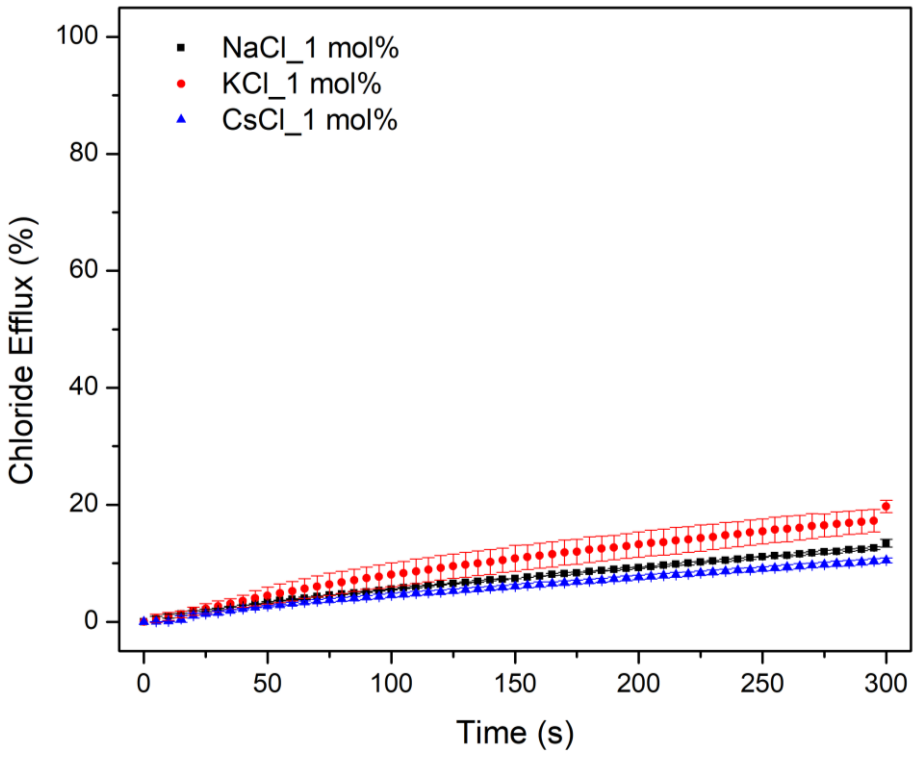

Figure S76. Comparison of the Cl^- transport by **7** (1 mol%) in the Cl^-/NO_3^- exchange assay with a NaCl (black), KCl (red), and CsCl (blue) internal solution.

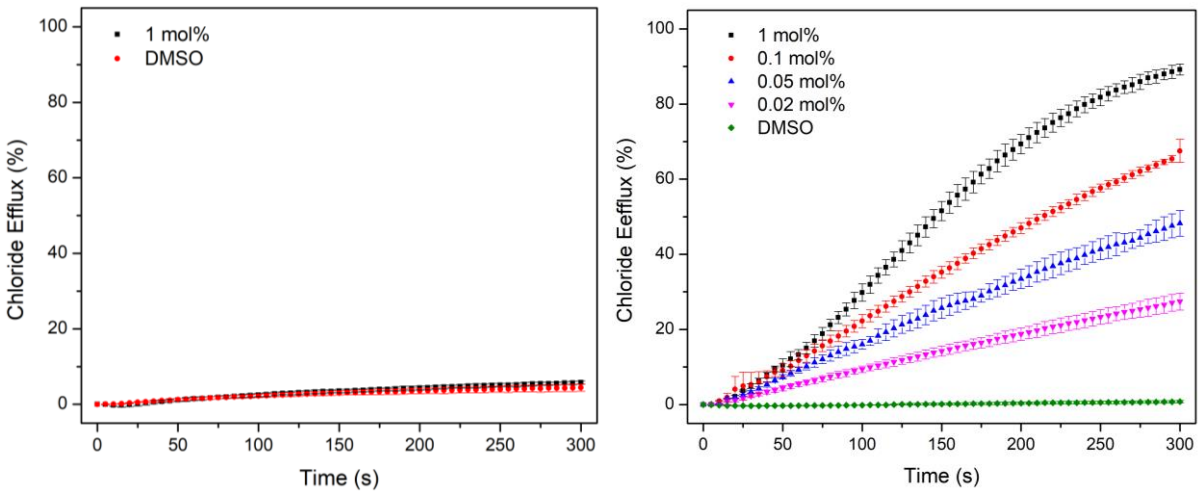

Figure S77. Chloride transport facilitated by OMCP **8** in the Cl^-/NO_3^- exchange assay with a NaCl (left) and CsCl (right) internal solution. Each data point is the average of three repeats with error bars showing the standard deviation. DMSO was used as a control.

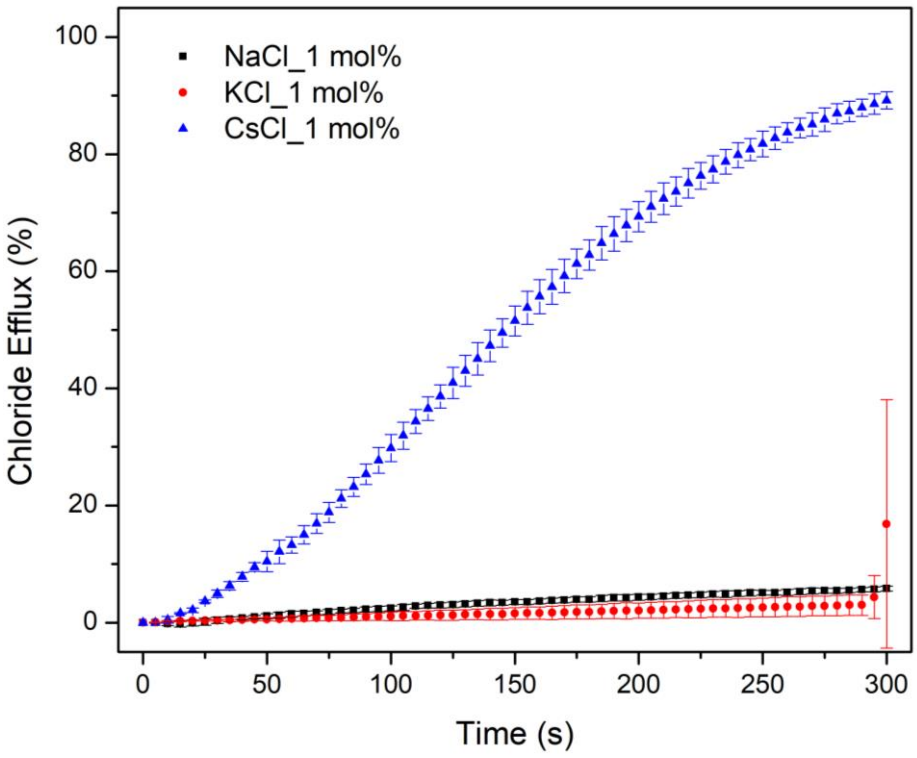

Figure S78. Comparison of the Cl^- transport by OMCP **8** (1 mol%) in the Cl^-/NO_3^- exchange assay with a NaCl (black), KCl (red), and CsCl (blue) internal solution.

ISE Cationophore Coupled Transport

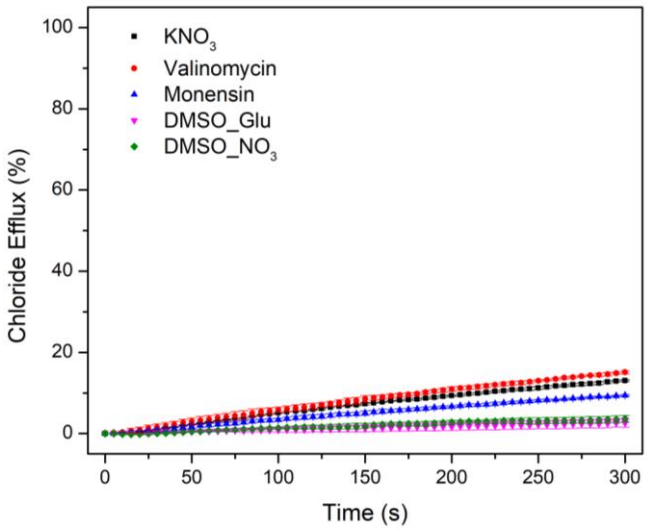

Figure S79. Chloride efflux by **1** (1 mol%) in POPC vesicles loaded with KCl (300 mM) and suspended in an isotonic external solution containing either KNO_3 (300 mM) or KGlu (300 mM) in the presence of valinomycin (0.1 mol%) and monensin (0.1 mol%). Each data point is the average of two repeats, with error bars showing the standard deviation.

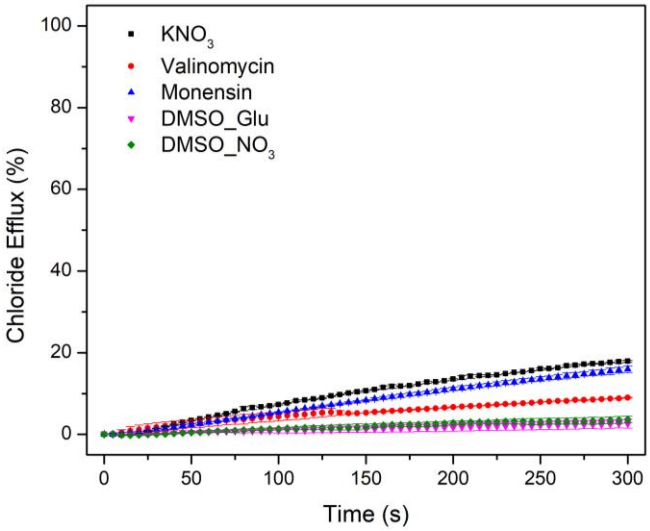

Figure S80. Chloride efflux by **2** (0.2 mol%) in POPC vesicles loaded with KCl (300 mM) and suspended in an isotonic external solution containing either KNO_3 (300 mM) or KGlu (300 mM) in the presence of valinomycin (0.1 mol%) and monensin (0.1 mol%). Each data point is the average of two repeats, with error bars showing the standard deviation.

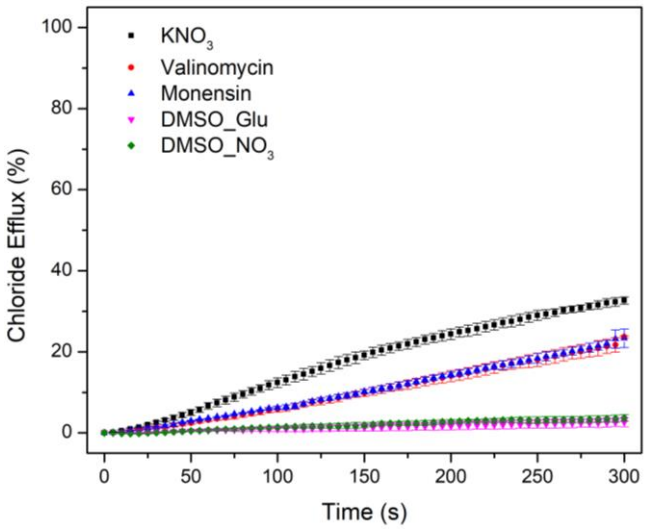

Figure S81. Chloride efflux by **3** (1 mol%) in POPC vesicles loaded with KCl (300 mM) and suspended in an isotonic external solution containing either KNO_3 (300 mM) or KGlu (300 mM) in the presence of valinomycin (0.1 mol%) and monensin (0.1 mol%). Each data point is the average of two repeats, with error bars showing the standard deviation.

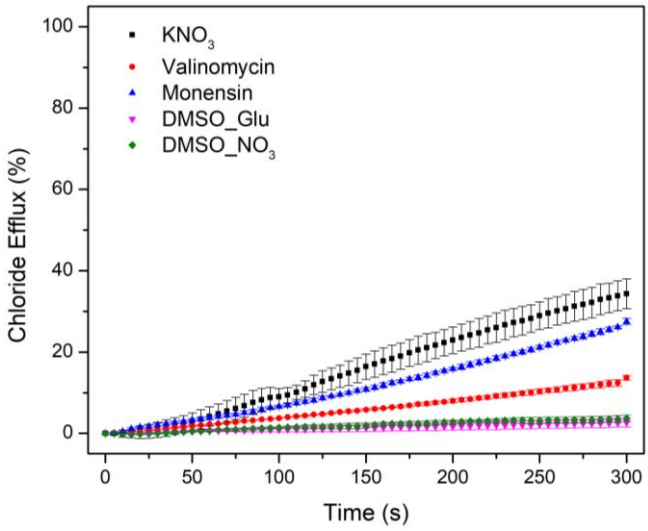

Figure S82. Chloride efflux by **4** (1 mol%) in POPC vesicles loaded with KCl (300 mM) and suspended in an isotonic external solution containing either KNO_3 (300 mM) or KGlu (300 mM) in the presence of valinomycin (0.1 mol%) and monensin (0.1 mol%). Each data point is the average of two repeats, with error bars showing the standard deviation.

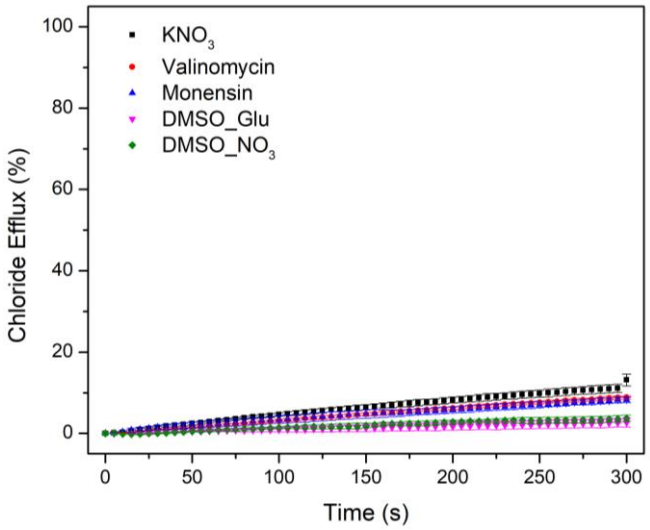

Figure S83. Chloride efflux by **5** (1 mol%) in POPC vesicles loaded with KCl (300 mM) and suspended in an isotonic external solution containing either KNO_3 (300 mM) or KGlu (300 mM) in the presence of valinomycin (0.1 mol%) and monensin (0.1 mol%). Each data point is the average of two repeats, with error bars showing the standard deviation.

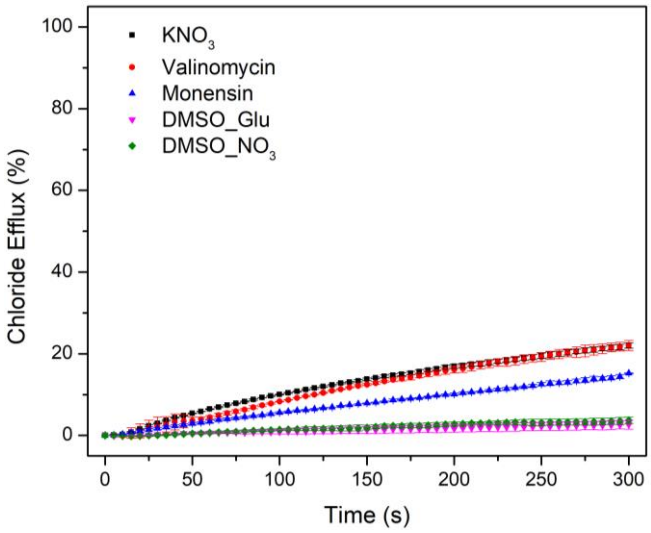

Figure S84. Chloride efflux by **6** (1 mol%) in POPC vesicles loaded with KCl (300 mM) and suspended in an isotonic external solution containing either KNO_3 (300 mM) or KGlu (300 mM) in the presence of valinomycin (0.1 mol%) and monensin (0.1 mol%). Each data point is the average of two repeats, with error bars showing the standard deviation.

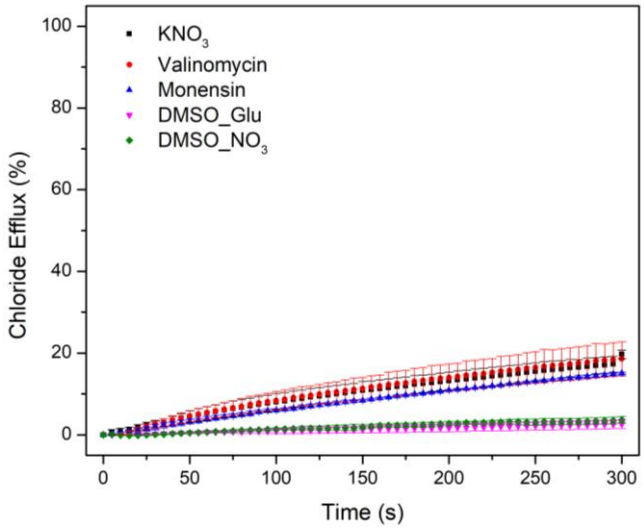

Figure S85. Chloride efflux by **7** (1 mol%) in POPC vesicles loaded with KCl (300 mM) and suspended in an isotonic external solution containing either KNO_3 (300 mM) or KGlu (300 mM) in the presence of valinomycin (0.1 mol%) and monensin (0.1 mol%). Each data point is the average of two repeats, with error bars showing the standard deviation.

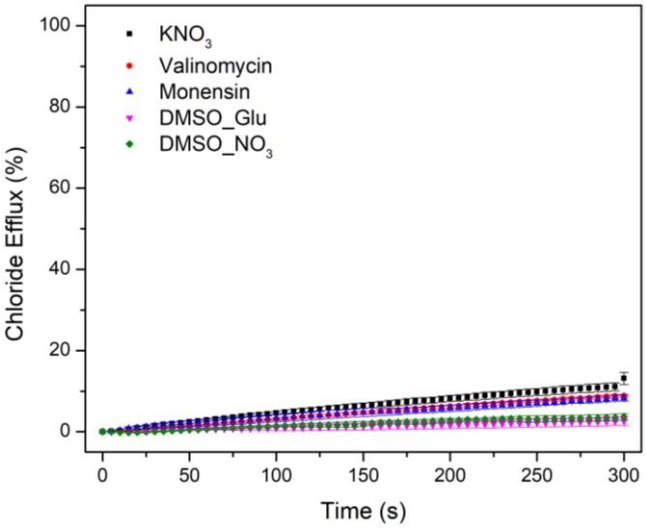

Figure S86. Chloride efflux by OMCP **8** (1 mol%) in POPC vesicles loaded with KCl (300 mM) and suspended in an isotonic external solution containing either KNO_3 (300 mM) or KGlu (300 mM) in the presence of valinomycin (0.1 mol%) and monensin (0.1 mol%). Each data point is the average of two repeats, with error bars showing the standard deviation.

HPTS Assay

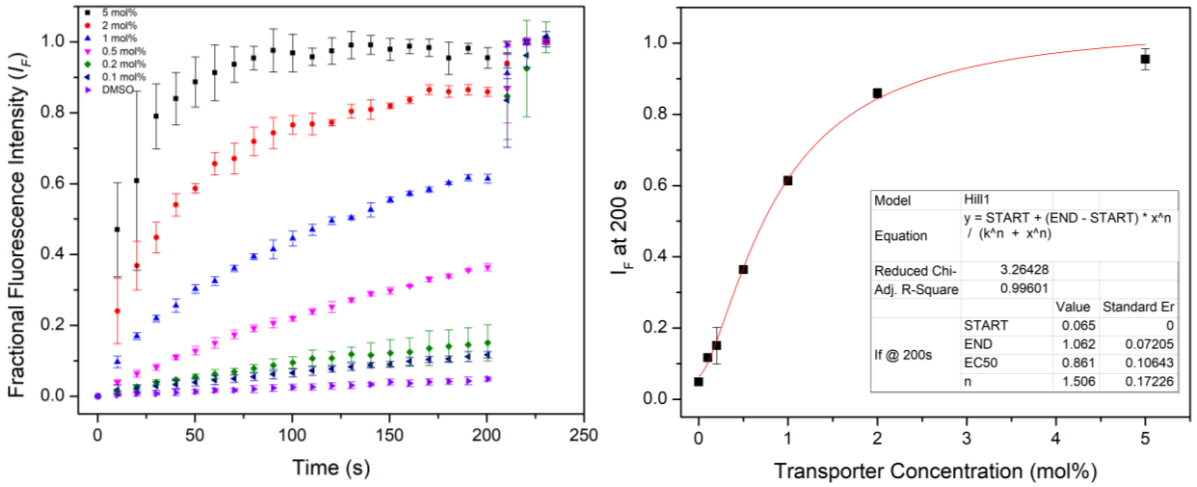

Figure S87. Hill analysis of the H^+/Cl^- symport (or Cl^-/OH^- antiport) facilitated by **1** in the HPTS assay. Each data point is the average of three repeats with error bars showing the standard deviation.

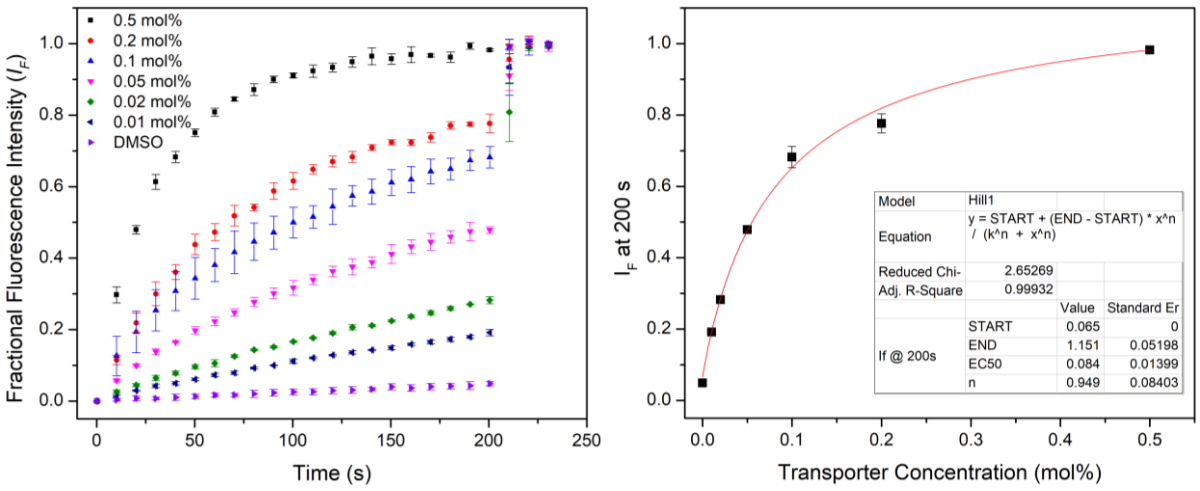

Figure S88. Hill analysis of the H^+/Cl^- symport (or Cl^-/OH^- antiport) facilitated by **2** in the HPTS assay. Each data point is the average of three repeats with error bars showing the standard deviation.

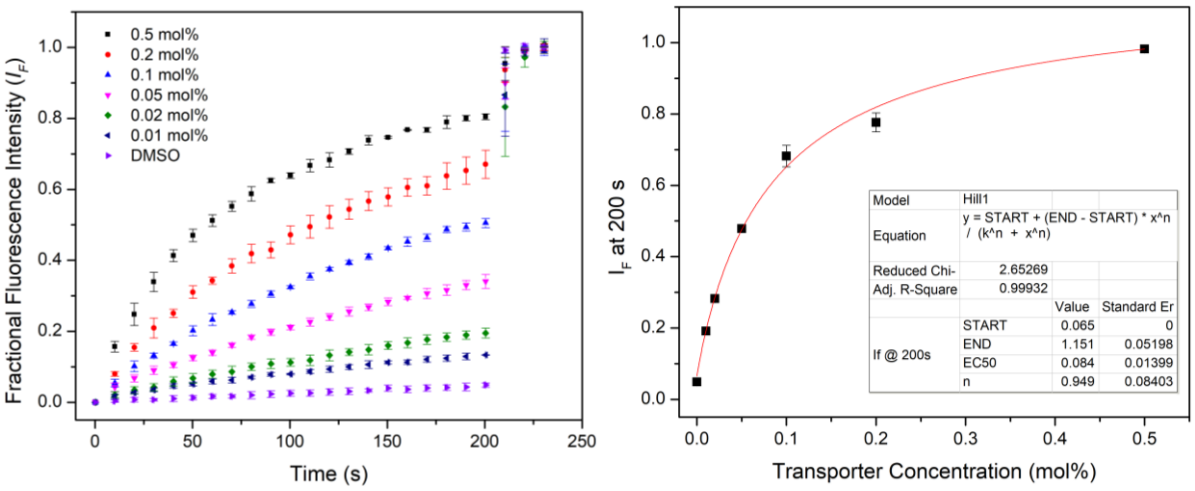

Figure S89. Hill analysis of the H^+/Cl^- symport (or Cl^-/OH^- antiport) facilitated by **3** in the HPTS assay. Each data point is the average of three repeats with error bars showing the standard deviation.

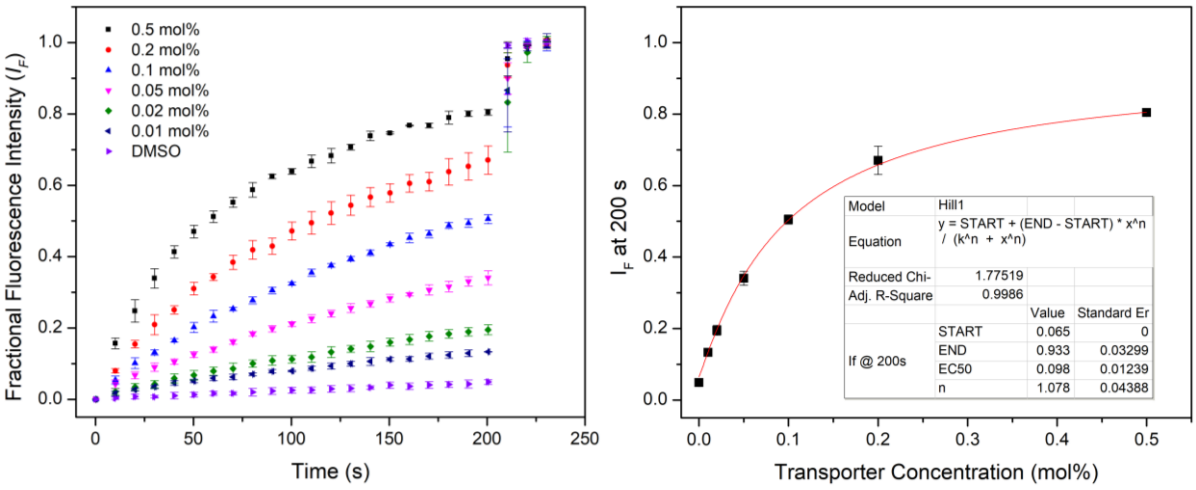

Figure S90. Hill analysis of the H^+/Cl^- symport (or Cl^-/OH^- antiport) facilitated by **4** in the HPTS assay. Each data point is the average of three repeats with error bars showing the standard deviation.

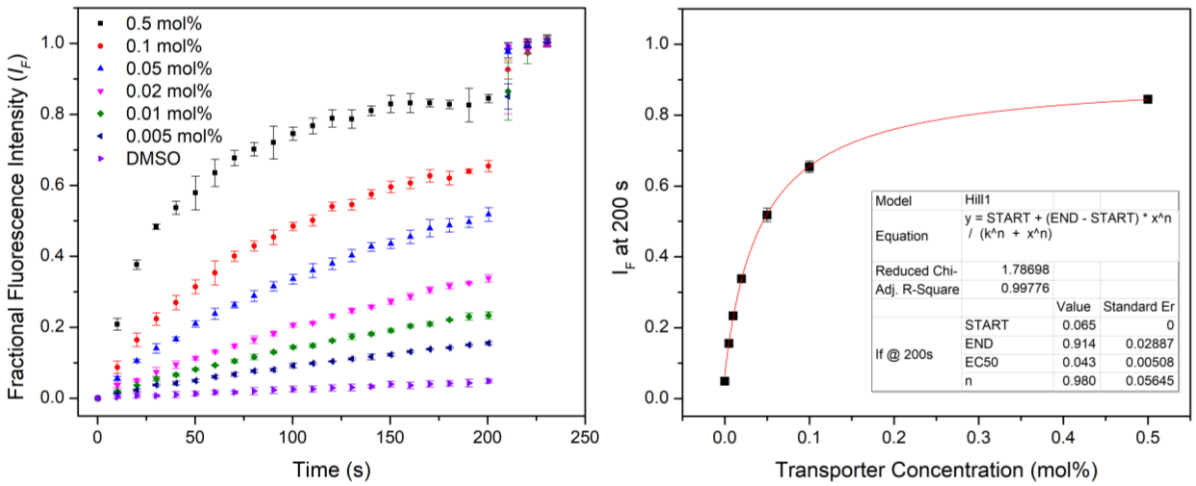

Figure S91. Hill analysis of the H^+/Cl^- symport (or Cl^-/OH^- antiport) facilitated by **5** in the HPTS assay. Each data point is the average of three repeats with error bars showing the standard deviation.

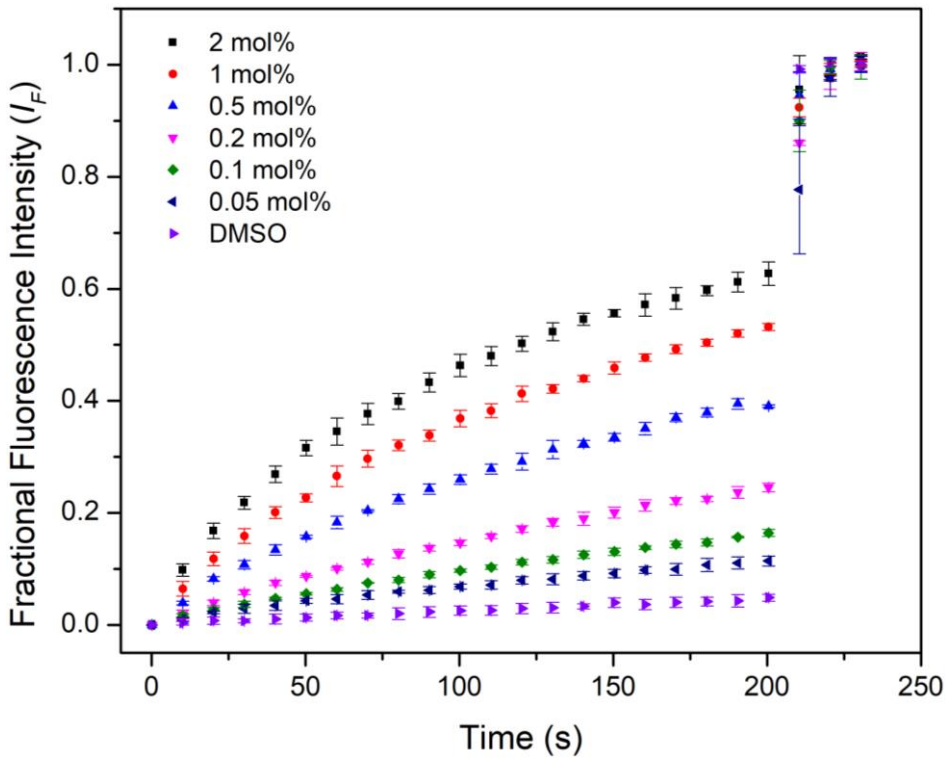

Figure S92. H^+/Cl^- symport (or Cl^-/OH^- antiport) facilitated by **6** in the HPTS assay. Each data point is the average of three repeats with error bars showing the standard deviation. A Hill fit analysis could not be accurately performed for **6** due to insufficient transport activity before the compound precipitated.

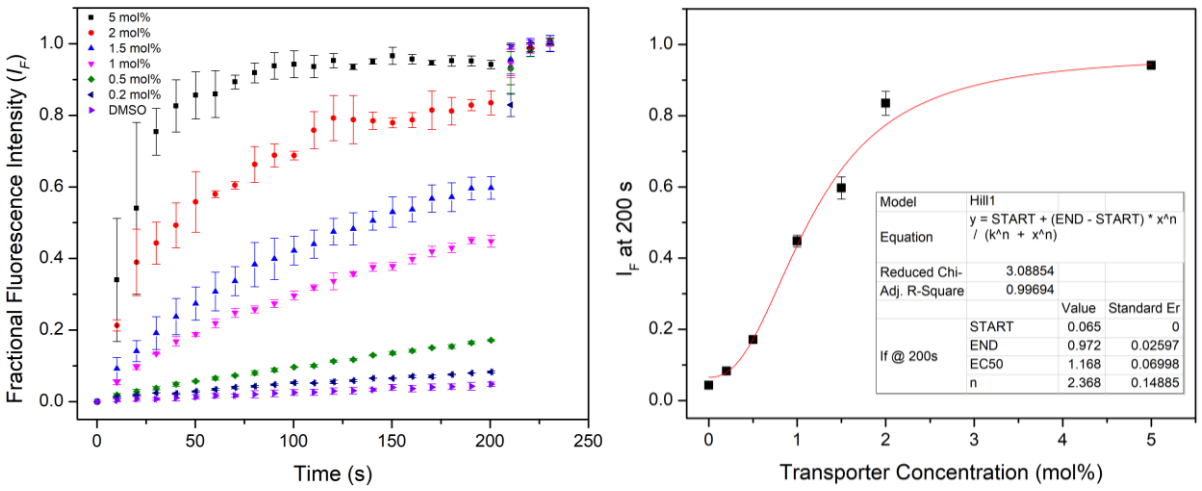

Figure S93. Hill analysis of the H^+/Cl^- symport (or Cl^-/OH^- antiport) facilitated by **5** in the HPTS assay. Each data point is the average of three repeats with error bars showing the standard deviation.

HPTS Mechanistic Studies

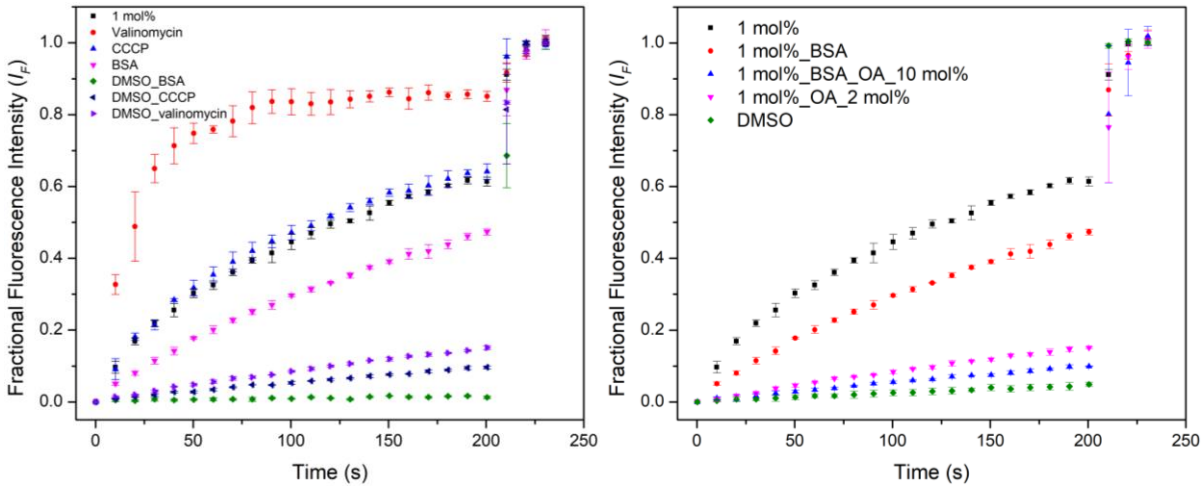

Figure S94. Chloride efflux by **1** (1 mol%) in the HPTS assay in POPC vesicles (left) in the presence of BSA, CCCP, and valinomycin. Chloride efflux of **1** (1 mol%) in low fatty acid content vesicles (right) in the presence of OA and BSA. Each data point represents the average of 3 repeats, and error bars show the standard deviation.

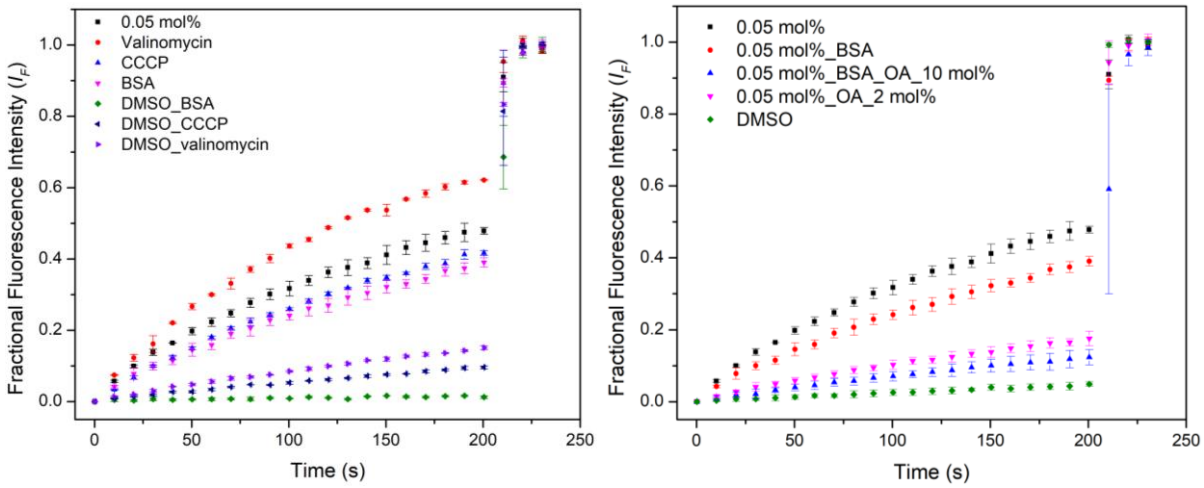

Figure S95. Chloride efflux by **2** (0.05 mol%) in the HPTS assay in POPC vesicles (left) in the presence of BSA, CCCP, and valinomycin. Chloride efflux of **2** (0.05 mol%) in low fatty acid content vesicles (right) in the presence of OA and BSA. Each data point represents the average of 3 repeats, and error bars show the standard deviation.

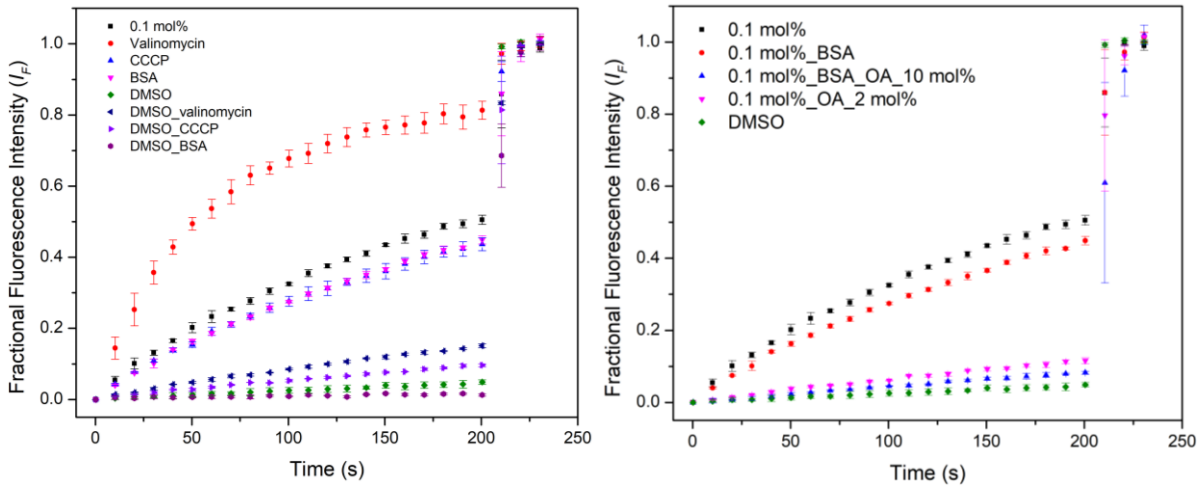

Figure S96. Chloride efflux by **3** (0.1 mol%) in the HPTS assay in POPC vesicles (left) in the presence of BSA, CCCP, and valinomycin. Chloride efflux of **3** (0.1 mol%) in low fatty acid content vesicles (right) in the presence of OA and BSA. Each data point represents the average of 3 repeats, and error bars show the standard deviation.

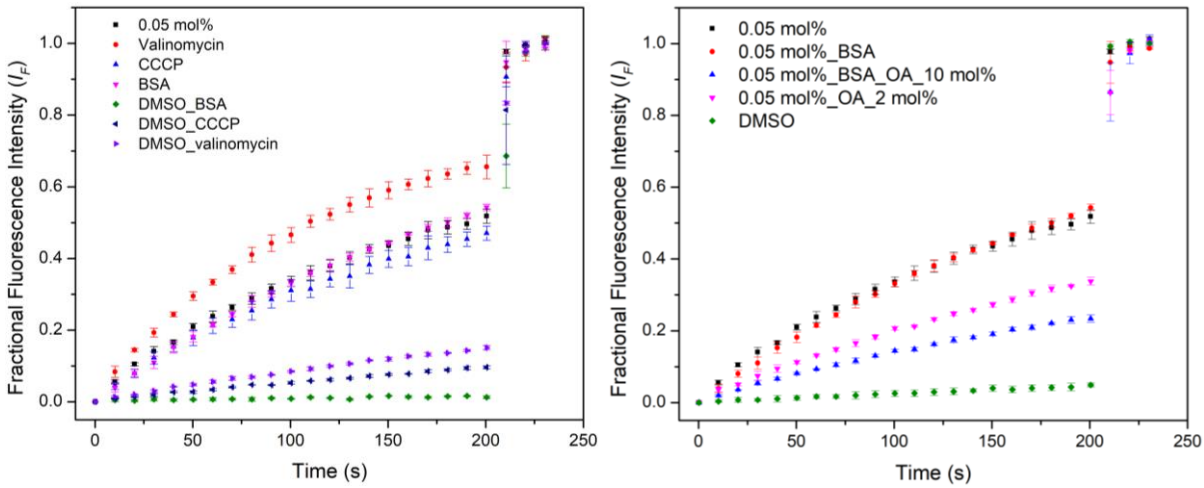

Figure S97. Chloride efflux by **4** (0.05 mol%) in the HPTS assay in POPC vesicles (left) in the presence of BSA, CCCP, and valinomycin. Chloride efflux of **4** (0.05 mol%) in low fatty acid content vesicles (right) in the presence of OA and BSA. Each data point represents the average of 3 repeats, and error bars show the standard deviation.

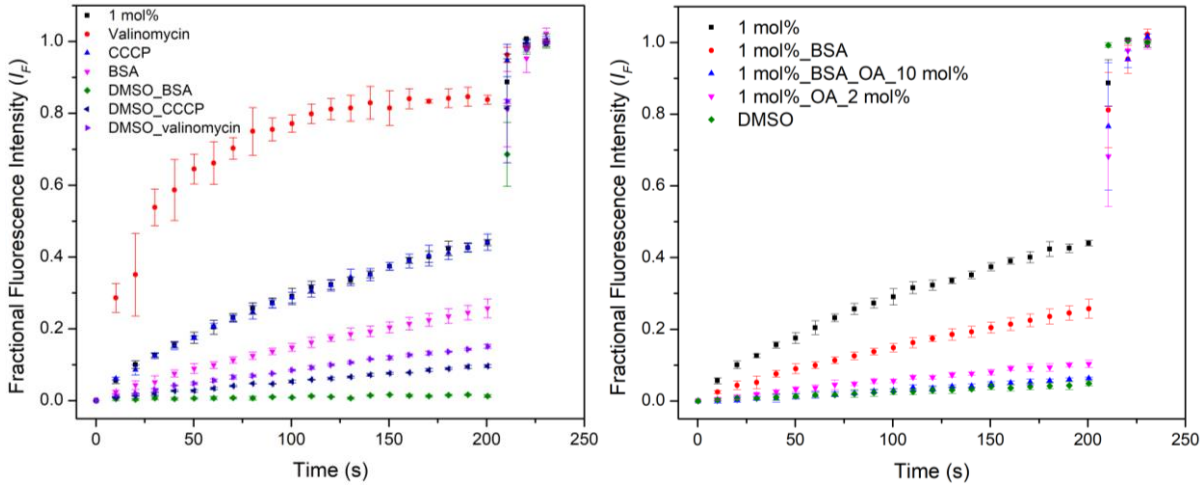

Figure S98. Chloride efflux by **5** (1 mol%) in the HPTS assay in POPC vesicles (left) in the presence of BSA, CCCP, and valinomycin. Chloride efflux of **5** (1 mol%) in low fatty acid content vesicles (right) in the presence of OA and BSA. Each data point represents the average of 3 repeats, and error bars show the standard deviation.HPTS Anion Selectivity Assay

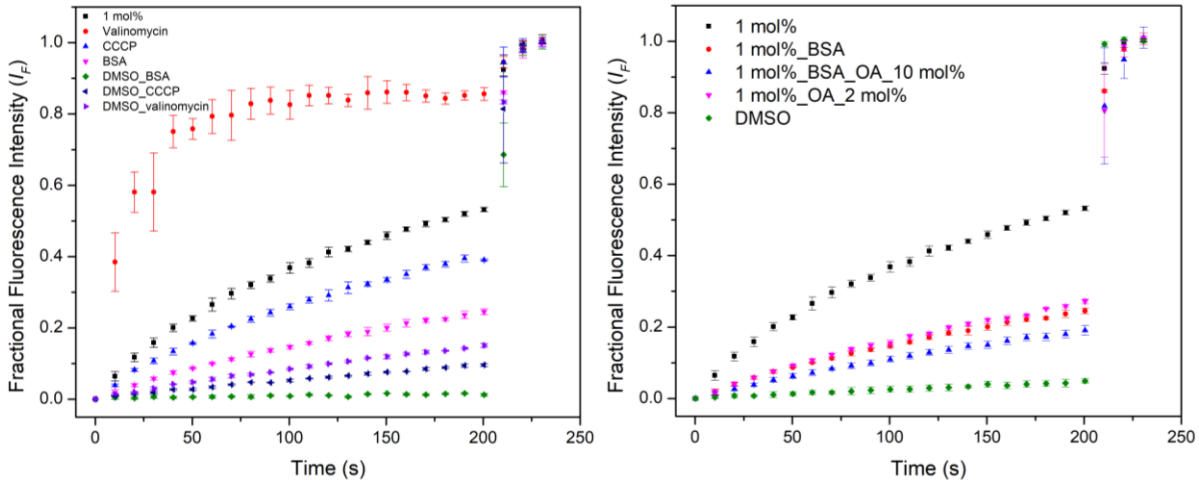

Figure S99. Chloride efflux by **6** (1 mol%) in the HPTS assay in POPC vesicles (left) in the presence of BSA, CCCP, and valinomycin. Chloride efflux of **6** (1 mol%) in low fatty acid content vesicles (right) in the presence of OA and BSA. Each data point represents the average of 3 repeats, and error bars show the standard deviation.

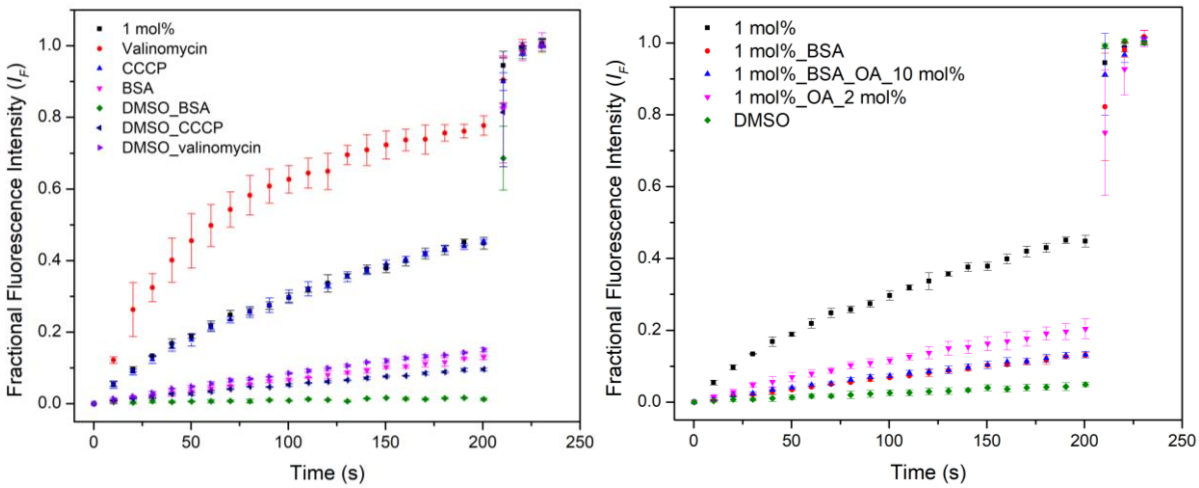

Figure S100. Chloride efflux by **7** (1 mol%) in the HPTS assay in POPC vesicles (left) in the presence of BSA, CCCP, and valinomycin. Chloride efflux of **7** (1 mol%) in low fatty acid content vesicles (right) in the presence of OA and BSA. Each data point represents the average of 3 repeats, and error bars show the standard deviation.

HPTS Anion Selectivity Studies

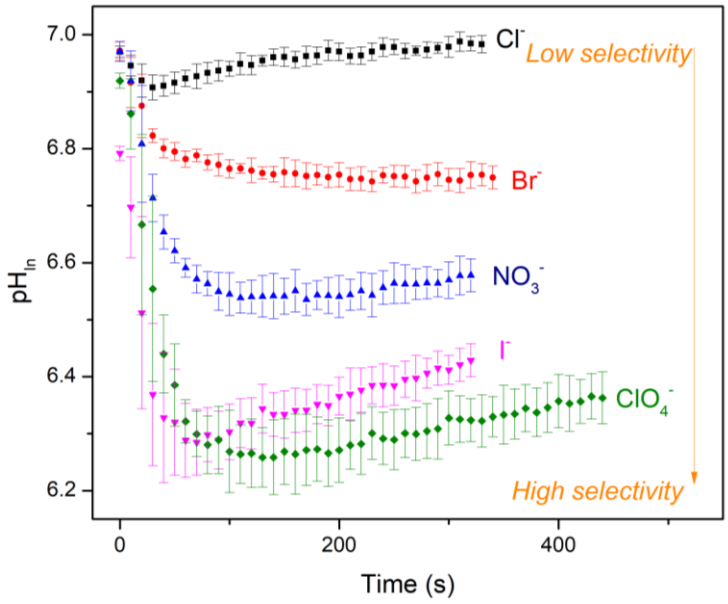

Figure S101. The intravesicular pH over time in the HPTS anion selectivity assay in the presence of **1** (1 mol%). Vesicles containing NaCl (100 mM) were suspended in different external solutions (100 mM) containing either Cl^-, Br^-, NO_3^-, I^-, or ClO_4^-. Error bars represent the standard deviation of three runs.

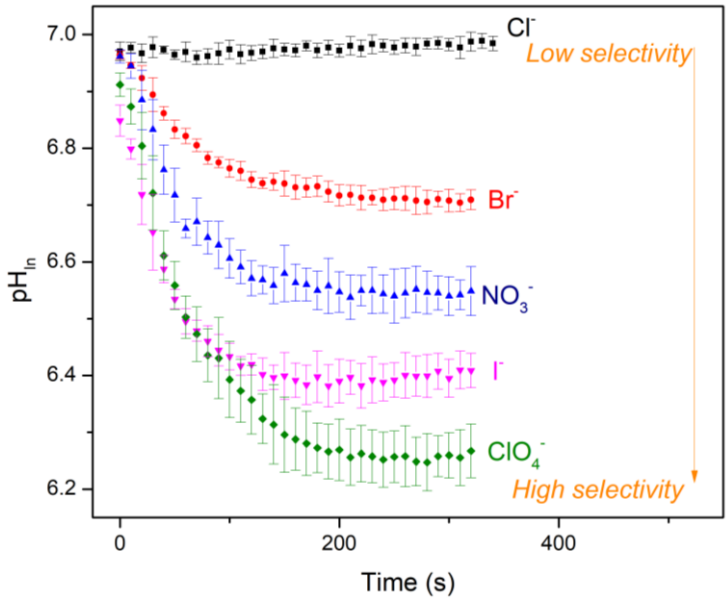

Figure S102. The intravesicular pH over time in the HPTS anion selectivity assay in the presence of **2** (0.05 mol%). Vesicles containing NaCl (100 mM) were suspended in different external solutions (100 mM) containing either Cl^-, Br^-, NO_3^-, I^-, or ClO_4^-. Error bars represent the standard deviation of three runs.

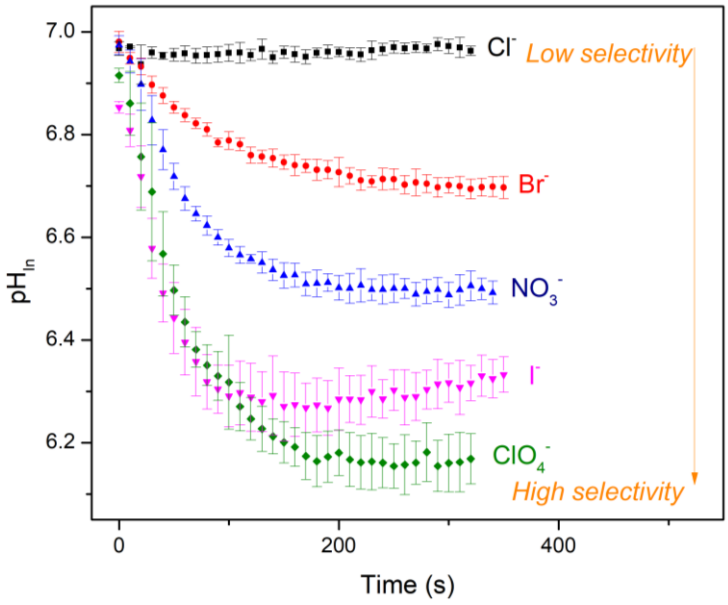

Figure S103. The intravesicular pH over time in the HPTS anion selectivity assay in the presence of **3** (0.1 mol%). Vesicles containing NaCl (100 mM) were suspended in different external solutions (100 mM) containing either Cl^-, Br^-, NO_3^-, I^-, or ClO_4^-. Error bars represent the standard deviation of three runs.

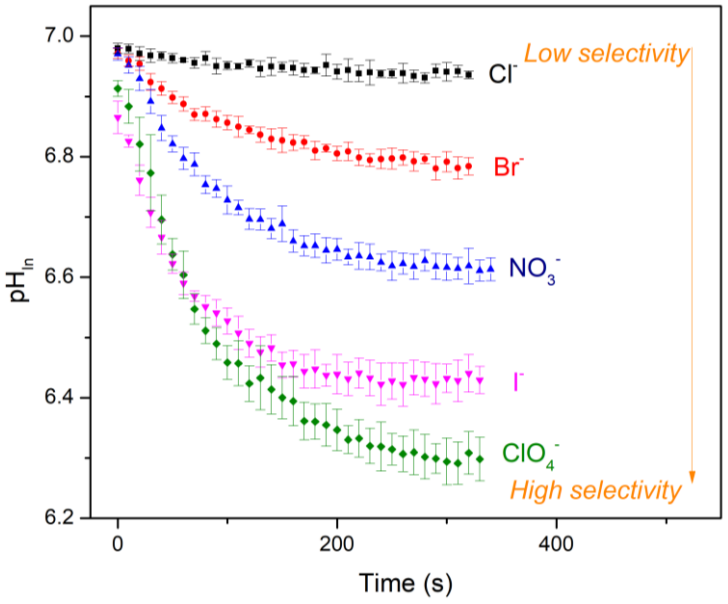

Figure S104. The intravesicular pH over time in the HPTS anion selectivity assay in the presence of **4** (0.05 mol%). Vesicles containing NaCl (100 mM) were suspended in different external solutions (100 mM) containing either Cl^-, Br^-, NO_3^-, I^-, or ClO_4^-. Error bars represent the standard deviation of three runs.

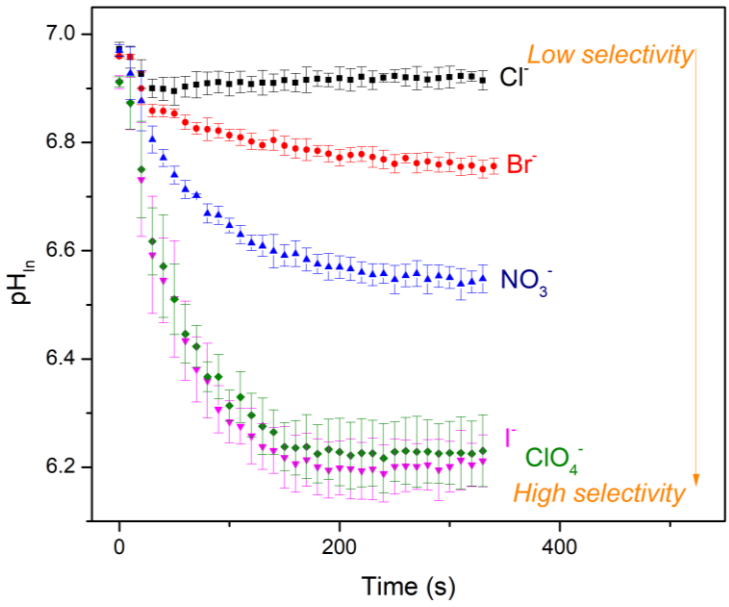

Figure S105. The intravesicular pH over time in the HPTS anion selectivity assay in the presence of **5** (1 mol%). Vesicles containing NaCl (100 mM) were suspended in different external solutions (100 mM) containing either Cl^-, Br^-, NO_3^-, I^-, or ClO_4^-. Error bars represent the standard deviation of three runs.

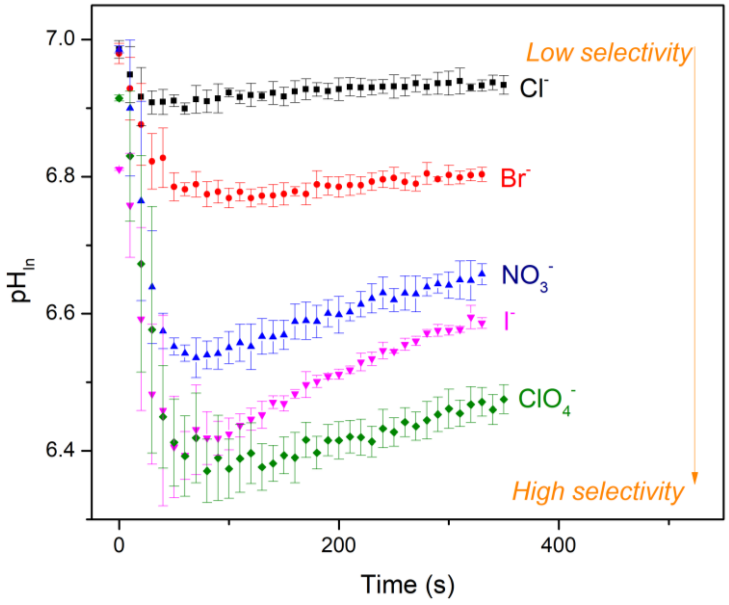

Figure S106. The intravesicular pH over time in the HPTS anion selectivity assay in the presence of **6** (1 mol%). Vesicles containing NaCl (100 mM) were suspended in different external solutions (100 mM) containing either Cl^-, Br^-, NO_3^-, I^-, or ClO_4^-. Error bars represent the standard deviation of three runs.

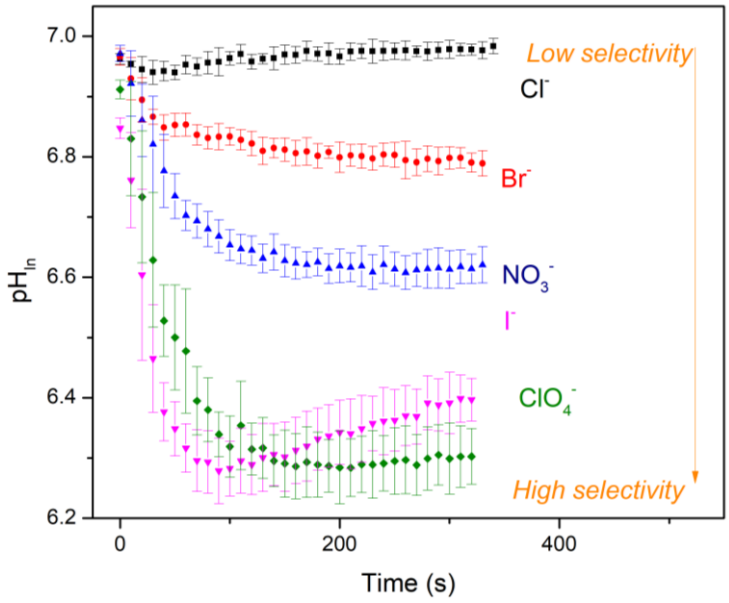

Figure S107. The intravesicular pH over time in the HPTS anion selectivity assay in the presence of **7** (1 mol%). Vesicles containing NaCl (100 mM) were suspended in different external solutions (100 mM) containing either Cl^-, Br^-, NO_3^-, I^-, or ClO_4^-. Error bars represent the standard deviation of three runs.

References

1. http://app.supramolecular.org/bindfit/ (accessed May, 2024).
2. P. Thordarson, Determining association constants from titration experiments in supramolecular chemistry, *Chem. Soc. Rev.*, 2011, **40**, 1305-1323.
3. L. A. Jowett and P. A. Gale, Supramolecular methods: the chloride/nitrate transmembrane exchange assay, *Supramol. Chem.*, 2019, **31**, 297-312.
4. A. M. Gilchrist, P. Wang, I. Carreira-Barral, D. Alonso-Carrillo, X. Wu, R. Quesada and P. A. Gale, Supramolecular methods: the 8-hydroxypyrene-1, 3, 6-trisulfonic acid (HPTS) transport assay, *Supramol. Chem.*, 2021, **33**, 325-344.
5. X. Wu and P. A. Gale, Measuring anion transport selectivity: a cautionary tale, *Chem. Commun.*, 2021, **57**, 3979-3982.